Design and engineering of human TRAIL variants

RIJKSUNIVERSITEIT GRONINGEN

Design and engineering of human TRAIL variants

Proefschrift

ter verkrijging van het doctoraat in de
Wiskunde en Natuurwetenschappen
aan de Rijksuniversiteit Groningen
op gezag van de
Rector Magnificus, dr. F. Zwarts,
in het openbaar te verdedigen op
vrijdag 24 november 2006
om 13.15 uur

door

Albert Martinus van der Sloot

geboren op 8 november 1974
te Sneek

Promotor:	Prof. Dr. W.J. Quax
Beoordelingscommissie:	Prof. Dr. K. Poelstra Prof. Dr. L. Serrano Dr. A. Samali

Paranimfen: Carlos Reis

Barry Swets

The studies described in this thesis were performed at the Department of Pharmaceutical Biology of the University of Groningen, the Netherlands. Publication of the thesis was financially supported by the Graduate School for Drug Exploration (GUIDE).

Cover design: Carlos Reis

Printed by Print Partners Ipskamp, Enschede

ISBN printed version: 90-367-2878-9

ISBN digital version: 90-367-2879-7

Contents

Chapter 1:	General introduction and scope of the thesis	9
Chapter 2:	Review: Computational design methods for optimizing protein therapeutics	15
Chapter 3:	Stabilization of TRAIL, an all-β-sheet multimeric protein, using computational redesign	33
Chapter 4:	Designed tumor necrosis factor-related apoptosis-inducing ligand variants initiating apoptosis exclusively via the DR5 receptor	49
Chapter 5:	Towards the design of a DR4 selective TRAIL variant	67
Chapter 6:	Enhanced anti-cancer activity of a DR5 selective TRAIL variant in combination with a proteasome inhibitor or radiation therapy in a cervical cancer model	81
Chapter 7:	Summary and general discussion	93
	References	99
	Nederlandse samenvatting	121
	Dankwoord	127
	List of publications	131
	Color figures	133

1

Introduction and scope of the thesis

Introduction

The TNF-ligand and TNF-receptor family

Tumor necrosis factor (TNF) ligand family members and their cognate receptors of the TNF receptor family activate several signaling pathways, eliciting activities ranging from cell-proliferation to the induction of apoptosis. TNF like ligands (TNF-L) and TNF like receptors (TNF-R) are involved in a variety of biological processes, such as host defense, development, (auto)immunity, inflammation and tumor surveillance[1-3]. TNF-L and TNF-R like molecules have been identified in a wide range of metazoans, from *Drosophila* to mammals[4]. Currently, nineteen TNF-ligands and twenty-nine TNF-receptors have been identified in humans (table 1)[2,5]. Several ligands have multiple receptors, and conversely, some receptors also bind multiple ligands (figure 1).

		TNF-ligands																		
Symbol	acronym	LTA TNFB	TNF TNFA	LTB TNFC	TNFSF4 OX-40L	TNFSF5 CD40L	TNFSF6 FASL	TNFSF7 CD70	TNFSF8 CD30LG	TNFSF9 4-1BB-L	TNFSF10 TRAIL	TNFSF11 RANKL	TNFSF12 TWEAK	TNFSF13 APRIL	TNFSF13B BAFF	TNFSF14 LIGHT	TNFSF15 TL1A	TNFSF18 GITRL	EDA EDA1	EDA EDA2
TNFRSF1A	TNF-R1	x	x	x																
TNFRSF1B	TNF-R2	x	x	x																
LTBR	TNF-R3			x												x				
TNFRSF4	OX40				x															
TNFRSF5	CD40					x														
TNFRSF6	FAS						x													
TNFRSF6B	DcR3						x									x	x			
TNFRSF7	CD27							x												
TNFRSF8	CD30								x											
TNFRSF9	4-1BB									x										
TNFRSF10A	DR4										x									
TNFRSF10B	DR5										x									
TNFRSF10C	DcR1										x									
TNFRSF10D	DcR2										x									
TNFRSF11A	RANK											x								
TNFRSF11B	OPG										x	x								
TNFRSF12	DR3												?				x			
TNFRSF12A	FN14												x							
TNFRSF12L	DR3L																			
TNFRSF13B	TACI													x	x					
TNFRSF13C	BAFF-R														x					
TNFRSF14	HVEM	x														x				
NGFR	NGFR																			
TNFRSF17	BCMA													x	x					
TNFRSF18	GITR																	x		
TNFRSF19	TROY																			
TNFRSF19L	RELT																			
TNFRSF21	DR6																			
EDAR	EDAR																		x	
EDA2R	XEDAR																			x

TNF-receptors

Figure 1. Interactions between human TNF-L and TNF-R family members. NGFR interacts with members of the Nerve growth factor family members and EDAR and EDR2 are splice variants.

The TNF-ligand family is characterized by a conserved C-terminal domain, the TNF homology domain (THD). The sequence identity between THDs of different TNF-L family members is ~20-30%. The THD causes trimerization of the TNF-L and is responsible for receptor binding. Sequence homology is highest between the (aromatic) residues responsible for trimer formation. All monomeric subunits of TNF-ligands consist of antiparallel β-sheets, organized in a jellyroll topology, and these subunits self associate in bell-shaped homotrimers, the bioactive form of the ligand. A trimer binds three subunits of a cognate receptor, each receptor subunit binds usually in the grooves between two adjacent monomer subunits. The ligands are type II transmembrane proteins (i.e. intra-cellular N-terminus and extra-cellular C-terminus), but the extracellular domain of some members can be proteolytically cleaved from the cell surface, yielding a bioactive soluble form of the ligand[1,2,6].

The distinguishing feature of the extra-cellular part of the TNF-like receptors is the cysteine-rich domain (CRD). These CRDs are pseudo-repeats of ~40 amino acids and typically contain six cysteine residues which are involved in the formation of three intra-chain disulfide bonds. The number of CRDs in a particular receptor varies usually from one

to four. TNF-R family members have an elongated shape due to the repeated arrangement of the CRDs. Most of the TNF-R family members are type I transmembrane proteins (i.e. intra-cellular C-terminus and extra-cellular N-terminus). However, several exceptions exist; for example some receptors lack a C-terminal part and are secreted as soluble receptors (OPG and DcR3) or are covalently linked to the cell membrane via a glycophosphatidylinositol (GPI) anchor (DcR1) and some other transmembrane TNF-R family members lack a signal peptide sequence and are consequently type III transmembrane proteins[1,2,6]. The canonical model of TNF ligand-receptor signaling proposes that three receptor monomers are recruited upon binding of a trimeric ligand into a signaling complex with 3:3 stoichiometry (ligand-monomer: receptor-monomer)[1,2,6]. Receptor monomers cross-linked in this manner by the ligand subsequently transduce the signal into the cell. This simple model has been challenged by the fact that several TNF-R family members contain a pre-ligand assembly domain (PLAD) which allows the receptors to self-assemble in the absence of a ligand[7,8]. Binding of a TNF ligand would then cause a rearrangement of the pre-assembled TNF-R complex and allow transduction of the signal. In addition, certain receptors are not fully activated upon stimulating with a soluble TNF-L but require the membrane bound form of the ligand for full activation.

Depending on whether the cytoplasmic or intra-cellular tail of a particular TNF-R harbors a death domain (DD) or TNF receptor-associated factor (TRAF) binding domain, two main modes of signaling can be recognized: signaling events governed by TRAF proteins or by DD containing molecules[1]. TRAF proteins physically and functionally connect TNF-Rs to downstream signaling pathways involved in regulation of diverse cellular responses, including activation, differentiation and survival[9]. A particular subset of TNF-receptors contains an intra-cellular DD and hence are known as "death receptors". Binding of a TNF-L to these receptors typically cause the recruitment of adaptor proteins such as TNF-R-associated DD protein (TRADD) or Fas-associated DD protein (FADD). Recruitment of these adaptors will cause the recruitment of caspase 8 or 10 and can ultimately result in cell death by a process called apoptosis or programmed cell death[10,11].

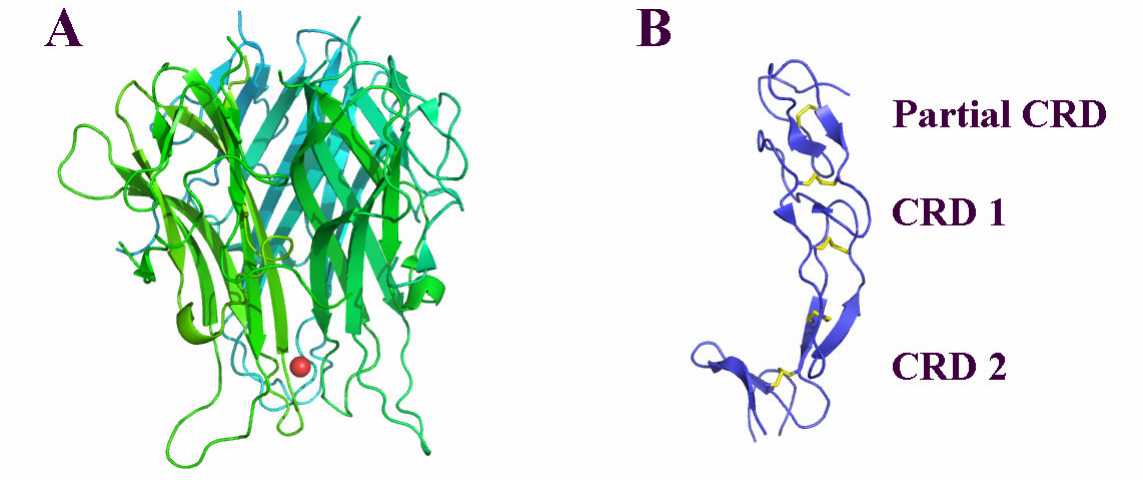

Figure 2. Structure of the TRAIL trimer and DR5. A) Sideview of the TRAIL trimer, the individual TRAIL monomers are depicted in different shades of green. The zinc atom in the center of the TRAIL trimer is depicted as a red sphere. B) DR5 receptor monomer, disulphide bridges are depicted in yellow. In this orientation, the cell membrane of the DR5 containing cell is at the bottom of the figure. Picture is based on the structure of Cha *et al.*,[12].

TRAIL and its receptors

A member of the TNF-ligand family, Tumor necrosis factor (TNF) related apoptosis inducing-ligand (TRAIL, Apo2L) is attracting great interest as a potential anti-cancer therapeutic as it selectively kills various types of tumor cells, and unlike other apoptosis inducing TNF-ligand family members, appears to be inactive against normal cells[13]. TRAIL kills tumor cells by inducing apoptosis and normal cells appear to be relatively resistant towards TRAIL induced apoptosis. Reports in which TRAIL induces apoptosis in normal cells could be attributed to the specific preparations of TRAIL used[14,15]. TRAIL is expressed as a transmembrane protein and it can be released from the cell membrane by proteolytic cleavage. Upon cleavage a soluble form of TRAIL is generated, both the soluble and the cell membrane-bound form are able to induce apoptosis. Like other TNF-ligand family members, TRAIL is a trimeric ligand and the β-sheets in a monomer are organized in a jellyroll topology (Figure 2A)[16-18]. Unlike other TNF-like ligands, TRAIL contains a single cysteine residue, which is involved in chelating a zinc ion located at the center of the TRAIL trimer[17]. This zinc binding center is essential for the stability and biological activity of (soluble) TRAIL. The TRAIL trimer binds three receptor molecules, each at the interface between two of its monomers (figure 3A and B)[16,18].

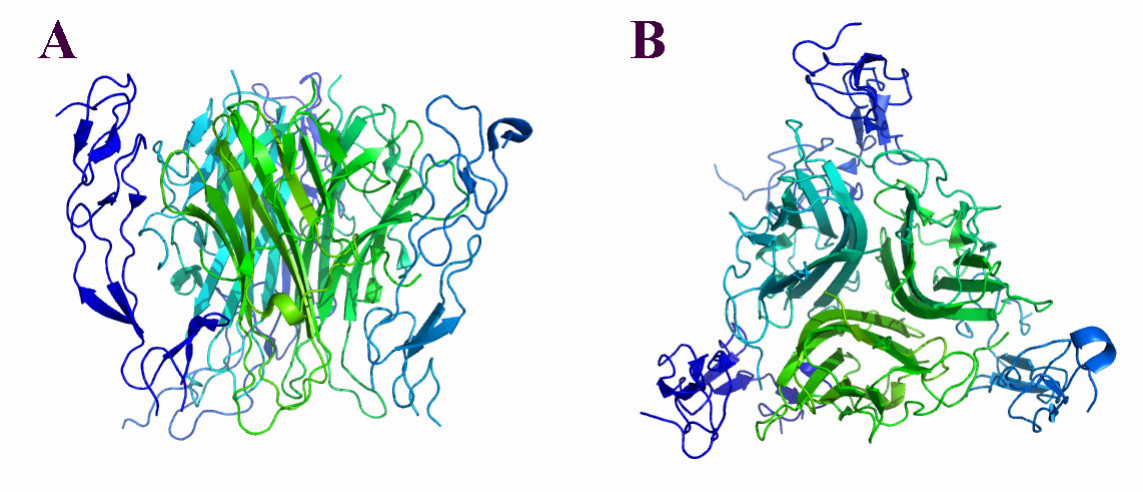

Figure 3. Structure of the 3:3 TRAIL-DR5 complex. A) side view (same orientation as in figure 1). B) top view along the N-terminal to C-terminal axis of the DR5 receptor (i.e. looking towards the cell surface of DR5). Picture is based on the structure of the TRAIL-DR5 complex of Cha *et al.*,[12].

TRAIL is a promiscuous ligand as it binds to five different cognate receptors of the TNF-receptor family; to the death receptor 4 (DR4, TRAIL-R1), death receptor 5 (DR5, TRAIL-R2, KILLER, TRICK-2) and to the decoy receptor 1 (DcR1, TRAIL-R3, TRIDD) and decoy receptor 2 (DcR2, TRAIL-R4, TRUNDD) and to the soluble secreted receptor osteoprotegerin (OPG)[19]. The death- and decoy receptors consist of two complete CRDs and one partial N-terminal CRD with unknown function (figure 2B)[16,18]. Binding of TRAIL to the DR4 and DR5 receptors induces apoptosis by activating the cell-extrinsic or death receptor-mediated apoptosis pathway. Upon binding with TRAIL the death receptors trimerize and an intracellular death-inducing signaling complex (DISC) is assembled; the intracellular death domains of DR4 and DR5 recruit FADD[20-22], which bind and activate the

apoptosis initiator caspases 8 and 10[23-26]. This leads to the activation of the apoptosis executioner caspase 3, followed by the activation of other proteases and nucleases resulting finally in apoptosis[27,28]. This process can be inhibited by the cellular FLICE like-inhibitory protein (cFLIP), an inhibitor of caspase activation[29]. DcR1 or DcR2 do not contain an intracellular death domain or contain a truncated death domain, respectively. Binding to these receptors does not induce apoptosis, in contrast, it could prevent apoptosis by sequestering available TRAIL or by interfering in the formation of a TRAIL-DR4 or DR5 signaling complex[30]. Recently, it was demonstrated that the PLADs overlapping the partial N-terminal CRD of DR5 and DcR2 were able to form pre-assembled hetero complexes in the absence of TRAIL and that DcR2 by virtue of this pre-assembled complex with DR5 was able to inhibit TRAIL-induced apoptosis[31].

At present, clinical phase I studies are performed with recombinant human TRAIL (Genentech, South San Francisco, USA). This recombinant TRAIL version is a fragment of the C-terminal extra-cellular part of human TRAIL comprising amino acids 114-281 and is expressed in *Escherichia coli* bacteria as a soluble protein without additional exogenous sequences (rhTRAIL WT)[13]. This TRAIL protein is purified as a trimer and optimized for its zinc content. No hepatotoxicity was observed in chimpanzees[32] after administration of rhTRAIL and neither was toxicity observed in human hepatocytes or other normal cells[13,14,32]. However, rhTRAIL will probably be rapidly cleared as it half-life in chimpanzees was only 25 minutes[32].

Scope of the thesis

Protein therapeutics currently are of increasing importance as approximately twenty five percent of all new therapeutics entering the market are protein based therapeutics. However, since endogenous proteins are not “designed” by Nature, or more accurately, not evolved to function as therapeutic agents, additional optimization might be required. Traditionally, expert design or directed evolution techniques were used to improve the characteristics of protein therapeutics. Computational protein design methods are a more recent powerful technology which is able to improve various properties important for protein therapeutics, such as stability, receptor specificity and immunogenicity. Application of this technology potentially allows a faster transition from laboratory bench to clinic for protein therapeutics. As yet, however, computational protein design is hardly applied for the improvement of protein therapeutics. In this thesis, the feasibility of computational protein design technology is demonstrated with the improvement of therapeutically relevant properties of the protein therapeutic rhTRAIL. Chapter 2 in this thesis describes the recent progress in the use of computational protein design methods to improve protein therapeutics and other potential applications of these methods in the field of medical biotechnology. Chapter 3 reports the design of rhTRAIL variants with higher thermostability. Chapter 4 describes the design of rhTRAIL variants selective for DR5, whereas the design of rhTRAIL variants selective for DR4 is described in chapter 5. The added value of using a DR5 selective rhTRAIL variant compared to using rhTRAIL WT in combination with radiation therapy or chemotherapy is demonstrated in chapter 6. Finally, in chapter 7 the results of the studies described in this thesis are summarized and future perspectives are discussed.

2

Computational design methods for optimising protein therapeutics

A.M. van der Sloot and W.J. Quax

Abstract

The use of computational methods in the (re)design of various properties of proteins has made an impressive progress in recent years. In this review we will discuss the use and impact of these methods in the design of biopharmaceuticals and in medical biotechnology.

Introduction

Until the nineteen eighties the only available protein therapeutics were those purified from material of human, animal or microbial origin. The advent of recombinant DNA (rDNA) technology in the early seventies enabled the introduction of the first human recombinant protein therapeutic, human insulin, in 1982. In the twenty plus years since, this has resulted in the introduction of over 70 recombinant protein therapeutic products currently on the market and approximately another 80 at various stages in clinical development[33]. The first recombinant protein therapeutics did have identical amino acid sequences as their natural counterpart. However, as natural occurring proteins are not evolved to be used as drugs, additional structure optimization might be required. Sequence optimization can be a useful strategy to improve several properties of a potential protein drug, such as stability, affinity, specificity, solubility, immunogenicity and pharmacokinetic (PK) properties, in order to obtain a variant with the desired characteristics.

Several methods have been developed to obtain optimized protein variants. These can be classified into three main categories: (I) "classical" protein engineering approaches (expert design), (II) molecular or directed evolution methods and, more recently, (III) computational protein design. Classical protein engineering methods or expert design can be defined as hypothesis driven sequence alternations based on structural information and/or information obtained from sequence alignments with a high degree of human intervention[34]. A disadvantage of this approach is that only a relatively small amount of possible sequence changes can be assessed; only a very small part of the total possible "sequence space" is sampled.

Directed evolution methods are being based on the creation of random sequence variation and subsequent selection of improved variants[35]. Several rounds of selection are generally employed and after each round the sequence alterations yielding improved variants can be recombined into a single variant. These methods allow for sampling of a much larger part of sequence space. Error-prone PCR (ep-PCR) mutagenesis is often used for the creation of random (DNA) sequence variation[35]. With epPCR genetic libraries encoding up to ~10^{15} unique variants can practically be created (assuming a 1000 bp gene)[36]. Saturation mutagenesis techniques can be used to create libraries with codons encoding all 20 natural amino-acids at certain site specific positions. Saturation of several sites in one template gene results in a "combinatorial explosion" of library size; a library "saturated" (randomized) at only 9 different codon positions already consists of 5.1×10^{11} unique variants. However, the majority of the introduced sequence variation will be detrimental or neutral for protein function; only a small portion of the variants contain sequence alterations (or mutations) beneficial for protein function. For less complex libraries with sizes up to ~10^6 variants high-throughput screening (HTS) might be used to select out the variants with optimized characteristics, however, for complex libraries with larger sizes such a screening approach is not feasible[37]. In these cases phage, cell or ribosome based display techniques are used to select out the improved variants. These techniques have in common a genotype/phenotype linkage, with the protein variant (phenotype) displayed on the outside of the cell or phage and the gene encoding the variant (genotype) inside the cell or phage. Using a "panning" procedure library members with superior binding

characteristics are selected from the vast pool of non-functional members or members with inferior binding characteristics. In a panning procedure the displayed library is incubated in the presence of immobilized target protein, a subsequent wash removes all the non-bound library members and finally the bound members are eluted from the target protein. Eluted library members are propagated and the panning procedure is generally repeated several times. This results in a gradual enrichment of members with superior binding characteristics. With DNA shuffling methods independent advantageous sequence alterations can be recombined. The amino acid sequence of thus improved members can be determined indirectly by DNA sequencing, taking advantage of the genotype/phenotype linkage[35,37].
Although directed evolution methods are powerful and have been very successful in improving binding or enzymatic properties of various proteins, several potential drawbacks can be noted. The practical obtained library size is often much smaller than the theoretical library size; the practical library size is restricted by physical and biological limitations such as transformation efficiency[38].

More recently, development of computational methods allows for combining rational and mathematical modeling of biophysical (and biological) knowledge in algorithms combining both approaches: computer design steps with *in silico* screening/selection, permitting screening of a much larger sequence space (up to 10^{80}) than is experimentally possible with selection methods or high-throughput screening techniques[39]. The use of structure based computational algorithms in recent years has resulted in impressive results such as several *de novo* design examples, for example the design of a new amino acid sequence able to fold into a predetermined structure[40] to the design of a completely new globular fold and structure[41]. Efficient algorithms are needed to search the vast sequence space and accurate scoring functions are required in order to rank the best designs[39,42]. Structure based computational design algorithms employ usually an inverse protein folding approach, i.e. the algorithm determines which amino acid sequence is most compatible with a protein 3-dimensional backbone structure. A particular 3-dimensional structure will have many sequences compatible with it while any given amino acid sequence only has one compatible 3-dimensional structure. This makes inverse folding more tractable to solve computationally than protein folding problems[39]. The algorithm places discrete conformations (rotamers) of the naturally occurring amino acids at the positions considered for design. After simultaneous optimization of the conformations of the amino acids interacting with the substituted amino acid the energy of the structure is determined, favorable substitutions are retained and unfavorable substitutions are discarded. In many algorithms and depending on the particular design problem, the details of this basic scheme will differ. Due to computational reasons the backbone conformation of the protein structure is often considered as being fixed, a reduced amino acid repertoire can be used or a backbone dependent rotamer library with only the common observed discrete conformational states of amino acids can be employed. However in certain types of design problem it is necessary to increase precision at expense of computational time. In such cases a certain degree of backbone flexibility can be considered or the use of a more continuous amino acid conformational state distribution by use of an expanded rotamer library, e.g. the common amino-acid discrete conformational states are expanded by several standard deviations around their rotatable bonds. The energy functions used to score the

fitness of the designs are based on several approaches such as physical models, statistical analysis, empirically derived functions and many of the successful algorithms use a combination hereof. These functions typically include van der Waals interactions, hydrogen bonding and electrostatic potentials, an implicit solvation term and side chain and backbone entropy terms[43,44]. Depending on the design problem and the particular algorithm, various search algorithms are used to find low-energy solutions to the design problem. There are two general classes of search algorithms; Stochastic methods and deterministic methods[45]. Using stochastic methods, such as Genetic algorithms[46] and Monte Carlo simulated annealing (MC)[47] the outcome is probabilistic. Self consistent mean field optimization[48] and dead end elimination (DEE)[49] are deterministic methods; upon rerunning a simulation these algorithms will produce the same outcome providing that the same parameters are used. Only the DEE algorithm can ensure, upon convergence, that the global minimum energy conformation is found. However, this algorithm can only be applied when the combination of sequence positions that need to be redesigned is relatively small. When DEE does not converge or in larger design problems several simulations using a stochastic method such as MC might be used to sample sequence and conformational space to find low energy solutions. The primary advantage of computational design algorithms is the much larger fraction of the sequence/conformational space that can be sampled in search for an optimal solution when compared with expert design or directed evolution methods. Moreover, these functions are objective and require a lower level of human intervention than both other methods.

In this review we will describe various computational protein engineering methods and their (potential) use in the design of protein therapeutics and other applications in the field of medical biotechnology.

Stability

Protein thermal stability is important for therapeutic proteins, both influencing the pharmacokinetic and pharmacodynamic properties and for stability during production and shelf-life of the final product. Stability issues concerning these latter two points can be addressed by protein formulation technology. However it is also possible to enhance the intrinsic stability of a protein structure by redesigning its amino acid sequence; an often used read out for structural stability is to measure the thermostability of a protein. Several strategies are used to augment the thermal stability of proteins[50,51]. Both rational[52-55] and directed evolution methods[56-58] have been successfully used to improve stability. However, suitable selection/screening procedures are required, which often rely on the susceptibility of partly unfolded proteins to proteases, and the finally improvement in stability is limited to the temperature used in the selection assay were the host (phage, bacteria) is still viable. More recently, both sequence based algorithms and structure based computational design algorithms have been successfully employed to enhance stability of various proteins.

Structure based computational design algorithms have been used for example, to generate a hyper-thermophilic variant of streptococcal Gβ1 domain protein[59], to enhance the stability of the spectrin SH3 domain[60], to completely redesign nine globular proteins[61] and to increase the thermostability of yeast cyosine deaminase[62]. Computational design algorithms

were also proven successful in the improvement of (thermo) stability of therapeutically interesting proteins. Dahiyat and co-workers used their PDA algorithm to design variants with enhanced stability of human granulocyte-colony stimulation factor (hG-CSF)[63] and human growth hormone (hGH)[64]. In order to reduce the risk of an immunogenic response directed against the mutated proteins, only buried and partial buried amino acids in the interior of the protein were amendable for mutation in the design process. Besides immunological reasons, focusing the design on (partial) buried amino acids also had the added advantage that the design process became more straightforward as charge-charge interactions did not have to be taken into account. Using a homology model of hG-CSF, based on a crystal structure of bovine G-CSF, multiple residues in the interior of the protein were changed. The resulting hG-CSF designs, each having 10 to 14 mutations, showed a significant improvement in thermal stability of up to 13 ^{o}C. This increase in thermal stability resulted in improvement of pharmaceutically relevant properties; shelf-lives of these hG-CSF designs were extended between 5 and 10 fold. These designs were biologically active *in vitro* and one of the designs showed a 2-fold increase in bio-availability, after subcutaneous administration. However, after *intra venous* administration this variant showed an enhanced clearance[63]. Employing similar methodology, hGH designs containing 6 to 10 mutations showed improvements in thermal stability of up to 16 ^{o}C[64]. As these and other examples show, modifications ("repacking") of the interior of a protein results often in multiple interdependent amino acid substitutions. To prevent the complete "repacking" of the protein core of the trimeric Tumor necrosis factor-related apoptosis-inducing ligand (TRAIL) and to reduce the amount of required amino acid substitutions, Van der Sloot *et al.,* used a TNF-ligand family alignment to focus the design on non-conserved residues only[65]. Conserved residues are often retained in a family for good reason, such as structural stability (see below). Focusing on non-conserved residues only left the existing stability causing amino acid residue networks intact and, as additional benefit, this approach also reduced the use of computational resources. The automated design algorithms PERLA/FOLD-X were subsequently employed to identify favorable substitutions at those non-conserved residue positions. A TRAIL variant containing only 2 mutations showed an 8 ^{o}C increase in thermal stability and, in an accelerated thermal stability study, retained full biological activity upon incubation for 1 hour at 73 ^{o}C[65].

In addition to structure based computational design approaches also sequence based approaches are used to improve the stability of proteins without explicitly using 3d structural information. Serrano and co-workers used a combination of expert design and the helix/coil transition theory algorithm Agadir, which calculates the helical behavior of monomeric peptides, to stabilize the 4-helix bundle cytokine Interleukin-4 and improve its refolding yield[66]. A sequence based approach was used by Lehmann et al., to construct thermostable phytase variants[67]. It was already known that information extracted from a sequence comparison of homologous proteins could be useful to stabilize proteins[52,68-70], this premise was extended by Lehmann *et al.,* into the "consensus approach"[71]. The consensus approach is based on the hypothesis that in an amino acid sequence alignment of homologous proteins, at any given residue position, the respective consensus amino acid contributes more than average to the stability of the protein than non-consensus amino acids. This was demonstrated for fungal phytases, based on a sequence alignment of several homologous mesophylic phytases, consensus amino acid sequences were calculated for

phytases. These consensus phytases proved to be 15-33 ^{o}C more stable than the parent phytases while retaining enzymatic activity[67,72]. Despite the large improvement in thermo stability of the consensus phytases, a subsequent analysis revealed that, of the 24 residue positions analyzed, only 10 consensus residues contributed positively to the increase in stability, 4 residue showed a neutral contribution to stability and 10 consensus residues had a negative impact on stability[72]. Applying the consensus approach to stabilize fibroblast growth factor 1 (FGF-1) yielded a quadruple mutant variant having its thermostability improved by 7.8 ^{o}C. Upon structural inspection, non-conserved residues in the receptor binding interface or involved in heparin binding were excluded from optimization as were mutations judged to have a detrimental effect on stability[73,74]. Other sequence based approaches make use of machine learning methods. A neural network algorithm was employed to predict stability changes in Staphylococcal nuclease upon mutation[75]. Although no structural data is required in this particular implementation, experimental stability data needs to be available or to be generated in order to train the network and it can only predict stability changes for residue positions it was trained to work with[75]. Two machine learning approaches, using support-vector-machine algorithms, overcome this limitation. These methods do not rely on the availability of external training data sets and works on all positions in the protein sequence. Predicting capabilities of these two algorithms with regard to stability changes upon mutation are almost equally well when only relying on sequence information compared when there is also structural information available[76,77].

Aggregation

Aggregation of proteins and peptides into insoluble deposits constitutes a serious problem during production, storage and administration of (potential) protein therapeutics[78]. It results in a decrease in activity of the drug formulation and it can induce immune responses, which can result in resistance to the drug by antibody mediated clearance or in allergic responses[79]. Two algorithms have recently been developed that are able to predict the aggregation propensity of a given sequence irrespectively of the morphology (amyloid, non-amyloid) of the aggregated product; the Zyggregator algorithm developed by Dobson and co-workers[80,81] and the statistical mechanics algorithm TANGO algorithm by Serrano and co-workers[82]. Recently, aggregation resistant variants of human calcitonin (hCT) were designed using the Zyggregator algorithm[83]. The 32 residue peptide hormone hCT shows an extremely high tendency to self aggregate thereby limiting its clinical potential. Salmon CT (sCT) has a much lower tendency to aggregate and is therefore the clinically preferred agent. However, the sequence identity between sCT and hCT is only 50% and immunogenic responses could cause antibody related secondary resistance in long term treatment with sCT[84]. More than 600 sequence variants of hCT were evaluated *in silico* for their aggregation propensity and three of these sequences were selected for experimental validation. All three variants had a sequence identity of more than 80% with hCT and showed a much decreased tendency to aggregate while the physiological activity of the variants was improved when compared to both sCT and hCT[83].

Receptor binding specificity and affinity

Increasing the affinity for a target receptor or reducing receptor binding promiscuity of a protein with therapeutic potential can have beneficial implications for its use as a therapeutic agent. A higher affinity for a particular target receptor can result in increased physiological activity and use of the therapeutic agent at a lower dose. Reducing receptor binding promiscuity by preventing interactions with non-target receptors can limit undesirable physiological activities and reduce side-effects.

In recent years, computational design has successfully been employed in the redesign of affinity and specificity of a wide variety of protein-protein interactions, previously this was the realm of phage display and related techniques. Some of the first proofs of concept are for example; Reina *et al.,* applied the PERLA algorithm in redesigning the specificity of the protein-protein interactions of PDZ domains, resulting in the recognition of novel target sequences by the designed PDZ domains [85]. Coiled-Coil interfaces were designed by Havranek and Harbury which direct the formation of either homodimers or heterodimers[86]. The substrate specificity of calmodulin towards smooth muscle myosin light chain kinase was improved by Shifman and Mayo using their ORBITAL algorithm[87,88]. Kortemme *et al.,* used the Rosetta algorithm to design new colicin E7 DNase/Im7 inhibitor protein pairs[89]. In addition, analogous to experimental alanine-scanning mutagenesis[90], computational alanine-scanning can be employed to analyze important interactions in protein-protein interfaces[91-93]. Although details differ, the strategy for improving affinity or binding specificity of a protein with one of its binding partners is not that different from the ones used to design more stable proteins using the structure based computational design algorithms. However, instead of finding a sequence compatible with the structure of the parent but with a lower energy, a sequence is obtained that is compatible with the structure of the parent in *complex* with its binding partner and having a lower energy when it is in complex with the binding partner. When improving only the affinity of a certain protein-protein interaction such a stabilization of a desired interaction is sufficient, this is also known as a positive design strategy. On the other hand, in order to improve the specificity of an interaction one would ideally optimize the interaction with the target binding partner but also make interactions with any non-target partner less favorable. In addition to a positive design strategy a negative design strategy can then be used[86]. Using a negative design strategy, interactions with any competing non-target binding partners are destabilized. For closely related target binding partners and competing non-target binding partners the use of a negative design strategy was found to be essential in attaining binding specificity[86,94]. Focusing only on improving the charge complementary between patches of charged residues of a pair of interacting proteins can also be used to improve the affinity between two interacting partners, instead of optimizing all the interactions in the binding interface between two partners. Schreiber and co-workers improved the Coulombic complementary of the β-lactamase inhibitor protein BLIP for TEM-1 β-lactamase, their electrostatic optimization algorithm PARE predicted amino acid substitutions in the vicinity of—but not in—the TEM-1 binding surface of BLIP with enhanced complementary to the BLIP binding area of TEM-1. Because of this enhanced electrostatic complementary, the BLIP mutants showed a 250-fold enhanced rate of association (k_{on}) upon complex formation with TEM-1 while the dissociation rate constant (k_{off}) was unchanged. This

improvement in k_{on} resulted in an improved affinity constant K_D because of the relationship $K_D = k_{off} / k_{on}$ (for a 1:1 interaction)[95]. This work, and one using similar methodology to design Ral mutants which bind faster and tighter to Ras[96], show that not only the direct contact interface might be targeted to improve an interaction but also surface patches in the vicinity but outside the actual interface might be targeted to improve affinity. This electrostatic optimization approach has the advantage that it requires a less detailed knowledge of the short range interactions (h-bonds, salt-bridges, hydrophobic and van der Waals interactions) governing the interaction between two proteins although it does not use the available possibilities in the interaction interface itself to stabilize the interaction as it is not able to decrease the k_{off} in a predictable manner.

Structure based computational design algorithms have already been used to improve the affinity and/or receptor binding specificity of several proteins in order to create promising novel protein therapeutic agents. Antibody (Ab) based protein therapeutics are currently the most widely used format of biopharmaceuticals. Apart from improving the affinity of an antibody for its antigen any further for therapeutic reasons, it is usually also required for antibodies after humanization as the CDR-grafting process generally reduces the antigen binding affinity. Clark *et al.,* used several computational protein design approaches to improve the affinity of an antibody fragment to the I-domain of the integrin VLA-1[97]. The affinity could be improved by an order of magnitude, despite the moderate resolution (2.8 Å) of starting crystal structure of template antibody in complex with VLA-1 and the already reasonable high affinity (7 nM). Employing two different methodologies, e.g. fixed backbone side-chain repacking using the Dezymer algorithm and an electrostatic optimization method, yielded 9 mutants with improved affinity out of 40 mutants total. Although most of the individual mutations contributed <1 kcal/mol, subsequent combination of four of the higher affinity mutations yielded a ~10 fold improvement in affinity. Use of a side chain repacking protocol incorporating backbone flexibility only yielded one mutant with improved affinity[97]. An electrostatic optimization method was used by Marvin and Lowman to enhance the rate of association (k_{on}) of an Ab directed against VEGF 6-fold which resulted in a 2.5 fold improvement in affinity at physiological ionic strength[98].
The therapeutic efficacy of Abs is not only determined by the affinity for its antigen but also with its ability to trigger (immune) effector activity. The complement-dependent cytotoxicity (CDC) is determined by interactions between the IgGs Fc domain and hinge region with C1qs. Interaction of the IgG Fc domain with receptors of Fcγ family (FcγRs) cause different effector functions, such as Ab-dependent cell-mediated phagocytosis (ADCP) and Ab-dependent cell-mediated cytotoxicity (ADCC). Depending on the interaction with the specific type of FcγR, an effector activating response (FcγRI, FcγRIIa/c and FcγRIIIa) or an inhibitory (FcγRIIb) response is obtained. Furthermore, also the pharmacokinetics (plasma half-life) of IgG type Abs is governed by the interaction of the Fc domain with the FcγRn type of receptor. Engineering Fc domains of antibodies in order to modulate binding to C1qs and FcγRs might therefore improve the clinical efficacy of Abs. For example, it has been demonstrated that activation FcγR receptors are necessary for the effect of ritximab and trastuzumab and that inhibitory FcγRIIb receptor have a detrimental effect on the efficacy of these Abs[99]. To address this issue, Dahiyat and co-workers engineered the antibody Fc domain to obtain a set of Fc domains with enhanced

effector function due to improved affinity and specificity for activation receptors. Using the crystal structure of the Fc/FcγRIIIb and homology models of other complexes, interactions between the Fc domain and the activating receptors were directly optimized or library combining "directed diversity" and "quality diversity" was generated. This library contained sequences consisting of variants enriched for stability and solubility. Variants having the desired receptor binding properties were finally selected using a semi-automated *in vitro* screen receptor binding assay. The antibodies having an engineered Fc domain showed >100 fold improvement in *in vitro* effector function and enhanced cytotoxicity in an *in vivo* preclinical macaque model. Moreover, these variants bound also tighter to both the high affinity Val158 allelic form of the FγRIIIa activating receptor and the more common but less responsive low affinity Phe158 allelic form[100].

In addition to have been used in optimizing the therapeutic potential of antibody based therapeutics, structure based computational design methods have also been employed in optimizing binding specificity and affinity of several non-antibody protein molecules. Springer and co-workers designed Intercellular adhesion molecule-1 (ICAM-1) variants with increased affinity for its receptor integrin lymphocyte function-associated antigen-1 (LFA-1). The interaction between ICAM-1 and LFA-1 is critical for immunological and inflammatory reactions and inhibiting this interaction can be beneficial in autoimmune disease and allograft rejection[101,102]. Soluble ICAM-1 could be used as a competitive antagonist, blocking the binding of endogenous membrane bound ICAM-1 to LFA-1. The affinity between ICAM-1 and LFA-1 is relatively low (185 nM) enhancing the affinity of soluble ICAM-1 with its target receptor is therefore essential for therapeutic applications. Using a combination of expert design, design algorithms (PDA/SPA and Rosetta) and a low throughput *in vitro* empirical screen, Springer and co-workers succeeded in generating ICAM-1 variants with twenty fold enhanced affinity for LFA-1, in spite of the low resolution crystal structure of ICAM-1/LFA-1 (3.3Å). The design algorithms were most successful in predicting non-polar and aromatic stabilizing mutations in the interaction interface and less successful in predicting favorable electrostatic interactions or in optimizations of the hydrogen bond network. Furthermore, predictions of the two design algorithms were complementary as some of the predicted mutations were not suggested by the other algorithm[103]. Molecules that inhibit tumor necrosis factor-alpha (TNF-α) signaling have demonstrated clinical efficacy. The currently used molecules are antibodies or soluble TNF receptors which sequester TNF-α. Steed *et al.,* used the PDA algorithm to design dominant negative TNF-alpha (DN-TNF) variants that prevent formation of active TNF-α trimers[104]. These DN-TNF variants were designed to show a significantly reduced binding to the TNF-R1 and TNF-R2 receptors. In the presence of endogenous TNF-α the subunits exchange and TNF-α/DN-TNF heterotrimers are formed, which are unable to transduce signals, and consequently, is inhibited. Using crystal structures of TNF-α and a TNF-α variant as templates, a total of 151 variants were designed and tested. By applying an *in silico* screen, only non-immunogenic amino acid substitutions were selected and considered for testing. Empirical validation showed both *in vitro* and *in vivo* a large reduction in TNF-α mediated effects[104]. One of these DN-TNF variants will become the first example of a protein therapeutic designed by computational design algorithm to enter in a phase-1 clinical trial end of 2006. Another member of the TNF ligand family, tumor necrosis factor-related apoptosis-inducing ligand (TRAIL), draws a lot of interest as a potential anticancer drug that selectively induces apoptosis in a variety of cancer cells[105,106]. TRAIL induces

apoptosis by interacting with death receptors DR4 and DR5. TRAIL can also bind to decoy receptors (DcR1, DcR2 and OPG) that cannot induce apoptosis. Use of TRAIL receptor-selective variants could permit a more tumor-specific therapy through escape from decoy receptor-mediated antagonism. Moreover, irradiation appears to specifically up-regulate DR5 receptor expression and the combination of irradiation and TRAIL treatment has been demonstrated to have an additive or synergistic effect[107]. Using a crystal structure of the TRAIL/DR5 complex and homology models of TRAIL in complex with the other receptors, van der Sloot *et al.,* designed DR5 selective TRAIL variants employing the FOLD-X protein design algorithm[108]. Both positive design (improved affinity for DR5) and negative design (decreased binding to DR4, DcR1 and DcR2) was used. To prevent the complete redesign of the receptor binding interface, which would increase the chance of introducing immunogenic epitopes, only single amino acid substitutions were considered in the initial design, subsequently double substitution variants sufficiently separated in the structure were generated by combining single substitution variants. An *in vitro* surface plasmon resonance based receptor binding screening assay was used to select the variants with the most favorable DR5 specificity characteristics. *In vitro* receptor binding assays and biological activity assays demonstrated that the designed DR5 variants showed indeed an increase in affinity and a much improved specificity for the DR5 receptor, a double mutant variant was not capable of binding to the DR4 receptor at all[108]. Interestingly, Kelley *et al.,* used phage display to generate DR4 and DR5 selective TRAIL variants. Their best DR5 selective variant contained six amino acid substitutions. After a partial dissection to determine the role of each individual mutation in selectivity of the phage display variants, Kelley *et al.,* concluded that it was not possible to eliminate any mutation without compromising selectivity and/or losing biological activity[109]. The phage display approach did not identify any of the selectivity causing mutations as determined with the computational design approach. These last two studies demonstrate the power of the use of computational design algorithms and show that both computational design algorithms and directed evolution methods can be complementary.

Not only protein-protein interactions are subjected to design. Interactions involving proteins with small molecule receptor functionality, enzyme-substrate and protein-nucleic acid interactions have been modified—or created—using computational design approaches[110]. Proteins having novel ligand binding properties or catalytic properties can for example be used in diagnostics, drug delivery devices, as biosensors, in molecular therapeutics, as components in nanotechnology or as devices in synthetic biology or in systems biology. For gene therapy applications, DNA binding proteins can be designed into new transcription factors able to trigger the activation of specific genes or the design of site specific endonucleases stimulating gene targeting and promoting the repair of disease associated genes by gene specific homologous recombination[111]. The targeting and repair of specific genes was recently demonstrated using site-specific zinc finger nucleases, indiscriminate nuclease domains coupled to a site specific zinc finger[112-115]. Catalytic efficacy might be improved by incorporating the DNA binding and nuclease functionality in one structural unit. Chevalier *et al.,* designed an artificial and highly specific homing endonuclease by fusing domains of I-*Dmo*I and I-*Cre*I and subsequently using computational design in combination with an in vivo protein folding screen to engineer a new interface between these (protein) domains. The new enzyme bound specifically to long chimeric DNA

sequence with nanomolar affinity and the cleaving rate was similar to the parent enzymes[116]. Continuing on this, Ashworth *et al.,* redesigned the DNA binding and cleavage specificity of the homing endonuclease I-*Mso*I directly. In order to redesign the cleavage specificity, an *in silico* screen was performed to search for base-pair changes predicted to disrupt binding of the parent enzyme. This was followed by redesign of amino acids in the vicinity of the substituted base in order to accommodate and stabilize the new base-pair. Experimental characterization show that the redesigned enzyme binds and cleaves the redesigned recognition site approximately 10.000 times more effectively than the wild-type enzyme[117].

Considerable advances have also been made in the design of metal-ion binding sites and small molecule ligand binding sites in proteins. Hellinga and co-workers introduced a zinc binding site in maltose binding protein (MBP), a member of the periplasmic binding protein (PBP) superfamily. Amino acid residues interacting directly with metal according to a predefined geometry, the primary coordination sphere (PCS), were introduced using the Dezymer algorithm[118]. However, surrounding residues interacting with the PCS make also important contributions to metal affinity. Residues in this second coordination sphere (SCS) were optimized after the introduction of a zinc PCS in ribose binding protein, another member of PBP superfamily. Zinc binding RBPs with an optimized SCS, in comparison with RBPs having only a zinc binding PCS, had a significantly improved affinity for zinc (K_d 1-2 μM) and improved thermostability. These zinc binding RBPs were subsequently used to control *in vivo* gene expression in *E. coli* by coupling the zinc binding RBP to a synthetic signal transduction pathway. In response to Zn^{2+}, β-galactosidase reporter gene expression response showed a 6-10 fold increase[119]**.** Similar methodology was used to construct a calcium binding site PCS with high coordination number (seven) in the N-terminal domain of the cell surface adhesion receptor CD2[120]. Degrado and co-workers used computational design to construct a four-helix bundle protein de novo capable of selectively binding a non-biological metalloporphyrin cofactor[121].

Members of the *E. coli* periplasmic binding protein (PBP) superfamily comprising novel ligand binding properties were designed by Hellinga and co-workers. Trinitrotoluene (TNT), l-lactate or serotonin bindingsites were engineered in the PBPs in place of the wild-type sugar or amino acid ligands. Starting from high resolution crystal structures of the PBSs, the algorithm identified amino acid sequences forming a complementary surface with the novel ligand. The method combined a docking procedure with amino acid mutations in the vicinity of the binding site. The combinatorial problem (10^{53}-10^{76} choices) was solved with an algorithm based on dead-end elimination theorems, the resulting designs contained 12-18 mutations. Affinities of top scoring designs for the respective ligands were experimentally determined; PBPs for TNT, l-lactate or serotonin were obtained having affinities in the low micro-molar range (<5 μM) one particular TNT-binding PBP did even have an affinity for TNT in the low nanomolar range (2 nM). For creating the high affinity interactions fine grained sampling using a highly expanded rotamer library was required. Subsequent incorporation of a TNT and a l-lactate binding PBP into a bacterial synthetic signal transduction pathway allowed *E. coli* to respond with gene expression in the presence of extracellular TNT or l-lactate[122]. Using similar

methodology, a biosensor for the organophosphate surrogate of the nerve agent Soman was designed[123].

The next challenge after the engineering of novel ligand-binding sites, the design of enzymatic activity, requires not only providing stabilizing interactions between protein and ligand for a single state of the ligand but for all the intermediate (transition) states along the reaction coordinate. Moreover, amino acid residues and co-factors have to be precisely positioned and the binding surface has to be stereochemically complementary to all the intermediate states. The binding surface needs also to adapt to the different requirements of the various stages of catalysis (substrate binding, catalysis and product release)[124,125]. Not surprisingly, design of catalytic activity presents a formidable challenge and is testing the current understanding of the mechanics and forces governing enzyme catalysis.

Bolon and Mayo used their Orbital algorithm to create novel enzymatic functionality—*p*-nitrophenyl acetate hydrolysis—using the catalytically inert *E. coli* thioredoxin as a scaffold. The designed enzyme exhibited a 25-fold rate enhancement over the uncatalyzed reaction[126]. Kaplan and Degrado designed *de novo* a catalytic scaffold capable of catalyzing the two-electron oxidation of 4-aminophenol to the corresponding quinone monoimine by using a diiron cofactor. The four-helix bundle was designed using computational design while the catalytic activity was introduced by expert design[127]. Hellinga and co-workers designed the catalytically inert bacterial ribose-binding protein (RBP) into analogs of the glycolytic triose phosphate isomerase enzyme using the Dezymer algorithm. The design process consisted of three parts. First, a geometrical definition of constraints governing key interactions with catalytic residues (His, Gln, Lys) was defined. Secondly, positions were identified were substrate and catalytic residues simultaneously satisfied the constraints using a combinatorial search algorithm. Third, the complementary surface around the substrate was generated using the receptor design algorithm. The resulting designs contained 18 to 22 mutations and exhibited 10^5- to 10^6-fold rate enhancements over the uncatalyzed reaction[128]. Although these rate enhancements are still a factor 100 below that of the natural occurring TIM enzyme, the designed enzyme was able to sustain growth in an *E. coli* TIM knockout strain. This methodology will allow the design of enzymatic reactions and, eventually, metabolic pathways not seen in nature and can for example be used in the "bio"synthesis of pharmaceuticals.

Pharmacokinetics and immunogenicity.

Pharmacokinetics is a critical factor in the efficacy of protein therapeutics. Most protein drugs are delivered by injection and the *in vivo* half-lives vary from minutes to days. Elimination and disposition mechanisms of protein drugs differ considerably from those of small-molecule drugs. Elimination is governed by several specific and non-specific events, such as; renal clearance (depending on size and charge), specific and aspecific proteolysis, receptor-mediated clearance or antibody mediated mechanisms in addition to structural stability and solubility of the protein[129,130]. Susceptibility to proteolysis can be attenuated by removing protease recognition sites. Pegylation or engineering of additional glycosylation sites in protein drugs can reduce renal clearance and improve plasma half-life. A substantial part of a cytokine protein drug can also be cleared due to interaction with (one of) its target receptors. Due to the generally high affinity constants—with low off-rates—of protein drugs with its target receptor in combination with the relatively large fraction of the drug

bound to the target receptor, are the pharmacokinetic properties of the protein drug also closely coupled to the turnover of the target receptor. For example, protein therapeutics bound to their target receptor can be internalized and degraded inside the cell or the protein drug can be subjected to phagocytosis. In order to engineer a G-CSF with a longer half-life, Lauffenburger and co-workers addressed the issue of receptor mediated endocytosis of G-CSF[131]. Their method suggests being broadly applicable to enhance the PK/PD properties of protein therapeutics. G-CSF is rapidly depleted from the bloodstream by neutrophils expressing the G-CSF receptor (G-CSFR). A computational design approach was used to design histidine (His) substitution variants of G-CSF. The introduced histidines should function as a pH activated switch; at neutral pH these variants should retain high binding affinity towards the G-CSFR (neutral His) but upon internalization of the G-CSF/G-CSFR complex the complex should dissociate due to the acidic pH in the endosomal compartment (positively charged His). Based on a crystal structure of G-CSF in complex with G-CSFR favorable candidate sites in the receptor interface for substitution with His were identified. After *in silico* mutagenesis to neutral His and positively charged His the electrostatic free binding energy of the mutant complexes was calculated in both cases. Mutants calculated to have a similar affinity for C-GSFR as wild-type at neutral pH but a reduced affinity for the C-GSFR at acidic pH were selected for experimental validation. Despite the fact that two predicted Asp to His substitution variants had a slightly decreased or unchanged affinity for the C-GSFR at neutral pH, these variants were shown to have an order of magnitude increase in (medium) half-life along with an enhanced potency due to enhanced endocytic recycling[131]. Antibodies directed against the protein drug or soluble variants of the target receptor (or closely related receptors), so called "decoy" receptors, can sequester a substantial fraction of the available drug and thereby reducing the drugs efficacy. Antibody mediated antagonism can be alleviated by reducing the proteins immunogencity and/or increasing its thermostability and/or reducing aggregation propensity (see above). Van der Sloot *et al.,* used a computational design strategy to reduce the affinity of TRAIL for its decoy receptors (see above)[108].

Immunogenicity of biopharmaceuticals is both associated with safety and efficacy concerns[79,132,133]. Neutralizing antibodies directed against the biopharmaceutical can cause loss of efficacy and failure of the therapy[134]. In some cases neutralizing antibodies are not only directed to the protein therapeutic but also cross reacting with the native counterpart. This was for example demonstrated in patients treated with a particular recombinant erythropoietin product (Eprex J&J); in this case patients developed antibodies against both the recombinant product and the native product which resulted in pure red cell anaplasia[135,136]. One of the major determinants of eliciting an immunogenic response is the amino acid sequence of a protein. The degree of sequence divergence from the human amino acid sequence determines the immunogenic response proteins elicit. However, also proteins similar in amino acid sequence as the native counterpart can illicit an immunogenic response and, in contrast, proteins that differ in sequence from the native counter do not have to induce an (considerable) immunogenic response (e.g. consensus IFN-α and methionyl hGH)[79]. Physicochemical factors are another important determent; aggregated or partly unfolded proteins can induce an immunogenic response as can oxidation or deamidation of amino acid residues. Other factors connected to the induction of immunogenic responses, but not further discussed here are for example: deglycosylation,

the production host, production impurities, formulation and storage, route of administration and dose and length of treatment[79]. Physicochemical factors can be addressed applying computational design methods as discussed above, structural stability and solubility can be improved and the tendency to aggregate can be reduced. Residues prone to oxidation or deamidation can be substituted with another amino acid without sacrificing structural stability and functionality. Pegylation or glycosylation can also be used to improve the solubility of a protein, in addition, both pegylation and glycosylation are thought to shield hydrophobic immunogenic epitopes at the surface of the protein. Several algorithms are available that scan amino acid sequences for MHC I or II binding epitopes, this information can subsequently be used to de-immunize a potential protein therapeutic. Reviewed in[137-139]. Immuno dominant epitopes can be removed using a structure based algorithm, this allows the removal of such an epitope without sacrificing structural stability or functionality.

Library design, screening and selection

Although the number of sequences that can be screened or, especially, selected appears to be enormous, it is even for a small protein only a tiny fraction of the potential sequence space that can be sampled. Moreover, only a fraction of the library created by traditional means (ep-pcr, saturation mutagenesis) is compatible with a viable protein structure. Computational design in combination with *in silico* screening allows sampling of a much larger fraction of the total sequence space (~10^{60} sequences)[140-142]. Therefore computational design allows for the creation of high quality libraries, only targeting sequence positions that can be changed without compromising structural integrity of the protein. These *in silico* screened libraries can therefore contain an increased diversity of *viable* structures which can result in obtaining more sequences with the desired property as well as being more improved for the desired property. Voigt *et al.,* used a structure based computational method applying mean-field theory to probe each residue's structural tolerance. This tolerance is defined by the residue's local sequence entropy, e.g. the number of amino acids that are permitted at that site. Mutations casing increase in stability or activity are most likely to accumulate at sites having high sequence entropy. Therefore, libraries focusing on positions most likely to lead to improvement of desired properties can be constructed[140]. *In vitro* recombination libraries can also be optimized using computational tools. The SCHEMA algorithm identifies fragments that can be recombined without disturbing the structural integrity of a protein. Libraries with targeted crossover points can be generated in order to increase the fraction of folded and functional variants[143]. This was recently demonstrated by Arnold and coworkers applying the SCHEMA algorithm to create an artificial family of Cytochromes P450[144]. The IPRO computational procedure allows for the one step optimization of the entire library by identifying mutations in the parent sequences which upon propagation in the combinatorial library systematically optimize the desired properties of offspring sequences[145].

The value of designing a quality enriched library was demonstrated by selecting a library of TEM-1 β-lactamase variants for improved resistance to the antibiotic cefotaxime. Starting from the TEM-1 β-lactamase crystal structure residues within 5 Å of the active site residues were considered for the library construction. This resulted in 7 x 10^{23} sequences, a number that can be easily screened *in silico*, but not experimentally. The PDA algorithm was used in combination with Monte Carlo simulated annealing to calculate a rank ordered list of the

1000 lowest energy sequences and amino acid occurrences were subsequently counted for all the variable positions. In case an amino acid had a greater than 10% probability of occurrence at a position it was included in the library, this resulted in library with a diversity of 172000 unique sequences. After just one round of selection with this library, variants were obtained showing an almost 1300 fold increase in cefotaxime resistance and all the resistance causing mutations identified from this library were not identified before in directed evolution experiments or in naturally occurring TEM-1 β-lactamase variants[146].

Concluding remarks and Future directions

The use of computational methods in the (re)design of various properties of proteins has made an impressive progress in recent years. Several of the described methodologies are already being applied in the development of protein therapeutics or will be used in the near future. The thermostability and structural stability of a protein can be effectively enhanced by applying both structure based computational design methods or sequence based methods with a high rate of success. Sequence based algorithms and structural based computational design algorithms can also be interfaced, for example a sequence based algorithm can be used to scan the protein sequence for immuno-dominant epitopes or aggregation prone regions followed by a structural based algorithm finding an optimal solution to remove these sequence motives without sacrificing structural stability and activity. Both structure based methods which optimize all relevant interactions and structure based methods which only focus on improving the electrostatic complementary of protein-protein interactions have been successfully applied in improving affinity or engineering the specificity of protein-protein interactions. In these cases the design process is frequently combined with a small screening assay to remove any false positives due to usually greater complexity of redesigning protein-protein interactions when compared to improving the stability of a single protein. Although the examples of design of affinity and specificity of protein-nucleic acid or protein small molecule interactions and the design of novel enzymatic activity are yet relatively sparse, in coming years more examples, in areas such as medical biotechnology, will undoubtly follow. The combination of computational design methods in combination with the design of libraries and high-throughput screening or selection methods also holds great promise, providing higher quality libraries with increased diversity in properly folded and functional members.

Despite the progress made, several challenges remain to be addressed. Structure based algorithms require 3d structural information, in general the rule is that a higher resolution of the design target's (crystal) structure yields a more reliable design outcome. Notwithstanding this requirement, several design exercises described in this review successfully relied (partly) on low resolution structural models or homology models as template structure. Normally, in such cases one could use multiple sequence alignment information to guide the design process and screen several of predicted sequences experimentally to increase the success rate and to remove false positives[147]. Structural genomics initiatives will make an increasing proportion of the protein sequence space amendable to design by structure based computational design algorithms either by directly using an experimentally determined structure or providing structural templates to build reliable homology models[148]. Recent progress in *de novo* protein structure prediction, using

structure based computational design algorithms, could in the future also contribute to make an even larger proportion of the sequence space amendable to structure based design[149]. Protein design algorithms, in addition, are continuously improved as well. The development of more accurate energy functions used to evaluate the designs requires improvement in variety of factors, such as, backbone flexibility, (surface) electrostatics, hydrogen bonding potentials, solvent (water) mediated interactions and the statistical terms describing entropy[150-152]. Expanding the design algorithms with parameterization for various non-natural amino acids, as for example developed by Schultz and co-workers[153], will allow the design of protein sequences possessing entirely new chemical functionality and reactivity. Improvements in search- and sampling optimization algorithms will allow finding low energy solutions more efficiently by covering a larger fraction of sequence- and conformational space in a reduced amount of time[154]. Improvements in statistical analysis of multiple sequence alignments will allow sequence based algorithms to extract higher order information encoded in these alignments. For example statistical coupling analysis was used to construct artifical WW domain sequences able to fold into a native structure[155]. These improvements in protein design algorithms will favor both future protein design and *de novo* structure prediction.

The examples discussed in this review show that protein design algorithms have matured enough to be a valuable addition to the protein engineers' toolbox, in addition to expert design and directed evolution methods. Application of current protein design methodology and future developments will allow development of novel medical biotechnology applications. Furthermore it permits the design of protein therapeutics with enhanced clinical efficacy by optimizing their amino acid sequences for various clinical important properties such as potency, specificity, immunogenicity and pharmacokinetics. By addressing these clinical properties of biopharmaceuticals early on in drug discovery and development as well as the optimization of its production properties, these computational methods will allow a faster transition from laboratory bench to clinic.

3

Stabilization of TRAIL, an all β-sheet multimeric protein, using computational redesign.

Almer M. van der Sloot, Margaret M. Mullally, Gregorio Fernandez-Ballester, Luis Serrano and Wim J. Quax

Protein Eng. Des. Sel. (2004) 17:673-680

Abstract

Protein thermal stability is important for therapeutic proteins, both influencing the pharmacokinetic and pharmacodynamic properties and for stability during production and shelf-life of the final product. In this study we show the redesign of a therapeutically interesting trimeric all beta-sheet protein, the cytokine TRAIL, yielding variants with improved thermal stability. A combination of TNF ligand family alignment information and the computational design algorithm, PERLA, were used to propose several mutants with improved thermal stability. The design was focused on non-conserved residues only, thus reducing use of computational resources. Several of the proposed mutants showed a significant increase in thermal stability as experimentally monitored by far-UV CD thermal denaturation. Stabilization of the biologically active trimer was achieved by monomer subunit or monomer-monomer interface modifications. A double mutant showed an increase in apparent T_m of 8 ^oC in comparison to rhTRAIL WT and remained biologically active after incubation at 73 ^oC for 1h. To our knowledge, this is the first study that improves the stability of a large multimeric β-sheet protein structure by computational redesign. A similar approach can be used to alter the characteristics of other multimeric proteins, including other TNF ligand family members.

Introduction

Besides influencing the final pharmacokinetic and pharmacodynamic properties of a protein therapeutic, stability is also important throughout the production process and for the shelf-life of the final product[156]. Several strategies are used to augment the thermal stability of proteins[50,51]. Both rational[52-55] and directed evolution methods[56-58] have been successfully used to improve stability. A disadvantage of a rational approach is that one can design only a limited number of potentially improved variants. In contrast, directed evolution methods allow large numbers of variants to be generated and screened. However, suitable selection/screening procedures are required, which are often not available or are very labour intensive. More recently, computational redesign algorithms have been employed to enhance stability, amongst other properties, of proteins[59-61,157]. These methods combine computer design steps with *in silico* screening, permitting screening of a much larger sequence space than is experimentally possible with high-throughput techniques. Efficient algorithms are needed to search the vast sequence space and accurate scoring functions are required in order to rank the best designs[39,42]. Recently, computational redesign has been used to generate a hyper-thermophilic variant of streptococcal Gβ1 domain protein[59], to enhance the stability of the spectrin SH3 domain[60] and to improve the (thermal) stability of the therapeutically interesting four helix bundle cytokines, granulocyte-colony stimulation factor (G-CSF)[63] and human growth hormone (hGH)[64].

In this study, we use the automated computer algorithm PERLA[158,159] and the empirical forcefield FOLD-X[160] to improve the thermal stability of a multimeric all β-sheet protein, tumor necrosis factor-related apoptosis inducing ligand (TRAIL; TNFSF10)[161,162]. TRAIL is a member of the tumor necrosis factor ligand family. Ligands belonging to this family are involved in a wide range of biological activities, ranging from cell proliferation to apoptosis, and they share similar structural characteristics. All monomeric subunits of these ligands consist of antiparallel β-sheets, organized in a jellyroll topology, and these subunits self associate in bell-shaped homotrimers, the bioactive form of the ligand. Sequence homology is highest between the aromatic residues responsible for trimer formation. A trimer binds three subunits of a cognate receptor, each receptor subunit binding in the grooves between two adjacent monomer subunits. The ligands are type II transmembrane proteins, but the extracellular domain of some members can be proteolytically cleaved from the cell surface, yielding a bioactive soluble form of the ligand. Recent reviews of the TNF ligand-family are readily available[1,2].

TRAIL in its soluble form selectively induces apoptosis in tumor cells *in vitro* and *in vivo*, by a death receptor mediated process[19]. Unlike other apoptosis-inducing TNF family members, it appears to be inactive against normal healthy tissue, therefore attracting great interest as a potential cancer therapeutic[13]. Several crystal structures of TRAIL[17,163] and TRAIL in complex with the death receptor 5 (DR5)[12,16,18] are available. Unlike other TNF family members TRAIL has a zinc binding site in its trimeric core and the presence of the zinc ion is known to be vital for the trimeric structure and bioactivity[17,164]. Several versions of recombinant soluble TRAIL with different N-terminal fusions tags have been reported, however these versions appear to have different bioactivity profiles in comparison to the

non-tagged 'wild-type' soluble TRAIL encoding amino acids 114-281[105]. The increased *in vitro* toxicity towards certain normal healthy cells is especially noticeable in the presence of exogenous tags[14]. We therefore chose to increase the stability of TRAIL by modification of the soluble ligand version (114-281), without addition of any exogenous tags. In view of a possible use as a therapeutic protein; a close resemblance to the wild-type structure is desirable. To our knowledge, this is the first study that shows improvement of the stability of a large multimeric protein structure by computational redesign. Methods used in this study are also applicable to other TNF family ligands.

Results

Computer screening.
Novel mutants of TRAIL have been designed in order to increase the stability of the bioactive trimer. Predictions were based on the automated computer algorithm, PERLA[158,165], as described in the methods section. Briefly, the program performs strict inverse folding: a fixed backbone structure is decorated with amino acid side chains from a rotamer library. Relaxation of strain in the protein structure is achieved via the generation of subrotamers. Most terms of the scoring function are balanced with respect to a reference state, to simulate the denatured protein. The side chain conformers are all weighted using the mean-field theory and finally candidate sequences with modelled structures (PDB coordinates) are produced. Energy evaluation of the modelled structures was carried-out by a modified version of FOLD-X[150,160], available at (http://fold-x.embl-heidelberg.de). The force field module evaluates the properties of the structure, such as its atomic contact map, the accessibility of its atoms and residues, the backbone dihedral angles, in addition to the H-bond network and electrostatic network of the protein. The contribution of water molecules making two or more H-bonds with the protein is also taken into account. The algorithm then proceeds to calculate all force field components: polar and hydrophobic solvation energies, van der Waals' interactions, van der Waals clashes', H-bond energies, electrostatics, and backbone and side chain entropies.

Selection of the template sequence
The template selected was 1DU3[12]. The crystal structure at 2.2 Å resolution contains the trimeric structure of human TRAIL in complex with the ectodomain of the DR5 receptor. The TRAIL monomer lacks an external, flexible loop (130-146), not involved in receptor binding or in monomer-monomer interaction. To complete the molecule, this loop was modeled using the structure of 1D4V (2.2 Å)[18], a monomeric TRAIL in complex with DR-5 receptor, having the atomic coordinates of the loop. Finally, the TRAIL molecule was isolated by removing the receptor molecules from the PDB file.

Computational design of mutants
The visual inspection of the isolated monomers, monomer-monomer interface and central core of TRAIL showed several residues as potential candidates for mutagenesis. The highly conserved hydrophobic residues were discarded from this list. After generating the mutants we identified if there were residues involved in receptor binding. These residues in principle could not be mutated without disrupting interactions with the receptor. However, it could be that a small decrease in binding affinity could be compensated by an increase in

stability. Thus one TRAIL variant (M2), that showed a significant predicted increase in stability but also contained residues involved in receptor interaction, was retained for subsequent experimental analysis.

Table 1. Residues initially considered for design

Monomer Set	**Dimer Set**	**Trimer Set**	**Misc. Set**
E194†	H125	R227†	A123
I196†	F163	C230	A272
	Y185	Y240	S225†
	Q187		V280
	S232		F163
	D234		A123
	Y237† (D203,Q205)		V208
	L239		
	S241		
	E271†		
	F274		

† Used in subsequent rounds of design

Mutants in parenthesis were added in subsequent rounds as interaction partners

The sequence space search for every position was simplified by checking the naturally occurring amino acids in a multiple sequence alignment of proteins belonging to the TNF ligand family, thus decreasing the computing time, and subsequently focusing on non-conserved residues. The use of protein rational design and force field algorithms allowed the identification of a list of mutant sequences with potential relevance for TRAIL stability. Four sets of residues were selected for design (Figure 1b and Table 1): (1) non-conserved residues at the surface of the monomer ('monomer' set), (2) non-conserved residues near positions close to the interface between two monomers ('dimer' set), (3) non-conserved residues along the central trimeric axis ('trimer' set) and (4) a miscellaneous set ('misc. set'). The automated computer design algorithm was applied as previously described[166]. Amino acid substitutions were introduced at the non conserved residue positions in conformations (side chain rotamers) compatible with the rest of the structure. Subsequently, favorable mutations were combined and evaluated in terms of free energy (kcal mol^{-1}), and unfavorable combinations (e.g. high Van der Waal clashes) were eliminated. An output of sequences and coordinates was produced and ranked in terms of free energy and subsequently reintroduced in the design algorithm for a 2^{nd}, 3^{rd} or 4^{th} round of design, if

necessary. Table 1 summarizes the list of mutants assayed *in silico* for increased stability of TRAIL. Some of these predictions were discarded directly after theoretical energy calculations, without further experimental analysis.

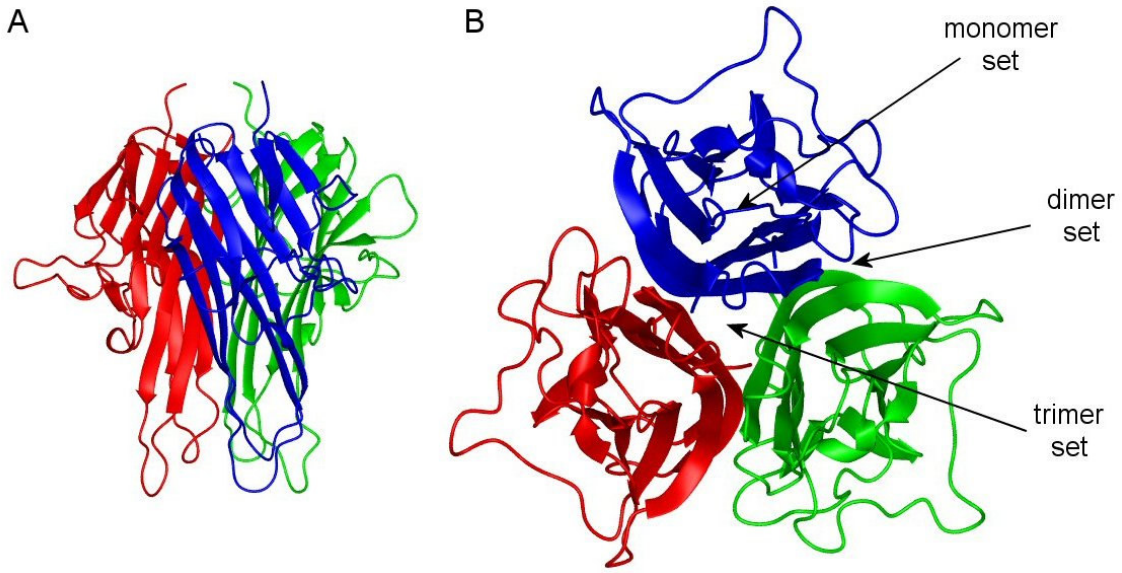

Figure 1. A) Side view of the TRAIL trimeric complex, showing the three monomers in red, blue and green. B) Top view of the same complex but viewed along the longitudinal axis, depicting the different sets used for design. Structure figures were generated using MOLMOL[167].

Description of the tested mutations

Predicted mutants were energy minimized and subsequently analyzed with FOLD-X. The energy values obtained were compared to that of the wild-type structure and used for discrimination of candidates. Mutants were selected based on an improvement in free energy relative to TRAIL WT (Table 2). In the monomeric set, M1 (E194I, I196S) was selected because of the large improvement of energy compared to TRAIL WT ($\Delta\Delta G$ = -9.7 kcal mol^{-1} $monomer^{-1}$). This low energy value is due to the fact that a trimer is being studied, in addition to the presence of significant van der Waals' clashes in the crystal structure (~5 kcal mol^{-1} $monomer^{-1}$), which are removed upon mutation. The mutations are located in the external loop connecting the C and D anti-parallel beta strands (CD loop), following the notation according to Eck[168]. The predicted increase in stability of M1 can be explained since Glu 194 is surrounded by hydrophobic groups (Trp 231, Phe 192, Ala 235) and the carboxyl group is uncompensated. The mutation Glu 194 to Ile rectifies this situation by replacing the charged residue for a medium sized hydrophobic residue. Conversely, Ile 196 is surrounded by polar residues (Asn 202, Lys 233) and is very close to the backbone, resulting in probable van der Waals clashes. Mutation to Ser avoids clashes and allows formation of a hydrogen bond to Asn 202, located in the opposite part of the CD loop (Figure 2a). Both mutations improve polar solvation energy, in addition to ameliorating side chain and backbone entropy.

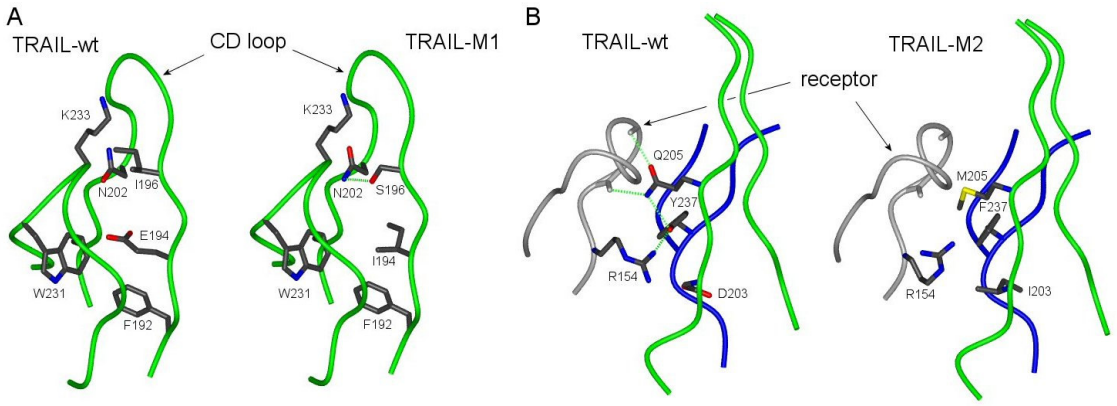

Figure 2. A) Comparison, between rhTRAIL WT and M1, of the local environment around residues 194 and 196. B) Comparison between rhTRAIL WT and M2. Backbones of the two adjacent monomers are in green and blue, respectively, and the backbone of the DR5 receptor is in grey. Hydrogen bond interactions are depicted in dashed green lines.

In the dimeric set (Table 2), the design of M2 (D203I, Q205M, Y237F) leads to the creation of a hydrophobic cluster to stabilize the interaction between residues 203 and 205 (D strand) of one monomer, and residue 237 (F strand) of the adjacent monomer. Gln 205 and Tyr 237 together form an intermolecular hydrogen bond, and Asp 203 points to a gap in the monomer-monomer interface. Mutation to Ile (203), Met (205) and Phe (237) breaks the Q205-Y237 hydrogen bond, but facilitates the tight packing of these residues, improving van der Waals interactions, hydrophobic and polar solvation energies of the entire TRAIL molecule, without a further increase of van der Waals clashes (Figure 2b). Although FOLD-X predicted that the affinity of M2 for the DR5 receptor is lower ($\Delta\Delta G_{binding}$=7.3 kcal mol^{-1} monomer^{-1}) than for TRAIL WT, this mutant was retained as a control to evaluate the accuracy of the procedure.

Residue 225 of M3 (S225A), belonging to the 'Miscellaneous set', is located in strand E and is solvent exposed in the monomeric form. However, after trimerization, this position becomes buried in a small pocket, leaving the side chain of the hydrogen bond donor Ser uncompensated. After mutation to Ala, the energy of the model is better than TRAIL WT for both polar and hydrophobic solvation energies, in addition to side chain entropy.

The Arg 227 residues of the trimeric set mutant (M4) are located in strand E, equidistantly opposed in a central position along the longitudinal axis of the TRAIL trimer. The three arginines are surrounded by hydrophobic (Ile242), polar (Ser241, Ser225) and aromatic (Tyr 240, Tyr 243) residues. These tyrosines direct the hydroxyl groups away from Arg 227, thus creating a rather hydrophobic cavity. The high concentration of positive charges is apparently not well compensated, since it forms only hydrogen bonds with the backbone (carbonyl groups of Ser241). Thus, the mutation of these positions to Met could help to accommodate the hydrophobic environment, as well as to decrease the repulsion of monomers due to uncompensated positive charges.

Mutagenesis and Purification of Mutants

The highest ranking mutant from each of the four sets was selected for further experimental analysis (Table 2). A mutant (C1) combining the mutations of M1 and M3 was also

constructed. All the designed TRAIL mutants were expressed in *E. coli* and purified successfully with a protein yield of ~ 0.7-2 mg/l. Far-UV CD wavelength spectra indicated that all mutants were properly folded with characteristics of a β-sheet containing protein, similar to that of rhTRAIL WT. Gel-filtration and dynamic light scattering measurements showed that all mutant protein solutions contained a single molecule species, consistent with a trimeric oligomerization state. Analytical ultracentrifugation with rhTRAIL WT and M1 corroborated this finding (data not shown).

Table 2 Computational design results

	$\Delta\Delta G_{stability}$ *	$\Delta\Delta G_{binding}$ *‡	**Set**	**Mutations**
M1	-9.7	0.4	Monomer	E194I, I196S
M2	-4.0	7.3	Dimer	D203I, Q205M, Y237F
M3	-7.0	-0.5	Misc.	S225A
M4	-9.1	-1.2	Trimer	R227M
C1	-11.4	-0.9	Combination	M1+M3

* Energy in kcal mol^{-1}, calculated per monomer

‡ $\Delta G_{binding} = \Delta G_{complex} - (\Sigma \Delta G_{chain})$; $\Delta\Delta G_{binding} = \Delta G_{binding}$ mutant $- \Delta G_{binding}$ wild-type

Thermal unfolding

The thermal unfolding of rhTRAIL WT and TRAIL mutants was monitored by CD, measuring changes in molar ellipticity at 222 nm upon heating. Figure 3 shows the heat induced changes of rhTRAIL WT and TRAIL mutants. TRAIL shows an onset of unfolding at approximately 70 °C and has a transition midpoint of 77 °C. The TRAIL mutants show however, onset of unfolding at increased temperatures and higher transition midpoints (Figure 3). For M1 the onset of unfolding was at approximately 76 ° C and the transition midpoint was at 85 °C. M2 showed an onset of unfolding at approximately 74 °C. M3 gave intermediate values between those of rhTRAIL WT and M1, with an onset of unfolding of 73 °C and a transition midpoint of 80 °C. Mutant C1, representing the combined mutations of M1 and M3 showed values comparable to that of M1. The mutant belonging to the trimeric set (M4), however, showed an experimentally determined stability of approximately 3 ºC less than rhTRAIL WT, and was therefore discontinued. The initial increase in molar ellipticity around 76 °C for M2 is due to an overall change of the far UV spectrum, reflecting a loss of structural properties of the starting material (data not shown). Upon cooling all protein solutions were turbid, indicating irreversible aggregation, therefore no thermodynamic parameters could be derived. Far and near UV wavelength CD scans at increasing temperatures confirmed the above findings (data not shown).

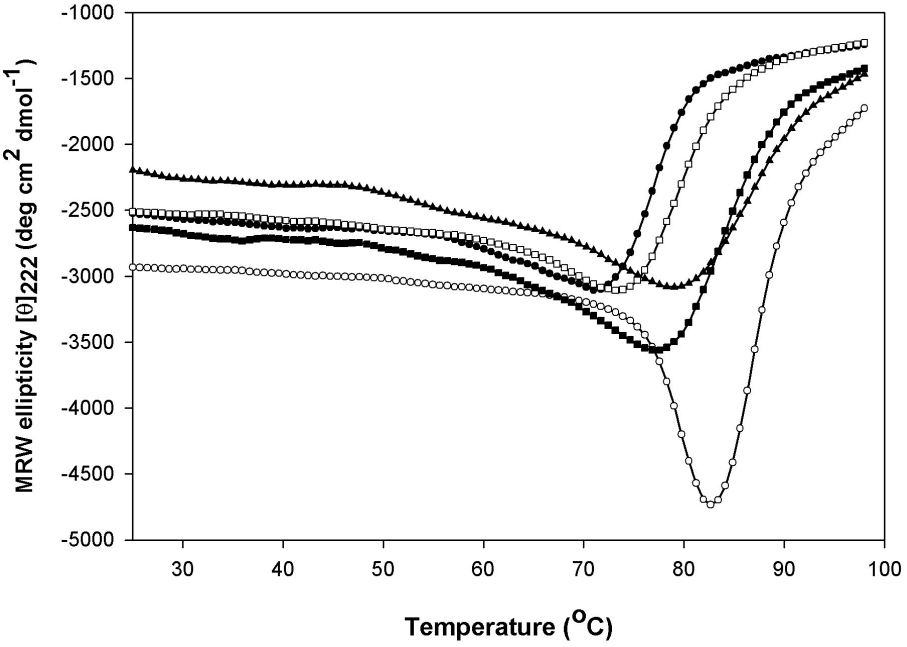

Figure 3. Thermal denaturation profiles of rhTRAIL WT (closed circles), M1 (closed squares), M2 (open squares), M3 (open squares) and C1 (closed triangles).

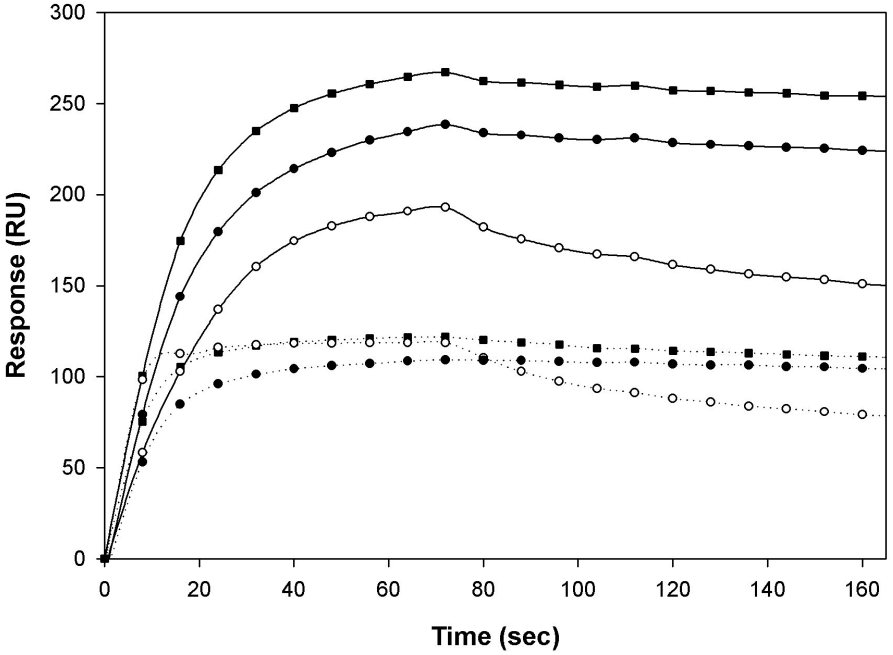

Figure 4. Binding of rhTRAIL WT (closed circles), M1 (closed squares) and M2 (open circles) to DR5 (dotted lines) and DR4 (solid lines) receptors.

***In vitro* bioactivity and binding of designed mutants**

Bioactivity of the TRAIL mutants was assessed *in vitro* using the Colo205 human colon cancer cell line with a MTT based viability assay. A reduction in viability was measured using increasing concentrations of rhTRAIL WT or TRAIL mutants relative to the control. While M1, M3 and C1 showed a bioactivity comparable to that of rhTRAIL WT (ED_{50} ~5 ng/ml), M2 exhibited bioactivity of nearly one order of magnitude lower (ED_{50} ~50 ng/ml). Real-time binding of rhTRAIL WT and TRAIL mutants to the death receptors DR4 and DR5 was assessed using surface plasmon resonance with a Biacore 3000 instrument. Sensorgrams of M1, M3 and C1 were identical to that of rhTRAIL WT. In contrast M2, whilst showing a similar level of binding to both receptors, displayed an increased off-rate when compared to the rhTRAIL WT sensorgram (Figure 4).

Accelerated thermal stability study

In order to test the stability of TRAIL and TRAIL mutants over time, an accelerated thermal stability measurement was performed. The temperature of 73 ^{o} C was chosen to measure effects on stability within a 1 h timeframe. At this temperature rhTRAIL WT starts to unfold, while the mutants are still properly folded (Figure 3). Protein solutions with the same concentration as used in the thermal unfolding measurements were incubated at 73 ^{o}C for 1 h and changes in molar ellipticity at 222 nm were measured (Figure 5). The ellipticity of rhTRAIL WT decreased from the onset, giving a half-life of approximately 13 min. The signal for the M1, M2 and C1 mutants remained essentially constant, indicating an increased thermal stability. M3 showed a half-life of approximately 24 min. These measurements, however, are not indicative of the bioactive trimeric structure of the TRAIL molecule, but of the secondary structure of the monomeric unit. To monitor a concomitant increase in biological activity at elevated temperatures of the mutants with unchanged biological activity (M1, M3 and C1), protein solutions with the same concentrations as used in the thermal unfolding measurements were incubated at 73 ^{o} C and samples were taken at regular intervals for 1 h. Samples were subsequently diluted in tissue culture medium and added to Colo205 cells, resulting in a final concentration of 100 ng/ml. After overnight incubation the viability of the cells was measured using a MTT assay. RhTRAIL WT showed decrease in bioactivity after 20 min of incubation, while M1 and C1 retained full bioactivity after incubation at 73 ^{o} C for 1 h (Figure 6). M3 displayed an intermediate bioactivity between rhTRAIL WT and the other mutants. The increases in thermal stability of the mutants as measured with CD could therefore be correlated with a more stable biologically active trimeric molecule.

Discussion

Others have previously applied computational engineering techniques to improve thermal stability of alpha-helical proteins or monomeric beta-sheet molecules[55,169,170]. However, frequently, monomeric proteins of less than 100 amino acids were used as targets. To our knowledge, this report is the first example of computational redesign of a large trimeric all-β-sheet protein towards a more thermal stable variant. Significantly, it shows that the principles learned from design and engineering of small proteins can also be applied for large multimeric protein complexes.

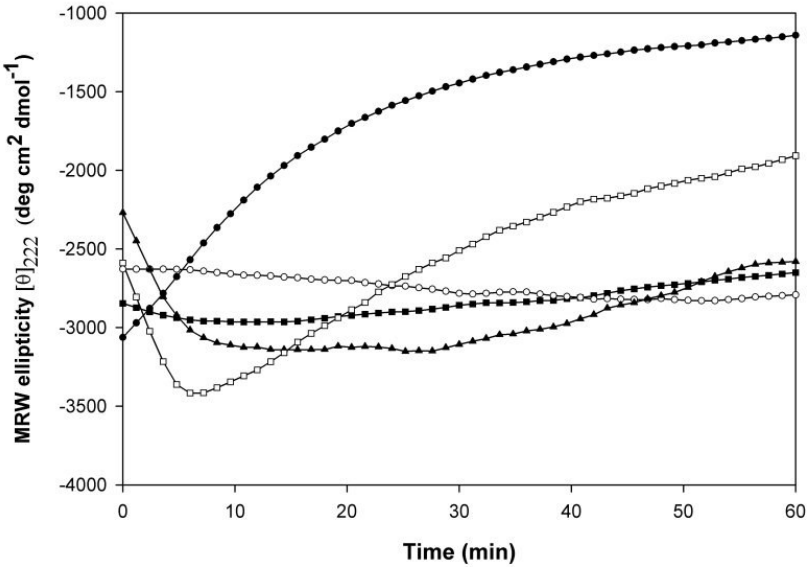

Figure 5. Stability of rhTRAIL WT (closed circles), M1(closed squares), M2 (open circles), M3 (open squares) and C1 (closed triangles) at 73 ºC for 60 min.

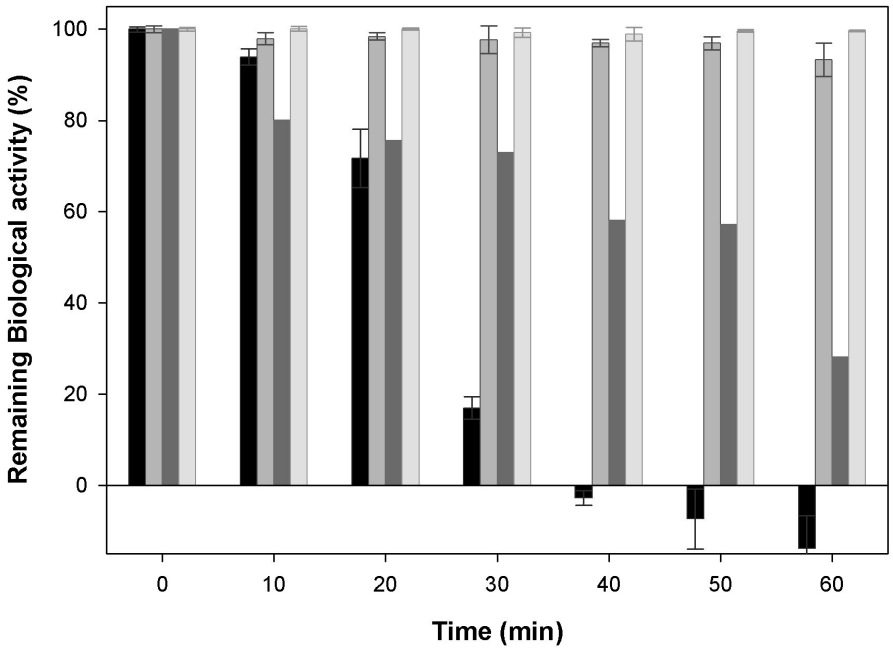

Figure 6. Remaining biological activity of rhTRAIL WT, M1, M3 and C1 (from left to right) upon incubation at 73 º C during 60 min. Biological activities are calculated relative to the value observed at 0 min.

The rhTRAIL WT (114-281) molecule has a relatively high thermal stability if compared to some members of the TNF ligand family. Human tumor necrosis factor alpha (TNF-α), for example, has an apparent T_m of 65 °C as measured with CD[171] and the CD40L receptor binding domain has an apparent T_m of 60 °C as measured with differential scanning calorimetry (DSC)[172]. In parallel investigations, we can show using CD that RANKL however, is more thermal stable than TRAIL, with an apparent T_m of 5 °C higher than rhTRAIL WT, confirming another study[173]. In this study, we investigated the possibility of further increasing the thermal stability of TRAIL, as a model for all-β-sheet proteins, through the use of computational engineering.

We succeeded in extending the thermal stability of the β-sheet protein by more than 5 °C by using a combined approach, employing both TNF ligand family alignment information and an automated computational design algorithm. Due to the non-reversible nature of the unfolding reaction, the apparent T_m is not a perfect indication of an increase in stability. From a functional point of view, therefore, it also makes sense to study the time taken for the protein to denature at high temperature and to relate this to an effect on biological activity. The accelerated thermal stability study showed that the increase in thermal stability of the mutants as measured with CD spectroscopy (Figure 5) can be correlated with the preservation of overall structural characteristics as highlighted by the lasting bioactivity of M1 during the experimental timeframe (Figure 6). When measuring the residual bioactivity of rhTRAIL WT and TRAIL mutants upon incubation at 73 °C for 1 h, it was shown that, while rhTRAIL WT was all but thermally inactivated after ~20 min, the mutants, significantly, had an improved stability with respect to rhTRAIL WT (Figure 5). According to the Arrhenius equation a measured increase in stability for M1 at 73 °C could also correlate with an increase in stability for M1 at more relevant temperatures, such as 37 °C or room temperature, provided that the type of degradation mechanism is the same at both temperatures. Although not tested in this study, it has been shown that in case of certain therapeutically interesting proteins, improvement of thermal stability can also be indicative of an improved *in vivo* half-life[174,175]. This could be of particular interest for the therapeutic use of TRAIL. Preclinical studies showed that rhTRAIL WT was rapidly eliminated from both rodents and non-human primates, with half-lives ranging from 3.6 min (mouse) to 27 min (Chimpanzee)[32].

It is advantageous to use alignment information in order to focus the design on non-conserved residue positions. The reason being that conserved residues are usually retained in a family for a good reason and it is probable that any mutation will decrease protein stability[69,176]. On the other hand, regions with high sequence variability are tolerant to mutation and it can be expected that variants that stabilize the protein can be found in these regions[69]. To accomplish our goal of redesigning a β-sheet protein, TRAIL, and to generate stable variants with the minimum number of mutations, the conserved residues forming the trimeric interface were therefore largely excluded from the prediction/optimization strategy. This resulted in an approach which focused mainly on improvement of the stability of the monomer (intra-chain stabilization; monomeric set) or improving monomer-monomer contacts (inter-chain stabilization; dimeric set). See Table 1.

M1, M2, M3 and C1 showed, in agreement with our predictions, an increase in thermal stability (Table 2; figure 3, 5, 6). Different basic principles were used in the M1, M2 and M3 designs. M1 shows an example of intra-chain stabilization. Stabilization of the flexible CD loop at the surface of each TRAIL monomer results in an increased stability of the entire trimer. This loop is not directly involved in receptor binding and is disordered in un-complexed rhTRAIL WT structures[17,163], but becomes ordered on binding to DR5[12,16,18]. M2, however, illustrates the optimization of the interactions between two adjacent monomers, i.e. inter-chain stabilization. Although we were successful with the above designs, in other cases like the combination mutant, C1 (M1 and M3 combined) or the M4 mutant, we failed in our predictions. There could be several reasons behind it, but it also shows the limitations of design methods. Inherent limitations on force fields, resolution of the structures used as templates and the omission of protein dynamics in the exercise are some of the factors behind protein design failures.

The increase in thermal stability did not affect the biological activity of M1, M3 and C1. M2 was more stable than rhTRAIL WT but the formation of an electrostatic interaction between Gln 205 and Arg 154 of the DR5 receptor was prevented (Figure 6b). This resulted in a subsequent 10-fold decrease in biological activity when compared to rhTRAIL WT, as predicted by FOLD-X ($\Delta\Delta G_{binding}$= 7.3 kcal mol^{-1} $monomer^{-1}$). Our findings confirmed an earlier study showing decreased bioactivity of alanine mutants at these positions[17]. Analysis of binding to the DR4 and DR5 receptors, using surface plasmon resonance, shows an increased off-rate for M2, indicating a lower affinity for both receptors, when compared to rhTRAIL WT and M1 (Figure 2). Since ligand-receptor binding sites are normally "high energy regions", the M2 mutations were expected to stabilize the TRAIL molecule. Thus, this could be regarded as an example of a possible increase in stability which is counterbalanced in evolution by loss of function.

Frequently, other computational redesign studies limited the screening for improvement of thermal stability to the core of the molecule[59,174,175]. Here we show that computational redesign techniques can also involve inter-chain interfaces and surface residues of the molecule, to successfully stabilize the structure.

Performance of PERLA/FOLD-X was successful in the case of the intra-chain (monomer) set, the inter-chain (dimeric) set and the miscellaneous set. The experimental data corresponding to these designs showed all variants within these sets were more stable than rhTRAIL WT. Significantly, we could show that stabilization of the CD loop in a single monomer resulted in stabilization of the entire trimeric molecule (Figure 2a).

Our studies have shown that computer redesign of a more thermal stable multimeric all β-sheet protein is achievable. Computational protein redesign is therefore a valuable addition to other protein engineering methodologies, such as directed evolution or experimental high throughput approaches, as a tool for the improvement of protein properties. Since the computational method used in our study is general applicable, our findings can be further applied to design other TNF ligand family members with improved thermal stability.

Methods

All reagents were of analytical grade unless specified otherwise. Isopropyl-β-D-1-thiogalactoside (IPTG), ampicillin and dithiotreitol (DTT) were from Duchefa. Chromatographic columns and media were from Amersham Biosciences. Restriction enzymes used were purchased from New England Biolabs. All other chemicals were from Sigma.

Computational design of mutants

A detailed description of the protein design algorithm, PERLA, is available elsewhere[159] (http://ProteinDesign.EMBL-Heidelberg.DE) and its use has been previously described[60,85,158,165]. In the case of oligomeric proteins such as TRAIL, protein design requires the following steps: Firstly, residues of a monomer that could establish specific interactions with the contiguous monomer must be identified and selected. Secondly, side chains that contact the residues to be mutated, must be identified to allow side chain movements that are necessary to accommodate the new residues introduced by the algorithm. The algorithm automatically selects these residues based on a geometrical approach that takes Cα-Cα distances and the angle between Cα-Cβ vectors into consideration. Thirdly, the algorithm places the amino acid repertoire at each position selected from a set of naturally occurring amino acids in a multiple sequence alignment of the TNF ligand family, and eliminates those side chain conformations and amino acids that are not compatible with the rest of the structure. Fourthly, all possible pair-wise interactions are explored to eliminate those combinations that are less favorable. Finally, an output of sequences and PDB coordinates corresponding to the best calculated solution (in terms of energy) is produced. The resultant PDB files containing the mutations were energy minimized using GROMOS 43B1 as implemented in Swiss-PdbViewer v3.7b2[177], and evaluated by FOLD-X[160] (http://fold-x.embl-heidelberg.de). The final energies of the models are compared to the reference rhTRAIL WT structure and expressed as ΔΔG (kcal mol^{-1}).

Cloning and PCR

cDNA corresponding to human soluble TRAIL (aa 114-281) was cloned in pET15B (Novagen) using *Nco*I and *BamH*I restriction sites. The N-terminal sequence encoding a His-tag and protease recognition site was therefore removed. Mutants were constructed by PCR using the Quick Change Method (Stratagene) or a modified megaprimer method[178]. The polymerase used was *Pfu* Turbo supplied by Stratagene. Purified mutagenic oligonucleotides were obtained from Invitrogen. Introduction of mutations was confirmed by DNA sequencing.

Expression and purification of rhTRAIL WT and mutants

The rhTRAIL WT and TRAIL mutant constructs were transformed to *Escherichia Coli* BL21 (DE3) (Invitrogen). RhTRAIL WT and M1 were grown at a 5 l batch scale in a 7.5 l fermentor (Applicon) using 4 x LB medium, 1 % (w/v) glucose, 100 µg/ml ampicillin and additional trace elements. The culture was grown to mid-log phase at 37 °C, 30 % oxygen saturation and subsequently induced with 1 mM IPTG. $ZnSO_4$ was added at a concentration of 100 µM to promote trimer formation. Temperature was lowered to 28 °C and the culture

was grown until stationary phase. Other mutants were grown in shake flasks at a 1 l scale at 250 rpm, using a similar protocol. Protein expression was induced when the culture reached OD_{600} 0.5 and induction was continued for 5 h. In this case, the medium used was 2 x LB without additional trace elements.

The isolated pellet was resuspended in 3 volumes extraction buffer (PBS pH 8, 10% (v/v) glycerol, 7 mM β-mercapto-ethanol). Cells were disrupted using sonication and extracts were clarified by centrifugation at 40,000 g. Subsequently, the supernatant was loaded on a nickel-charged IMAC Sepharose fast-flow column and rhTRAIL WT and TRAIL mutants were purified as described by Hymowitz[17] with the following modifications: 10 % (v/v) glycerol and a minimal concentration of 100 mM NaCl were used in all buffers. This prevented aggregation during purification. After the IMAC fractionation step, 20 μM $ZnSO_4$ and 5 mM of DTT (instead of β-mercapto-ethanol) was added in all buffers. Finally, a gelfiltration step, using a Hiload Superdex 75 column, was included. Purified proteins were more than 98 % pure as determined using a colloidal Coomasie brilliant blue stained SDS-PAGE gel. Purified protein solutions were flash frozen in liquid nitrogen and stored at -80 ^{o}C.

CD Spectroscopy

Circular dichroism (CD) spectra were recorded on a Jasco J-715 CD spectrophotometer (Jasco Inc.) equipped with a PFD350S Peltier temperature control unit (Jasco Inc.). Rectangular quartz cuvettes with a pathlength of 0.2 cm were used. Protein samples were dialyzed against PBS pH 7.3 and adjusted to a final concentration of 100 μg/ml. Wavelength spectra were recorded between 250-205 nm using a 0.2 nm stepsize and 1 nm band-width at 25 ^{o}C. Temperature scans from 25-98 ^{o}C were performed at 222 nm with a scan rate of 40 ^{o}C/h. Thermal decay measurements were performed at 73 ^{o}C for 1 h at 222 nm.

Bioactivity of TRAIL mutants *in vitro*

Bioactivity of rhTRAIL WT and TRAIL mutants was determined using a viability assay according to the manufacturer's instructions (Celltiter Aqueous One, Promega). Colo205 human colon carcinoma cells (ATCC number CCL-222) were cultured in RPMI 1640 Glutamax containing 10 % heat inactivated fetal calf serum and 100 units/ml Penicillin-Streptomycin. All reagents were supplied by Invitrogen. A concentration series of the rhTRAIL WT or TRAIL mutants was made in cell culture medium. Fifty μl of each dilution was added to a 96-well tissue culture micro plate (Greiner) and 100 μl of cell suspension was added, to a final cell number of $1x10^4$ cells/well. Mixtures were incubated for 16 h at 37 ^{o}C under a humidified atmosphere containing 5 % CO_2. Subsequently, 20 μl of MTS reagent was added. Cell viability was determined after 30 min incubation by measuring the absorption at 490 nm.

Receptor binding

Binding experiments were performed using a surface plasmon resonance-based biosensor Biacore 3000 (Biacore AB, Uppsala, Sweden), at 25 ^{o}C. Recombinant receptors were ordered from R&D systems (R&D systems, Minneapolis, MN, USA). Immobilization of the receptors on the sensor surface of a Biacore CM5 sensor chip was performed following

a standard amine coupling procedure according to the manufacturer's instructions. A reference surface was generated simultaneously under the same conditions but without receptor injection and used as a blank to correct for instrument and buffer artifacts. Purified rhTRAIL WT and TRAIL mutants were injected in two-fold at a concentration of 2 µg/ml and at a flow rate of 20 µl/min. Binding of ligands to the receptors was monitored in real-time. The receptor/sensor surface was regenerated using 3 M sodium acetate pH 5.2 injections.

Acknowledgements

We thank Dr. Rob van Weeghel and Ron Suk for providing purified rhTRAIL WT. We would also like to express gratitude to Afshin Samali and Eva Szegezdi for helpful discussions, and to Arie Geerlof, Sjouke Piersma and Johanna Vrielink for technical assistance. This research was partly funded by the EU 5th framework program (QLK3-CT-2001-00498).

4

Designed TRAIL variants initiating apoptosis exclusively via the DR5 receptor

Almer M. van der Sloot, Vicente Tur, Eva Szegezdi, Margaret M. Mullally, Robbert H. Cool, Afshin Samali, Luis Serrano and Wim J. Quax

Proc. Natl. Acad. Sci. U. S. A (2006) 103:8634-8639

Abstract

Tumor necrosis factor-related apoptosis inducing ligand (TRAIL) is a potential anticancer drug that selectively induces apoptosis in a variety of cancer cells, by interacting with death receptors DR4 and DR5. TRAIL can also bind to decoy receptors (DcR1, DcR2 and OPG receptor) that cannot induce apoptosis. The occurrence of DR5 responsive tumor cells indicates that a DR5-receptor specific TRAIL variant will permit new and selective tumor therapies. Using the automatic design algorithm FOLD-X, we successfully generated DR5-selective TRAIL variants. These variants do not induce apoptosis in DR4-responsive cell lines but show a large increase in biological activity in DR5-responsive cancer cell lines. Even rhTRAIL WT insensitive ovarian cancer cell line could be brought into apoptosis. In addition, our results demonstrate that there is no requirement for antibody mediated cross-linking or membrane bound TRAIL to induce apoptosis via DR5.

Introduction

Tumor necrosis factor (TNF) related apoptosis inducing-ligand (TRAIL) is currently attracting great interest as a potential anti-cancer therapeutic. TRAIL in its soluble form selectively induces apoptosis in tumor cells *in vitro* and *in vivo*, by a death receptor mediated process. Unlike other apoptosis inducing TNF family members, soluble TRAIL appears to be inactive against normal healthy tissue[13]. Reports in which TRAIL induces apoptosis in normal cells could be attributed to the specific preparations of TRAIL used[14]. TRAIL shows a high degree of promiscuity as it binds to five cognate receptors; DR4 (TRAIL-R1) and DR5 (TRAIL-R2) and to the decoy receptors DcR1 (TRAIL-R3), DcR2 (TRAIL-R4) and Osteoprotegerin (OPG)[19]. Upon binding to TRAIL, DR4 and DR5 receptors recruit Fas associated death domain (FADD), which bind and activate the initiator caspase 8, leading to apoptosis[23-25]. DcR1 or DcR2 do not contain a death domain or contain a truncated death domain, respectively, and therefore could prevent apoptosis by sequestering available TRAIL or by interfering in the formation of a TRAIL-DR4 or -DR5 signaling complex[30].

Use of TRAIL receptor selective variants could permit better tumor specific therapies through escape from the decoy receptor-mediated antagonism, resulting in a lower administrated dose, with possibly less side effects and as alternatives to existing agonistic receptor antibodies[179-181]. In experimental anti-cancer treatment, the receptors DR4 and/or DR5 were shown to be up-regulated after treatment with DNA damaging chemotherapeutic drugs and the response to TRAIL-induced apoptosis was significantly increased[19,182]. In addition, irradiation appears to specifically up-regulate DR5 receptor expression and the combination of irradiation and TRAIL treatment has been demonstrated to have an additive or synergistic effect[107]. Thus, we choose to develop DR5 receptor selective TRAIL variants using a computational design strategy. Computational design methods have been successfully employed to redesign several protein-protein interactions[85-87,89], but have as yet hardly been applied to therapeutic proteins. One exception is the design of dominant negative TNF-α variants that prevent formation of active TNF-alpha trimers[104]. Using the automatic design algorithm FOLD-X[150,160,183], we were able to redesign TRAIL into exclusively DR5-specific agonistic variants. Since the computational method used in our study is based on general applicable principles and has been successfully tested on a variety of proteins[65,85,183-185], our method can be further applied to design other protein therapeutics with reduced promiscuity and improved receptor binding characteristics.

Results

Modeling of TRAIL-receptor complexes

Monomeric subunits of TRAIL self associate in bell-shaped homotrimers, the bioactive form of the ligand, like other members of the TNF ligand-family[1,2]. A trimer binds three subunits of a cognate receptor, with each receptor subunit bound in the grooves between two adjacent monomer ligand subunits[16,18]. At present only crystal structures of TRAIL in complex with the DR5 receptor are known[12,16,18]. The sequence alignment of the different TRAIL receptors (figure 1A), shows a large overall sequence identity (except for OPG), practically no insertions or deletions and conservation of all cysteines involved in the

formation of internal disulfide bridges. Consequently, good quality homology models of DR4, DcR1 and DcR2 could be build, but not of OPG. The homology models were built using the WHAT IF web interface[186]. Afterwards, these models were refined using the protein design options of FOLD-X, removing incorrect side chain torsion angles, eliminating Van der Waals clashes and accommodating TRAIL and receptor residues to their new interface.

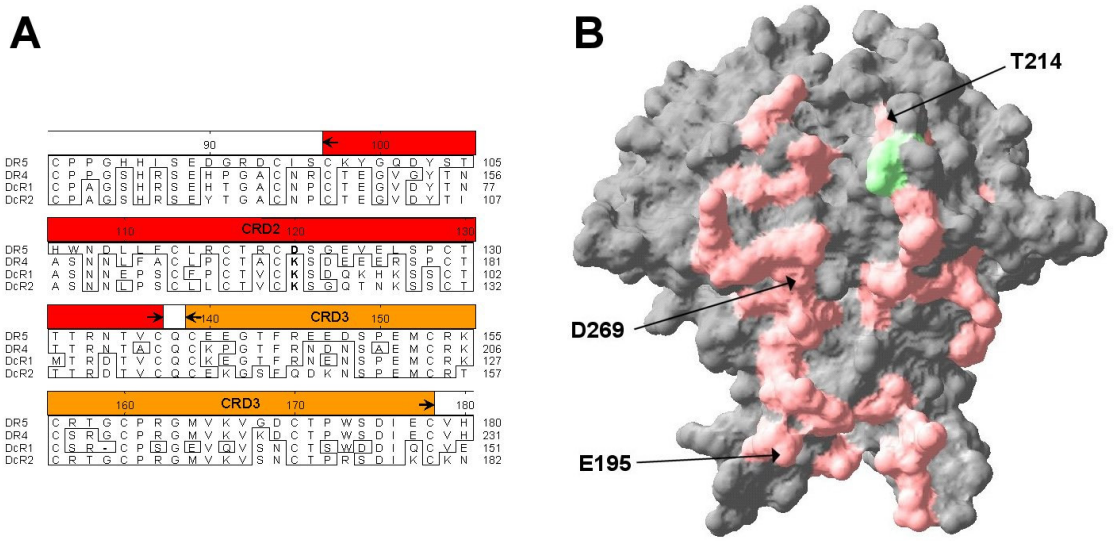

Figure 1. (A) Sequence alignment of the four different TRAIL membrane receptors. Both cystein rich domains involved in receptor binding are highly conserved. From the sequence alignment of the different TRAIL receptors[187] it is observed that the receptor cysteine rich domains (CRDs) involved in the interaction with TRAIL (CRD2 and CRD3) are highly conserved and the overall sequence identity when compared to DR5 is higher than 50%, with the exception of the soluble receptor OPG (not shown). In addition, there are neither insertions nor deletions in the sequence alignment (with the exception of a glycine deletion in the middle of CRD3 in DcR1) and all the cysteines involved in the formation of internal disulfide bridges are conserved. Position Asp 120 of DR5 and corresponding residues of the other receptors are depicted in bold, residues of CRD2 in red and residues of CRD3 in orange. Identical amino acids to DR5 are boxed. (B) Side view of TRAIL receptor binding interface formed by two TRAIL monomers, highlighted in light red are all amino acids selected for the *in silico* screening. Tyr216 (depicted in green) was used as a reference and control.

The accuracy of the models and the force field was tested using the data derived from the alanine scanning of rhTRAIL WT as performed by Hymowitz *et al.*[17]. The predictions of the energy change in the complex formation correlates with the changes in the dissociation constants measured (figure 2)**.** The calculated R^2 factor is 0.6 (R^2 factors calculated for DR4 and DR5 individually also amount to 0.6). However, several factors involved in accuracy should be taken into account. The methodology used focuses on energy changes in ligand-receptor complex formation, some mutations to alanine might be predicted as not changing receptor binding affinity but only producing slight changes on TRAIL stability, thereby affecting the correlation. The prediction error is on average within the error of this methodology (0.6 – 0.7 kcal/mol). Since many changes in affinity as measured in the alanine scanning are within this error it is not possible to obtain a better correlation. Taken together, this implies that our method can reliably predict mutations in the receptor binding interface that will most severely affect the complex formation.

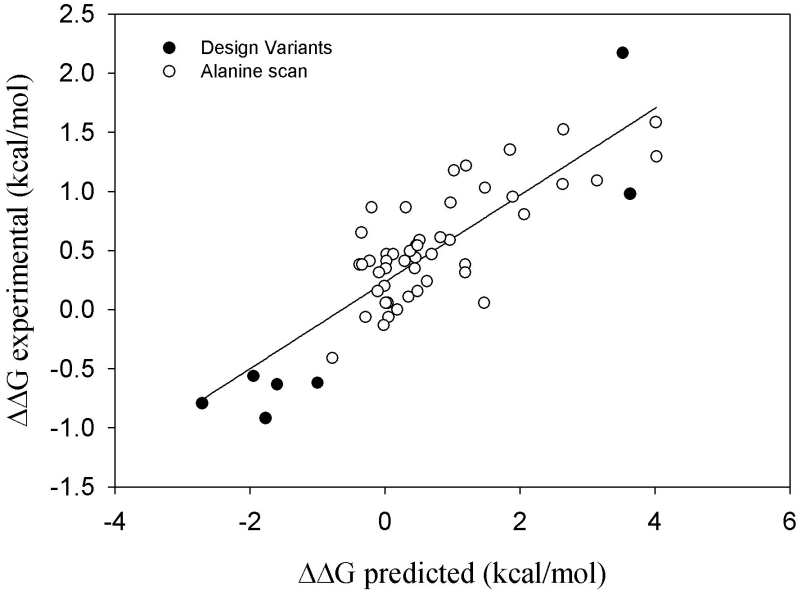

Figure 2. Correlation of the predicted changes in binding affinity compared with the experimental results of an alanine scanning performed by *Hymowitz et al.*[17] (open circles) and of the DR5 selective TRAIL variants (closed circles).

Computational design of the variants

For the computational screening, all residues from the TRAIL interface were considered. TRAIL residues interacting with a conserved amino acid environment in all four receptors were disregarded. Amino acids finally considered were Arg130, Gly131, Arg132, Lys145, Leu147, Gly148, Arg149, Lys150, Glu155, Arg158, Gly160, His161, Tyr189, Arg191, Phe192, Gln193, Glu195, Asn199, Thr200, Lys201, Asp203, Gln205, Val207, Gln208, Tyr209, Thr214, Asp218, Asp234, Glu236, His264, Ile266, Asp267 and Asp269. Tyr216 was included as a positive control due to its already known implication in receptor binding[16,18] and Ser165, located far away from the receptor binding interface, was used as a negative control (figure 1B). At each of the selected positions, FOLD-X placed the 20 natural amino acids whilst moving the neighbouring residues, obtaining a library of 2720 models in total (34 amino acid positions x 20 amino acids x 4 receptors). The energy of interaction was obtained calculating the sum of the individual energies of the receptor and ligand subunits and subtracting them from the global energy of the complex. In this way, a set of predicted energetic values for the complex formation was obtained and compared with the TRAIL WT values. After studying these values together with visual inspection of the mutant models, those in which a change in selectivity was predicted, were selected for experimental studies (Table 1).

Table 1. Predicted difference in binding energy (ΔΔG) of DR5-selective variants binding to different receptors when compared with TRAIL WT

Mutations	DR4	DR5	DcR1	DcR2
R130E	0.75	-0.2	1.76	1.52
G160M	-1.11	-1.52	-0.18	-0.65
E195R	0.11	-1.11	0.2	-0.79
T214R	1.85	-0.17	1.94	1.89
D269H	3.52	-1.6	3.78	4.43
D269R	1.95	-1.95	2.45	3.28
D269K	2.43	-1	2.94	3.71

Variants comprising these mutations were selected in the pre-screen assay from an initial set of 10 design proposals. Change in energy is measured in kcal/mol and applies to the change of a single binding interface bound to a single receptor.

Pre-screen for selective receptor binding

A fast surface plasmon resonance (SPR) based receptor binding pre-screen was used to further refine the *in silico* selection. TRAIL variant cell extracts were evaluated for binding to DR4, DR5 and DcR1 immobilized Ig fusion proteins. The ratios of binding to DR4 and DcR1 receptor with respect to DR5 receptor were calculated and compared to the ratio obtained for rhTRAIL WT. An increase in DR5/DR4 binding ratio of ≥25 % relative to the ratio of rhTRAIL WT was set as indicative of DR5 selectivity. Several variants comprising a substitution (His, Lys or Arg) at position Asp 269 and variants with a double mutation D269H/E195R and D269H/T214R with a reduced binding to the DR4 and increased binding to the DR5 receptor were chosen for further analysis. R191E/D267R, R130E, G160M, I220M and E195R were also selected, as they also showed an increased DR5/DR4 binding ratio. The effects, however, were smaller than that of the Asp 269 variants (data not shown).

Determination of Receptor binding

Selected TRAIL variants were purified as described before[65]. Analytical size exclusion chromatography (SEC) and dynamic light scattering (DLS) confirmed that the purified TRAIL variants were in a trimeric state and that higher order oligomeric species or aggregates were absent (data not show). Binding of the purified variants to immobilized DR4, DR5, DcR1 or DcR2 Ig receptor was assessed in real time using SPR. The TRAIL proteins were initially analyzed at two concentrations (30 and 60 nM). TRAIL variants R191E/D267R and G160M showed stability and folding problems and were therefore discarded. Binding curves of variants showing a significant change in the ratio DR5/DR4 binding were subsequently recorded for concentrations ranging from 0.1 to 250 nM. The D269H/T214R variant had a comparable improvement as the D269H single mutant variant in DR5 Ig binding, however no detectable binding to DR4 Ig was found (figure 3A and B). Apparent K_d values for DR5 binding ranged from 0.6 nM (D269H/E195R) to 2.5 nM (TRAIL), and for DR4 binding from 7.2 nM (TRAIL) to 244 nM (D269H). For D269H/T214R, D269K and D269R a proper apparent K_d for DR4 binding could not be determined. Binding of D269H and D269H/E195R towards the decoy DcR1 Ig receptor was >20 fold reduced when compared to rhTRAIL WT. Up to the highest concentration tested (250 nM) D269H/T214R did not show any observable binding to DcR1 Ig (figure

4A). D269H and D269H/E195R showed also reduced binding to DcR2 Ig, however this reduction was much less pronounced as the reduction observed in DcR1 binding. In contrast, D269H/T214R showed a large decrease in binding to DcR2 Ig relative to rhTRAIL WT (figure 4B). Binding to OPG Ig was also reduced for these three DR5 selective variants, with D269H/E195R showing the largest decrease in binding to this receptor (figure 4C). A competition ELISA experiment measuring the binding of TRAIL or variants towards immobilized DR5-Ig in the presences of soluble DR4, DR5 or DcR1 Ig corroborated the findings of the receptor binding experiment. Whereas TRAIL binding to immobilized DR5-Ig could be competed by soluble DR4, DR5 and DcR1, binding of the variants could only be antagonized by soluble DR5 Ig (figure 5).

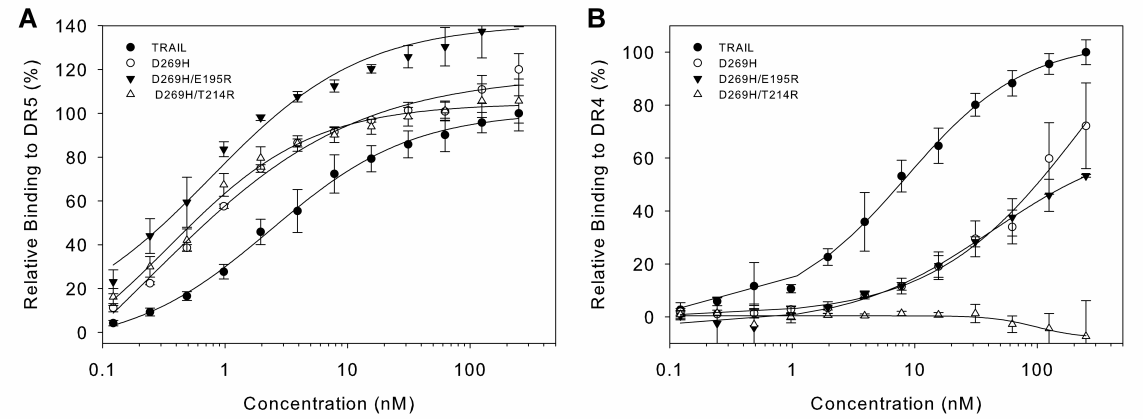

Figure 3. (A) Receptor binding of TRAIL and DR5 selective variants towards DR5-Ig as determined by SPR. (B) or towards DR4-Ig. Receptor binding is calculated relative to the response of rhTRAIL WT at 250 nM.

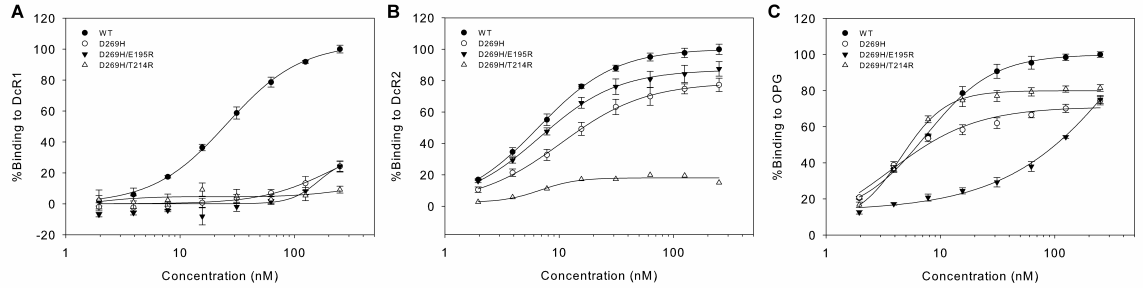

Figure 4. (A) Receptor binding of TRAIL and DR5 selective variants towards DcR1-Ig as determined by SPR, (B) towards DcR2-Ig or (C) towards OPG-Ig. Receptor binding is calculated relative to the response of rhTRAIL WT at 250 nM.

Comparison between predictions and experimentally obtained results

In order to calculate the correlation between predicted and experimentally obtained results of our DR5 selective variants, we compared the calculated ΔΔG values for DR4 and DR5 binding (table 1) with the ΔΔG values that stem from the experimentally determined apparent K_d values (see above). The calculated R^2 factor between these predicted and experimental ΔΔG values is 0.88. Adding these values to the alanine scan data set improved the overall calculated R^2 from 0.6 to 0.7 (figure 2).

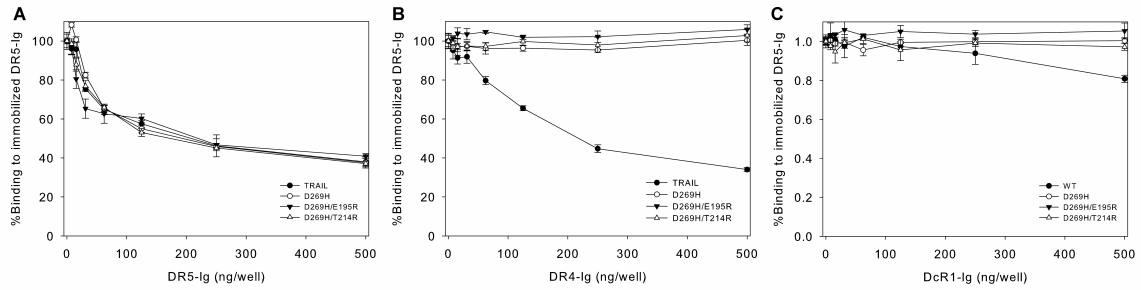

Figure 5. Competition ELISA. (A) Competition ELISA using soluble DR5-Ig as competitor, (B) soluble DR4-Ig as competitor or (C) soluble DcR1-Ig as competitor. Percentage bound to immobilized DR5-Ig is calculated relative to the amount bound at 0 ng/well soluble competitor. The selectivity of the DR5 selective variants towards the DR5 receptor in the presence of another TRAIL receptor was assessed using a competitive ELISA experiment. RhTRAIL WT or receptor selective variants were pre-incubated with 0-500 ng/well DR4, DR5 or DcR1 Ig during 30 min. Pre-incubated solutions were added to micro titer wells coated with DR5 Ig. Binding of the selective variants at various concentrations of soluble receptor towards the immobilized DR5 Ig was calculated relative to the value measured in the presence of 0 ng/well soluble receptor. Increasing concentrations of soluble DR4 Ig or DR5 Ig showed competition with immobilized DR5 Ig for rhTRAIL WT binding. In contrast, soluble DR4 Ig showed no competition with immobilized DR5 Ig for binding with the DR5 selective variants. However, soluble DR5 Ig displayed competition for binding with the immobilized DR5 Ig. Pre-incubation with increasing concentrations of DcR1 Ig did not affect the binding of the DR5 selective variants to immobilized DR5 Ig. RhTRAIL WT showed, in contrast, a 10-15% decrease in binding to immobilized DR5 when pre-incubated with the highest concentration of DcR1 Ig. The difference in level of competition of rhTRAIL WT binding between DcR1 Ig and DR5 Ig is caused by a ~100 fold difference in affinity of rhTRAIL WT for the two receptors, 200 nM and <2 nM, respectively[188].

Table 2. EC_{50} values Colo205 and A2780 Cells.

	Colo205		A2780	
Ligand	EC_{50} (+/- s.d)	Max. Effect	EC_{50} (+/- s.d)	Max. Effect
	(ng/ml)	%Cell death	(ng/ml)	%Cell death
TRAIL	8.6 (0.9)	78% (8%)	15.6 (3)	41% (3%)
D269H	1.8 (0.5)	80% (4%)	4.7 (0)	70% (5%)
D269H E195R	1.5 (0.4)	80% (6%)	4.2 (1)	69% (2%)
D269H T214R	5.1 (2.6)	66% (9%)	12.1 (4)	66% (11%)

Biological activity

To assess the biological activity related to DR5 binding, various cancer cells were used. Colo205 colon carcinoma cells and ML-1 chronic myeloid leukemia cells express all four TRAIL receptors on the cell surface as shown using FACS analysis, (figure 6A and B), and are sensitive to TRAIL-induced apoptosis. In order to test the involvement of DR4 versus DR5 in TRAIL-induced cell death Colo205 cells were treated with neutralizing anti-DR4 or anti-DR5 antibody for 1 h prior to addition of TRAIL. Both antibodies reduced TRAIL-mediated cell death and had an additive effect when used in combination (figure 7A). However, the DR5 neutralizing antibody was approximately 3 times more effective than the DR4 neutralizing antibody, demonstrating that TRAIL-induced apoptosis in Colo205 cells is primarily mediated by DR5. In contrast, the DR4 pathway is the major mediator of TRAIL-induced apoptosis in ML-1 cells (figure 7A). In order to examine whether the DR5 specific TRAIL variants induce cell death in Colo205 cells via the DR5 receptor, 1 µg/ml of neutralizing anti-DR4 or anti-DR5 antibodies were administered 1 h prior to ligand

treatment. The presence of the anti-DR4 antibody failed to prevent death induced by the DR5 specific variants. On the other hand 1 μg/ml of anti-DR5 antibody could significantly reduce the amount cell death (figure 7B).

Colo205 and ML-1 cells were then treated with increasing concentrations of TRAIL or the DR5 specific variants D269H, D269H/E195R and D269H/T214R and their cytotoxic potential was measured with a MTT assay. In Colo205 cells all TRAIL ligands were biologically active and induced cell death at levels that were either comparable to that of rhTRAIL WT or were up to five fold more active (figure 7C; table 2). Contrary to Colo205 cells, only TRAIL was able to induce cell death in ML-1 cells (figure 3D). Similar results were obtained using EM-2 chronic myeloid leukemia cells expressing only DR4 receptor and lacking the DR5 receptor, and the ovarian cancer cell line A2780 which expresses DR5 but lacks DR4 on its surface and is relatively insensitive towards TRAIL-induced cell death (S. de Jong, personal communication). Although EM-2 cells were sensitive to TRAIL induced cell death (50 ng/ml TRAIL initiating more than 80% cell death), treatment with any of the DR5 mutants failed to induce significant cell death (figure 8A). In A2780 cells, on the other hand, the cytotoxic activity of D269H, D269H/E195R and D269H/T214R is significantly increased, showing both an increased maximum response and drastically decreased EC_{50} values when compared to rhTRAIL WT (figure 7E; table 2). An additional experiment using D269H/E195R in wild-type BJAB cells responsive to both DR4- and DR5-mediated cell death ($BJAB^{wt}$), BJAB cells deficient in DR5 ($BJAB^{DR5\ DEF}$) and BJAB cells deficient in DR5 and stably transfected with D R5 ($BJAB^{DR5\ DEF}$+DR5)[189] confirm our findings. D269H/E195R was able to induce cell death in $BJAB^{wt}$ cells but was unable to induce significant cell death in $BJAB^{DR5\ DEF}$ cells when compared to rhTRAIL WT. In the DR5 transfected $BJAB^{DR5\ DEF}$+DR5 cells, however, the cytotoxic potential was restored (figure 7F). The cytotoxic effects of these TRAIL variants on non-cancerous cells human umbilical vein endothelial cells (HUVEC) was assessed by incubating these cells in the presence of 100 ng/ml rhTRAIL WT or TRAIL variants. However, no cytotoxic effects were observed for rhTRAIL WT and the receptor selective TRAIL variants (figure 8B). Taken together, the results obtained with the Colo205, ML-1, A2780 and BJAB cell lines show that the biological activity of the D269H, D269H/E195R and D269H/T214R variants is specifically directed towards the DR5 receptor.

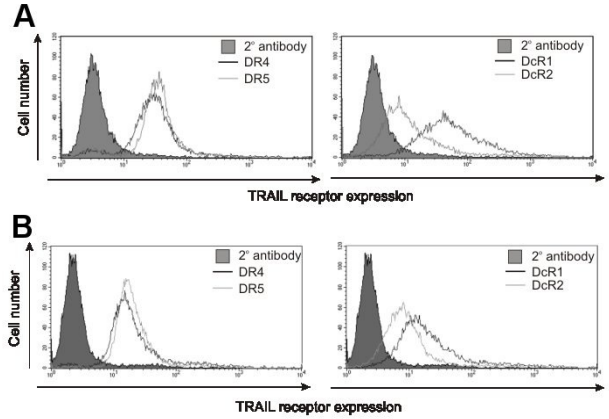

Figure 6. Cell surface expression of TRAIL receptors in A) Colo205 cells and B) ML-1 cells. Left panel: DR4 and DR5 receptor. Right panel: DcR1 and DcR2.

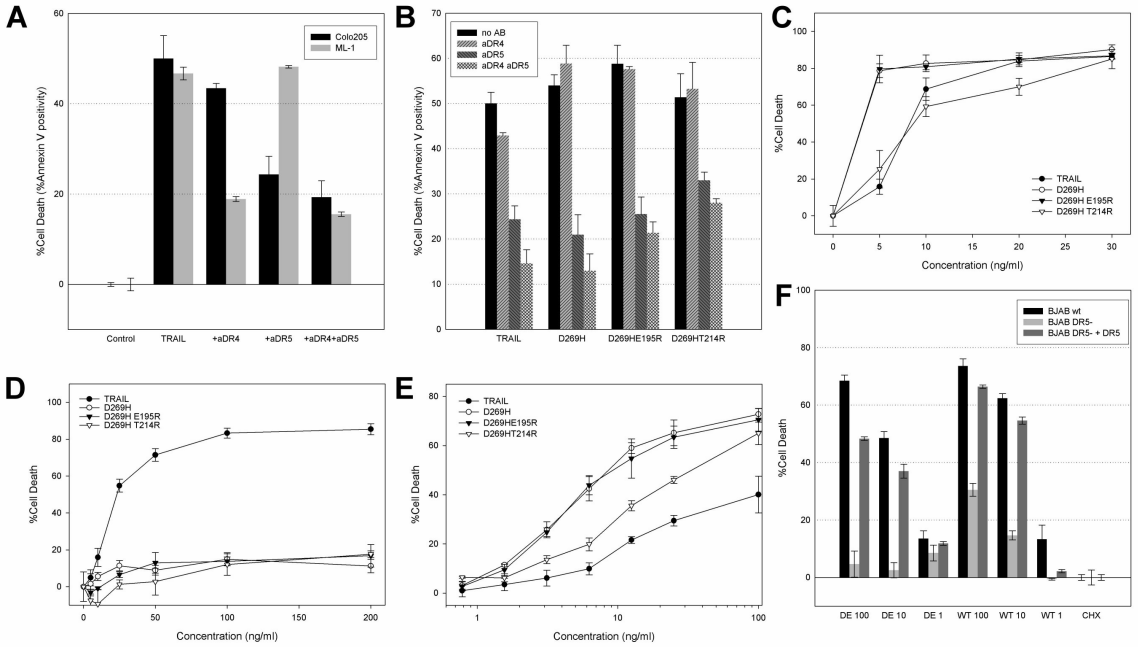

Figure 7. (A) Apoptosis inducing activity of 100 ng/ml TRAIL in the presence of 1 µg/ml DR4 (aDR4), DR5 (aDR5) or DR4 and DR5 (+aDR4+aDR5) receptor neutralizing antibodies in Colo205 and ML-1 cells. (B) Apoptosis inducing activity in Colo205 cells of 100 ng/ml TRAIL or DR5 selective variants without the presence of neutralizing DR4 or DR5 antibodies (no AB) or in the presence of neutralizing antibody (aDR4 or aDR5, or both, aDR4a DR5). Cytotoxic potential (%Cell death) of TRAIL or DR5 selective variants in: (C) Colo205 cells, (D) ML-1 cells, (E) A2780 cells and (F) of 1, 10 or 100 ng/ml TRAIL (WT) or D269H/E195R (DE) relative to cycloheximide control (0.33 µg/ml) in BJAB cells responsive to both DR4 and DR5 mediated cell death ($BJAB^{wt}$), BJAB cells deficient for DR5 ($BJAB^{DR5\ DEF}$)[189] and BJAB cells deficient for DR5 stably transfected with DR5 ($BJAB^{DR5\ DEF}$+DR5)[189].

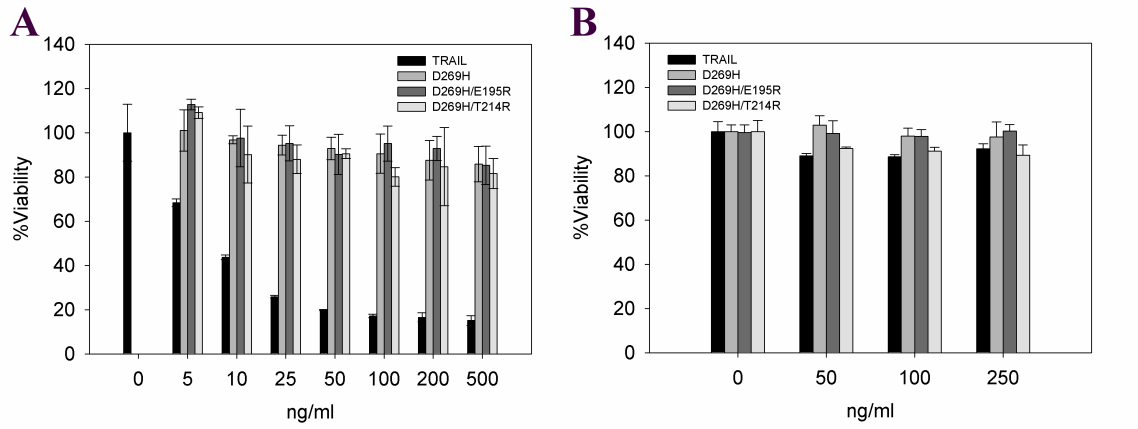

Figure 8. (A) Cytotoxic potential (%Viability) of TRAIL or DR5 selective variants in EM-2 cells. EM-2 cells express DR4 but not DR5. (B) Cytotoxic potential (%Viability) of rhTRAIL WT or DR5 selective variants in HUVEC cells.

Discussion

Since DR5 receptor is a good target for TRAIL cancer therapy (see Introduction) we choose to develop DR5 receptor selective variants of TRAIL by using a computational design strategy.

Structural basis for the changes in selectivity.
This study shows that residue 269 is one of the most important residues for DR5 selectivity. From the crystal structure of TRAIL in complex with DR5, it can be observed that this amino acid is not interacting directly with the receptor. Studying the models of TRAIL in complex with the other three receptors, reveals that Asp269 from TRAIL is interacting with Lys120 from the receptor. This lysine residue is conserved among the DR4, DcR1 and DcR2 receptors. In contrast, DR5 has an aspartate at this position (figure 9 A and B; figure 1A).

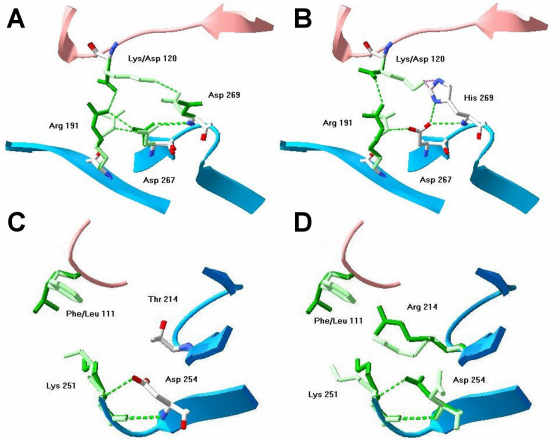

Figure 9. Area of interaction of TRAIL and DR4/DR5 receptor around position 269: A) TRAIL; B) D269H variant and around position 214: C) TRAIL; D) T214R variant. Ribbons color is red for receptor and blue for TRAIL. Residues in DR5-complexes are in dark green and residues in DR4-complexes in light green. Arg 191 and Asp 267 are key TRAIL amino acids for DR5 receptor binding in the corresponding binding pocket of the receptor, as observed in the crystal structure of TRAIL in complex with DR5.

Changing this amino acid to another with opposite charge, shows two cumulative effects. On one hand, breaking the Asp269-Lys120 interaction in the complex between TRAIL and receptors DR4, DcR1, and DcR2, would decrease TRAIL affinity towards them; furthermore, Lys120 has little space for re-accommodation, and this may even introduce some Van der Waals clashes in the area. On the other hand, Asp120 from DR5 receptor may interact with the protonated His269 of TRAIL, improving binding towards this receptor. In summary, this explains why a single mutation alone can greatly change the selectivity towards DR5, resulting in better binding to DR5 receptor and a substantial decrease in binding towards the other receptors. Residue 214 is also important for achieving DR5 selectivity. FOLD-X predicts for the T214R mutation a decrease in binding affinity for all receptors except DR5 (Table 1). This is due to the presence of a phenylalanine at position 111 in DR4 and a proline in DcR1 and DcR2, which prevent proper accommodation of Arg214 upon complex formation. As a result the arginine displaces

Asp254 and breaking intra-molecular H-bonds. In DR5 a leucine at position 111 allows accommodation of Arg214 without displacement of Asp254 (Fig. 4C and D). Additive effect of mutations towards selectivity can be expected in the cases where the positions of the mutations are far away enough from each other such that they cannot make any non-predictable interaction, e.g., mutations D269H and T214R.

Selective binding to different receptors.
Receptor binding experiments using SPR and competition ELISA experiments confirmed the modeling predictions. Variants D269H, D269H/E195R, D269K and D269R are between 70 to150 fold more selective for the DR5 receptor than for the DR4 when compared with rhTRAIL WT. The D269H/T214R variant showed no binding to the DR4 receptor at the highest concentration used in the assay (250 nM). The dissociation rates of TRAIL and the DR5 selective variants in complex with the DR5 and DR4 receptor were, however, too slow to measure accurately using SPR, thereby precluding the accurate determination of affinity constants. In the competition ELISA experiment, DR4 was unable to compete with immobilized DR5 for the binding to these designed selective variants, demonstrating that in the presence of both DR4 and DR5 these variants are markedly more selective towards DR5. The net gain in DR5 selectivity of these variants is the sum of both an increased preference for the DR5 and a reduced preference for the DR4 receptor, exemplifying both positive and negative design principles[86].
Binding of the D269H and D269H/E195R variants to the decoy DcR1 receptor was more than 20 fold reduced when compared to rhTRAIL WT. The D269H/T214R variant showed no binding to the DcR1 receptor at the highest concentration used in the assay (250 nM). Although binding of the D269H and D269H/E195R variants toward the decoy DcR2 receptor was reduced, the effect was much less pronounced when compared to the reduction in binding as observed with the other receptors. The different environment of Lys120 in receptor DcR2 when compared to DR4 and DcR1 could explain why the decrease in affinity is smaller in this case, in contrast to our predictions. However, the D269H/T214R variant showed a ~80% decrease in receptor binding to the DcR2 receptor when compared to rhTRAIL WT.

DR5 receptor produces apoptosis without additional cross-linking requirements
Using several different cancer cell lines, receptor selective behavior of the DR5 selective variants could also be demonstrated in several *in vitro* biological assays. In cells with the DR4 receptor as major mediator of TRAIL induced apoptosis (ML-1 and EM-2 cells), DR5 selective variants were unable to induce apoptosis even at high concentrations (200 ng/ml). These variants could however, induce apoptosis in cells with DR5 as the major mediator of TRAIL induced apoptosis (Colo205) and this induction could be antagonized using a neutralizing anti-DR5 antibody. The cell death inducing activity against Colo205 cells was comparable to rhTRAIL WT (EC_{50} ~8.6 ng/ml) in the case of D269H/T214R (EC_{50} ~5.1 ng/ml), or more than 5-fold increased in the case of D269H/E195R (EC_{50} ~1.5 ng/ml). In the DR5 positive and DR4 negative A2780 cells the increase in cell death inducing activity of the DR5 selective variants was even more pronounced. Using the various BJAB cell lines it could be confirmed that D269H/E195R mediated induction of cell death was dependant on the presence of the DR5 receptor and it was observed that the presence of the DR4 receptor only was not sufficient to induce cell death for this DR5 selective variant.

Taken together, the *in vitro* biological activity data convincingly demonstrates that differences in receptor selectivity as measured in the *in vitro* receptor binding assay is both relevant and significant in the *in vitro* biological context.
Both our results and results recently published[109] suggest that cross-linking TRAIL or membrane bound TRAIL are not an absolute prerequisite for DR5 mediated induction of apoptosis, as was concluded by others[190,191]. A 10-fold improvement in DR5 mediated activity of flag tagged TRAIL upon cross-linking was demonstrated, however this also resulted in toxicity in normal Cynomolgus monkey hepatocytes[109]. Our soluble trimeric DR5 selective TRAIL variants are capable of inducing DR5 receptor mediated apoptosis at lower concentrations than rhTRAIL WT, thus eliminating any requirement for antibody mediated cross-linking.

Designed versus Selected Variants
Other DR5 receptor selective TRAIL variants were recently isolated using phage display[109]. These variants were selected from saturation mutagenesis libraries that were constructed on the basis of a previously performed alanine scan[17]. Remarkably, the best DR5 selective mutant (DR5-8) contained 6 amino acid substitutions. Mutations found by us (e.g. D269H, E195R, T214R) to induce DR5 selectivity were not identified by the phage display approach. In a partial dissection to determine the role of each mutation in selectivity Kelley *et al.* could not eliminate any of the mutations without losing selectivity and/or biological activity[109]. It was concluded that to achieve receptor selectivity multiple amino acid substitutions were required. However our results clearly demonstrate that in case of the D269H/T214R variant, only two amino acid substitutions are required to obtain complete receptor selectivity. Having fewer mutations relative to the wild-type sequence appears favorable in view of a potential use of the DR5 selective variants as anticancer therapeutics, since fewer mutations are likely to reduce the risk of an immunogenic response.

Conclusion

This study shows that computational redesign of the receptor binding interface of TRAIL to obtain DR5 selective variants is achievable. In vitro analysis demonstrates that our DR5 selective mutants have increased affinity for DR5 whereas they do not bind to DR4. Our DR5 selective variants show high activity towards DR5 responsive cancer cells without the need for additional cross-linking. Consequently, these variants are of interest for the development as a potential anti-cancer therapeutic. Previously, we designed TRAIL variants with improved thermal stability using a computational redesign strategy[65]. Computational protein redesign methods are therefore a valuable addition to other protein engineering methodologies, such as directed evolution or experimental high throughput approaches, as a tool for the improvement of protein properties. Combining computational and experimental screening methods, is a powerful approach in protein engineering, a preliminary computational screening on proteins helps to identify the most important positions involved in protein-protein interactions and therefore decreases the number of variants to screen.

Methods

All reagents were of analytical grade unless specified otherwise. Recombinant TRAIL Ig receptor fusion proteins were ordered from R&D systems (R&D systems). PBS pH 7.4 and RPMI-1640 were obtained from Invitrogen. All other chemicals were from Sigma. All buffers used in SPR, ELISA and biological activity assays were of physiological pH and ionic strength.

Computational design of the mutants
Homology models of DR4, DcR1 and DcR2 were built using the WHAT IF[186] web interface based on human TRAIL in complex with the DR5 ectodomain[18]. Afterwards, these models were refined using the protein design options of FOLD-X, removing incorrect torsion angles, Van der Waal's clashes and accommodating TRAIL and receptor residues to their new interface and to build up the putative interactions between TRAIL and the three non-crystallized receptors through rotamer substitution. The crystal complex structure of TRAIL with DR5 receptor was also refined this way (see supplementary methods). A detailed description of the empirical force field FOLD-X is available elsewhere[160] (and at http://fold-x.embl-heidelberg.de).

In addition, the modified version of FOLD-X used in this work[150] is able to perform amino acid mutations accommodating this new residue and its surrounding amino acids the following way: It first mutates the selected position to alanine and annotates the side chain energies of the neighbour residues. Then it mutates this alanine to the selected amino acid and re-calculates the side chain energies of the same neighboring residues. Those that exhibit an energy difference are then mutated to themselves to see if another rotamer will be more favorable. This new feature allows proceeding through the whole computational design process using just one single force field. The method does not guarantee a global minimum, but we have found that it is able to find the WT side chain conformations when doing side chain-reconstruction from a poly-Ala backbone (Stricher, F. & Serrano, L "manuscript in preparation").

Side directed mutagenesis, Expression and Purification of selectivity mutants
cDNA corresponding to human soluble TRAIL (aa 114-281) was cloned in pET15B (Novagen) using *Nco*I and *BamH*I restriction sites. Mutants were constructed by PCR as described before.[65] Homotrimeric TRAIL proteins were purified using a 3 step purification as described before[65].

Determination of Receptor binding
Binding experiments were performed using a surface plasmon resonance-based biosensor Biacore 3000 (Biacore AB, Uppsala, Sweden). Immobilization of the DR4-Ig and DR5-Ig receptors on the sensor surface of a Biacore CM5 sensor chip was performed following a standard amine coupling procedure according to the manufacturer's instructions. Receptors were coated at a level of ~600-800 RU. Eighty µl TRAIL and variants were injected in three-fold at concentrations ranging from 250 nM to 0.1 nM at 70 µl/min and at 37 ^{o}C using PBS pH 7.4 supplemented with 0.005% v/v P20 (Biacore) as running and sample buffer. Binding of ligands to the receptors was monitored in real-time. Due to the very slow

dissociation of the TRAIL-receptor complex, only pre-steady state binding data could be obtained. Furthermore, a fast initial dissociation was observed directly after the end of injection, pointing at some heterogeneity in complex formation. In order to obtain data that represent proper high-affinity complex formation, the response at each concentration was recorded 30 s after the end of the injection. The response data as a function of TRAIL concentration were fitted using a four parameter equation to give an apparent affinity constant. Between injections the receptor/sensor surface was regenerated using 3 M sodium acetate pH 5.2 injections. DcR1-Ig and DcR2-Ig were captured using a protein A (Sigma) modified CM5 sensor chip and the protein A sensor surface was regenerated using 0.5 M glycine pH 2. For the pre-screening assay, 1:50 diluted clarified *E. coli* BL21 extracts were injected at 50 µl/min (see supplementary methods).

Biological activity

Cell line and treatment: Colo205 colon cancer cells, A2780 ovarium cancer cells, ML-1 myeloid leukaemia cells and the BJAB cell lines were maintained in RPMI1640 medium, 10% FCS, 1% penicillin, 1% streptomycin in humidified incubator, 37 °C, in 5 %CO2 environment. In the medium of $BJAB^{DR5\ DEF}$+DR5 cells puromycin (Sigma) was added to a final concentration of 1 µg/ml. TRAIL receptor inhibitors (neutralising antibodies) were always added 1h before TRAIL addition.

Annexin V staining: The Colo205 cells and ML-1 cells were seeded the day before the experiment at 10^5 cells/ml in 24 well plates (1ml/well) were treated with 1 µg/ml of anti-DR4 and/or anti-DR5 neutralising antibodies for 1h. 100 ng/ml rhTRAIL WT, D269H, D269H/E195R or D269H/T214R was added to the cells and incubated for 2h and 30 minutes. After treatment, the cells were harvested by scraping them gently off the wells and spun down. Control or treated Colo205 cells and ML-1 cells were harvested and collected by centrifugation, washed once in Annexin V incubation buffer and resuspended in 400µl fresh incubation buffer. 1 µl Annexin V was added to the samples, incubated at room temperature for 10 minutes and measured immediately on a FACSCalibur Flow cytometer (Beckton Dickinson), results being expressed as % of Annexin V positive cells.

MTT assay: MTT assay was performed as described before[65]. BJAB cell lines were incubated with 1, 10 or 100 ng/ml TRAIL or D269H/E195R in the presence of 0.33 ug/ml cycloheximide (Sigma) and for the EC_{50} determination Colo205 cells were treated with serial dilutions (25 ng/ml-0 ng/ml) of TRAIL or mutants and cytotoxicity was determined as described before[65]. EC_{50} values were calculated using a four parameter fit.

Supplementary Methods

Modeling of TRAIL-receptor Complexes. At present only crystal structures of TRAIL in complex with the DR5 receptor are known. The template selected was 1D4V[18], a structure at 2.2 Å resolution of human TRAIL in complex with the ectodomain of DR5 (TRAIL-R2) receptor. The complex of homotrimeric TRAIL and DR5 was generated using the protein quaternary structure server from the European Bioinformatics Institute (EBI) (http://pqs.ebi.ac.uk), using the symmetry coordinates in the PDB file. From the sequence alignment (Fig. 5*A*) of the different TRAIL receptors[187], it is observed that the receptor

cysteine-rich domains (CRDs) involved in the interaction with TRAIL (CRD2 and CRD3) are highly conserved, with the exception of the soluble receptor OPG. Indeed, when compared to DR5, the sequence identity of any other membrane-attached TRAIL receptor is >50% in each case, and there are neither insertions nor deletions in the sequence (with the exception of a glycine deletion in the middle of the CRD3 in DcR1). In addition, all the cysteines involved in the formation of internal disulfide bridges are conserved and share the same sequence position. Thus it is possible to build homology models of all TRAIL receptors except for OPG.

The homology models were built using the WHAT IF[186] web interface (http://swift.cmbi.kun.nl/WIWWWI//). The receptor models were superimposed on the DR5 receptor in complex with TRAIL, and after removal of the template receptor the initial complex models were obtained. Main chain conformation was not allowed to change during the homology modeling. After the reconstruction of the binding interfaces of TRAIL with the four different receptors a minimization round of 20 steps was performed, using Swiss-Pdb viewer (http://www.expasy.org/spdbv/) (4). This procedure reduces the possibility of having false energetic values due to slight van der Waals clashes produced by the binding interface reconstruction without changing the main chain conformation significantly. Afterward, these models were refined using the protein design options of FOLD-X, removing incorrect torsion angles, eliminating van der Waals clashes and accommodating TRAIL and receptor residues to their new interface. Similar results are obtained if the whole modeling exercise is done directly with FOLD-X; however, with the current FOLD-X version, the modeling is faster if WHAT IF is first used to place the side chains and subsequently followed by the use of FOLD-X to refine the structure (data not shown).

The FOLD-X force field calculates the free energy of unfolding (ΔG) of a target protein or protein complex combining the physical description of the interactions with empirical data obtained from experiments on proteins (5). Force field components (polar and hydrophobic solvation energies, van der Waals interactions, van der Waals clashes, H-bond energies, electrostatics in the complex and its effects on the rate of association (k_{on}) and backbone and side chain entropies) are calculated evaluating the properties of the structure, such as its atomic contact map, the accessibility of its atoms and residues, the backbone dihedral angles, the H-bond network and the electrostatic network of the protein (6). Water molecules making two or more H-bonds with the protein are also taken into account[183]. In addition, the modified version of FOLD-X used in this work[150] is able to perform amino acid mutations accommodating this new residue and its surrounding amino acids the following way: It first mutates the selected position to alanine and annotates the side chain energies of the neighboring residues. Then it mutates this alanine to the selected amino acid and recalculates the side chain energies of the same neighboring residues. Those residues that exhibit an energy difference are then mutated to themselves to see whether another rotamer will be more favorable. This new feature allows proceeding through the whole computational design process by using just a single force field, avoiding the use of PERLA[158,159] for rotamer substitution used in similar methodology works[65,85].

Screening for selectivity variants. TRAIL variant constructs were transformed to *Escherichia coli* BL21 (DE3) (Invitrogen). Variants and rhTRAIL WT were grown at a 10

ml scale by using a 2x LB medium. As controls, extracts of *Escherichia Coli* BL21 (DE3) without an overexpression plasmid and of an *E. coli* BL21 (DE3) culture with plasmid overexpressing SH3 domain were used. Cultures were grown as described in ref. 11. Cells were harvested by centrifugation. Pellet was resuspended in extraction buffer [PBS pH 7.4, 10% (vol/vol) glycerol and Complete Protease Inhibitor Cocktail (Roche)] in 25% of the original volume. Cells were disrupted by using sonication, and extracts were clarified by centrifugation at 20,000 g. TRAIL variant protein expression was assessed using SDS-PAGE. Clarified extracts of variants that were well expressed were subsequently diluted 1:50 in HBS-EP buffer (Biacore). These dilutions of the rhTRAIL WT and TRAIL variants were injected two-fold at a flow rate of 50 µl/min on a Biacore 2000. A Biacore CM5 sensor chip coated with ≈1500 Resonance Units (RU) of the TRAIL receptors DR4-Ig and DR5-Ig. A channel coated with ≈1500 RU of RANK-Ig receptor was used as control surface. Binding of ligands to the receptors was monitored in real time. The receptor/sensor surface was regenerated using 3 M sodium acetate (pH 5.2) injections. Ratios of binding for the different receptors were calculated relative to DR4 or DR5 binding.

Competitive ELISA. Nunc Maxisorb plates were coated for 2 h with DR5-Ig (100 ng per well) in 0.1 M sodium carbonate/bicarbonate buffer (pH 8.6), and remaining binding places were subsequently blocked with 2% BSA for 1 h. After washing for six times with Tris buffered saline/0.5% Tween 20 (TBST) (pH 7.5), preincubated (30 min) serial dilutions of soluble DR4-, DR5-, or DcR1-Ig (0-500 ng per well) and TRAIL or variants (10 ng per well) in PBS (pH 7.4) were added to the wells and incubated for 1 h at room temperature. After washing six times with TBST, a 1:200 dilution of anti-TRAIL antibody (R & D systems) was added and incubated for 1 h at room temperature, and, after washing six times with TBST, subsequently incubated with a 1:25,000 dilution of a horse radish peroxidase-conjugated swine-anti-goat antibody. After washing six times with TBST, 100 µl of 1-step Turbo TMB solution (Pierce) was added, and after ≈15 min, the reaction was quenched with 100 µl 1 M sulfuric acid. The absorbance was measured at 450 nM on a microplate reader (Thermolab systems, Breda, The Netherlands). Binding of TRAIL or variants to immobilized DR5-Ig with 0 ng per well of the soluble receptors was taken as 100%, and binding at other concentrations of soluble receptors was calculated relative to 0 ng per well of soluble receptor.

Acknowledgements

We would like to express gratitude to Dr. Andrew Thorburn for kindly providing the BJAB cell lines and Dr. Steven de Jong and Derk-Jan de Groot for providing and characterization of the A2780 cell line. We also thank Johanna Vrielink, Dr. Rob van Weeghel, Ron Suk, and Cátia Rodrigues for helpful discussions and technical assistance. This research was partly funded by the EU 5th framework program (QLK3-CT-2001-00498). R.H.C. was supported by the European Community initiative Interreg IIIA.

5

Towards the design of a DR4 selective TRAIL variant

Almer M. van der Sloot, Vicente Tur, Carlos Reis, Eva Szegezdi, Robbert H. Cool, Afshin Samali, Luis Serrano and Wim J. Quax

Abstract

Tumor necrosis factor-related apoptosis inducing ligand (TRAIL) is a potential anticancer drug that selectively induces apoptosis in a variety of cancer cells by interacting with death receptors DR4 and DR5. TRAIL can also bind to decoy receptors (DcR1, DcR2 and OPG receptor) that cannot induce apoptosis. The expression levels of DR4 and/or DR5 can be up-regulated in cancer cells in response to certain chemotherapeutic drugs. DR4 and DR5 receptor specific TRAIL variants will permit new and tumor selective therapies. The existence of certain cancer cells exclusively responding to DR4-mediated apoptosis, prompted us to make a DR4 selective TRAIL variant using computational protein design. Technically, the design of DR4 receptor selective TRAIL variants is still a considerable challenge due to the lack of a crystal structure of the TRAIL-DR4 complex. Nevertheless, our cell line assays indicate that the first designed variants induce apoptosis preferentially via DR4.

Introduction

Tumor necrosis factor (TNF) related apoptosis inducing-ligand (TRAIL) is currently attracting great interest as a potential anti-cancer therapeutic. TRAIL in its soluble form selectively induces apoptosis in tumor cells, *in vitro* and *in vivo*, by a death receptor mediated process. Unlike other apoptosis inducing TNF family members, soluble TRAIL appears to be inactive against normal healthy tissue[13]. TRAIL shows a high degree of promiscuity as it binds to five cognate receptors; DR4 (TRAIL-R1) and DR5 (TRAIL-R2) and to the decoy receptors DcR1 (TRAIL-R3), DcR2 (TRAIL-R4) and Osteoprotegerin (OPG)[19]. Upon binding to TRAIL, DR4 and DR5 receptors recruit Fas associated death domain (FADD)[20-22], which bind and activate the initiator caspases 8 and 10, leading to apoptosis[23-26]. DcR1 or DcR2 do not contain a death domain or contain a truncated death domain, respectively, and binding to these receptors does not induce apoptosis. In contrast, decoy receptors could prevent apoptosis by sequestering available TRAIL or by interfering in the formation of a TRAIL-DR4 or -DR5 signaling complex[30].

Use of DR4-receptor selective variants could permit better tumor specific therapies through escape from the decoy receptor-mediated antagonism, resulting in a higher efficacy with possibly less side effects as compared to rhTRAIL WT[179-181]. Receptors DR4 and/or DR5 were shown to be up-regulated after treatment with DNA damaging chemotherapeutic drugs and the response to TRAIL-induced apoptosis was significantly increased[19,182]. Previously, we described the design of DR5 selective TRAIL variants[108]. These variants showed an increased affinity for the DR5 receptor and decreased affinities for the DR4 and decoy receptors. The existence of certain cancer cells only responding to DR4-mediated apoptosis[108] and favorable results obtained with agonistic anti-DR4 antibodies[192], prompted us to design a DR4 selective TRAIL variant. Moreover, it was recently demonstrated that primary cells isolated from patients with chronic lymphocytic leukemia and mantle cell lymphoma were almost exclusively sensitive to DR4 mediated apoptosis[193,194].

In view of the observed lower affinity of rhTRAIL WT for DR4 than DR5[108,188], the design of an effective DR4 selective TRAIL variant preferably not only aims at decreased affinities for DR5 and decoy receptors, but also at an enhanced affinity for DR4. Consequently, it is essential to combine a positive design strategy strengthening the interactions between TRAIL and DR4 with a negative strategy that designs mutations disrupting interactions between TRAIL and the other receptors. Generally, it is less demanding to disrupt an existing interaction (or create an unfavorable one) by an amino acid substitution, than to create a new favorable interaction. A high quality structural model describing all the relevant interactions between the interacting partners is therefore of paramount importance. As no crystal structure of the TRAIL-DR4 complex is available, the design of a DR4 selective variant therefore critically depends on the quality of the homology model of the TRAIL-DR4 complex. We demonstrate here that the computational design of DR4-specific rhTRAIL variants is possible using a high quality homology model.

Results

Selectivity Design

For the design of a DR4 selective TRAIL variant, the procedure as previously used for the design of the DR5 selective TRAIL variants was used[108]. In short, the receptor binding interface of TRAIL was screened for single amino acid substitutions increasing the affinity for the DR4 receptor (=decreasing interaction energy ($\Delta\Delta G_i$)) or decreasing the affinity for DR5 and the decoy receptors. For the TRAIL-DR5-receptor complex a crystal structure was used and for the TRAIL-DR4-receptor complex a homology model consisting of TRAIL in complex with cysteine rich domains (CRDs) 2 and 3 of DR4 was constructed based on the TRAIL-DR5-receptor complex. FOLD-X was used to model and refine the TRAIL-DR4 receptor complex model. The accuracy of the models and the force field was tested using the affinity data derived from the alanine scanning of rhTRAIL WT as performed by Hymowitz *et al.* [17]. The predictions of the energy change in the complex formation correlates with the changes in the dissociation constants measured[108]. This implies that our method can reliably predict mutations at residue positions located at the receptor binding interface which will most severely affect the complex formation.

The FOLD-X design process proposed several TRAIL receptor interface positions and (single) amino-acid substitutions important for obtaining DR4 selectivity. One of the proposed mutations, K201R, was already present in a sextuple mutant selected by Kelley *et al.,*[109] again underlining the correctness of the DR4 model. In addition, new amino acid substitutions were calculated that have not been described before. From these, the D218Y and D218H mutations were predicted to cause the highest change in DR4 selectivity by improving the interaction with DR4 and decreasing the interaction with DR5 (figure 1). All mutations were made, produced and purified as described before[65,108].

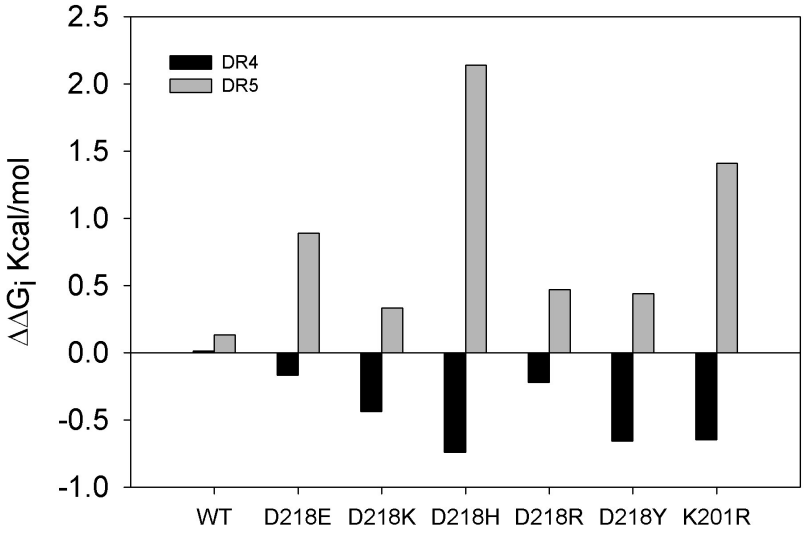

Figure 1. Results of FOLD-X calculation. A negative $\Delta\Delta G_i$ indicates an improvement in receptor binding and a positive $\Delta\Delta G_i$ indicates a decrease in receptor binding.

Receptor binding

Binding of the purified ligands to immobilized DR4- and DR5-Ig receptor chimeras was assessed in real-time using surface plasmon resonance (SPR). Receptor binding curves were recorded ranging from 0.5 nM to 250 nM (D218H) or 1 nM to 500 nM (D218Y) at 25 ^{o}C. The binding of D218Y and D218H towards immobilized DR5 Ig was more than 7-fold decreased when compared to rhTRAIL WT (rhTRAIL WT). In contrast, binding to immobilized DR4 Ig remained almost unchanged (figure 2A and B). These results show that the D218Y and D218H variants have become DR4 selective compared to rhTRAIL WT. As the DR4- and DR5-Ig chimera preparations were formulated with bovine serum albumin (BSA) upon lyophilization to stabilize the receptor chimera proteins, it was hard to precisely determine the exact amount of immobilized receptor chimeras. From maximum binding responses, it could be estimated that approximately 10 % of the immobilized protein was receptor-Ig conjugate.

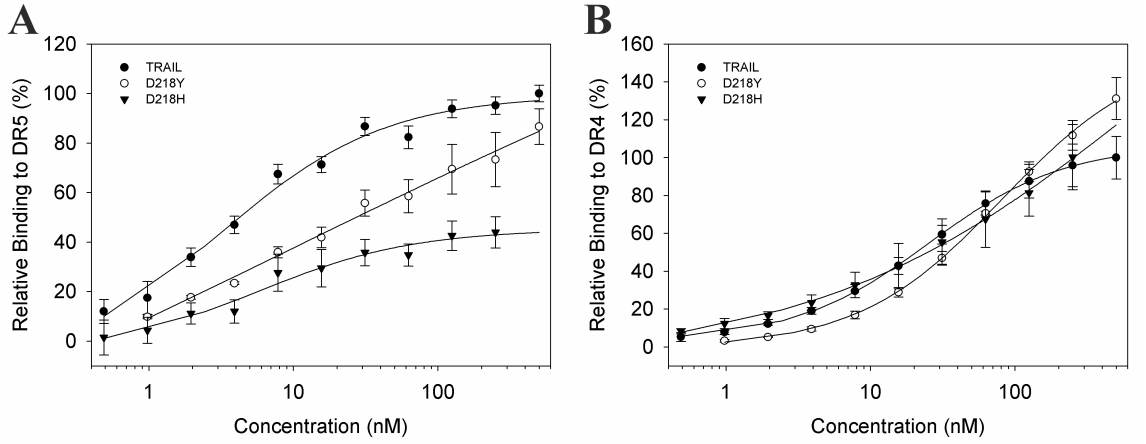

Figure 2. (A) Receptor binding of rhTRAIL WT and D218Y towards DR5-Ig as determined by SPR. (B) or towards DR4-Ig. (C) Receptor binding of rhTRAIL WT and D218Y or (D) towards DR4-Ig. Receptor binding was determined at 25 ^{o}C. DR4-Ig and DR5-Ig preparations formulated with BSA were immobilized on the sensor surface. Binding is calculated relative to the response of rhTRAIL WT at 250 nM.

In order to increase the signal to noise ratio it was decided to use DR4- and DR5-Ig receptor chimeras lyophilized without additional BSA. This allowed a more precise determination of the amount of receptor chimera immobilized on the SPR sensor surface. A SPR sensor chip was coated with ~800 RU of DR4 and DR5-Ig receptors, and receptor binding curves were recorded at 25 ^{o}C in real time at concentrations ranging from 0.5 nM to 250 nM of rhTRAIL WT, D218H and D218Y, respectively. As expected the measured response (in RU) was substantially increased. Unexpectedly, in this experiment the affinity of D218Y and D218H variants appeared to be decreased not only for the DR5 but also for the DR4 receptor (Figure 3A and B). Under these experimental conditions no change in receptor selectivity could be determined. The observed decrease in affinity for both receptors appeared not to change the DR4/DR5 receptor binding ratio. At this moment the reason for these deviating binding curves in presence and absence of BSA is not clear. It seems not logical that the presence of BSA would influence the DR4/DR5 binding ratio due to non specific interactions since binding to both DR4 and DR5 was simultaneously recorded. Any non specific interactions should then have been observed in both

sensorgrams. It should be realized that the SPR assay used for TRAIL-DR4 and -DR5 is not a simple 1:1 binding event; the injected TRAIL trimer has three receptor binding interfaces and the immobilized DR4- and DR5-Ig receptors are dimeric Fc construct based chimeras. Receptor chimera coating density dependent ligand binding effects can not be excluded, as it has been shown that several TNF-R family members including the TRAIL receptors contain a pre-ligand assembly domain (PLAD)[7,31], causing receptor oligomerization in the absence of ligand. Such effects are not easily detected since differences in immobilization densities not necessarily correlate to differences in physical densities on the flow cell surface; immobilization may primarily occur at the beginning of the flow cell, depending on the flow during immobilisation. Further testing is needed to clear this.

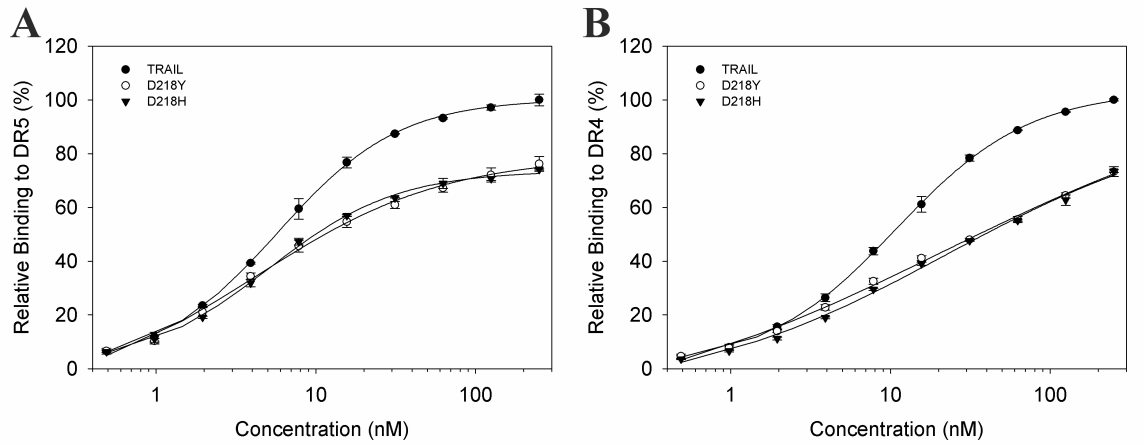

Figure 3. (A) Receptor binding of rhTRAIL WT, D218H and D218Y towards DR5-Ig as determined by SPR at 25 °C. (B) or towards DR4-Ig at 25 °C. DR4 and DR5-Ig preparations formulated without BSA were immobilized on the sensor surface. Binding is calculated relative to the response of rhTRAIL WT at 250 nM.

Interestingly, it has been reported that the affinity between rhTRAIL WT and especially DR4 is strongly dependent on temperature[188]. However, no significant changes in binding to DR4 or DR5 were observed for rhTRAIL WT, D218H and D218Y when repeating the assay at a temperature of 37 °C (Figure 4 A and B).

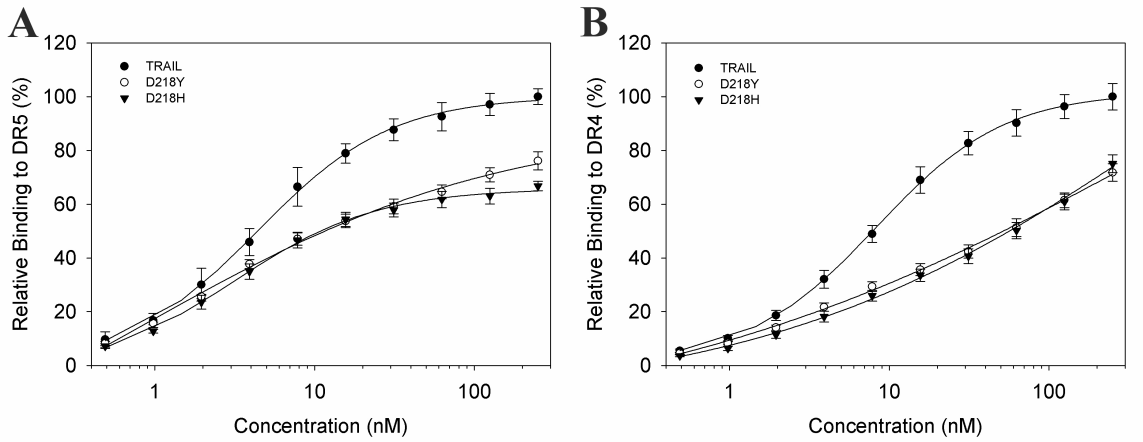

Figure 4. (A) Receptor binding of rhTRAIL WT, D218H and D218Y towards DR5-Ig as determined by SPR at 37 °C. (B) or towards DR4-Ig at 37 °C. DR4 and DR5-Ig preparations formulated without BSA were immobilized on the sensor surface. Binding is calculated relative to the response of rhTRAIL WT at 250 nM.

Extra experiments need to be performed to determine the cause of the observed differences between DR4 and DR5-Ig preparations with and without BSA. Visual inspection of the sensorgrams measured at 25 ^{o}C revealed that rhTRAIL WT virtually lacked an off-rate while both D218H and D218Y showed an initial increased off-rate at both receptors. However, the off-rate of D218H at DR4 appeared to be smaller than the off-rate of D218Y at DR4 while having approximately the same off-rate at the DR5 receptor, indicating that the affinity of D218H for DR4 might be higher than the affinity of D218Y for DR4 (Figure 5).

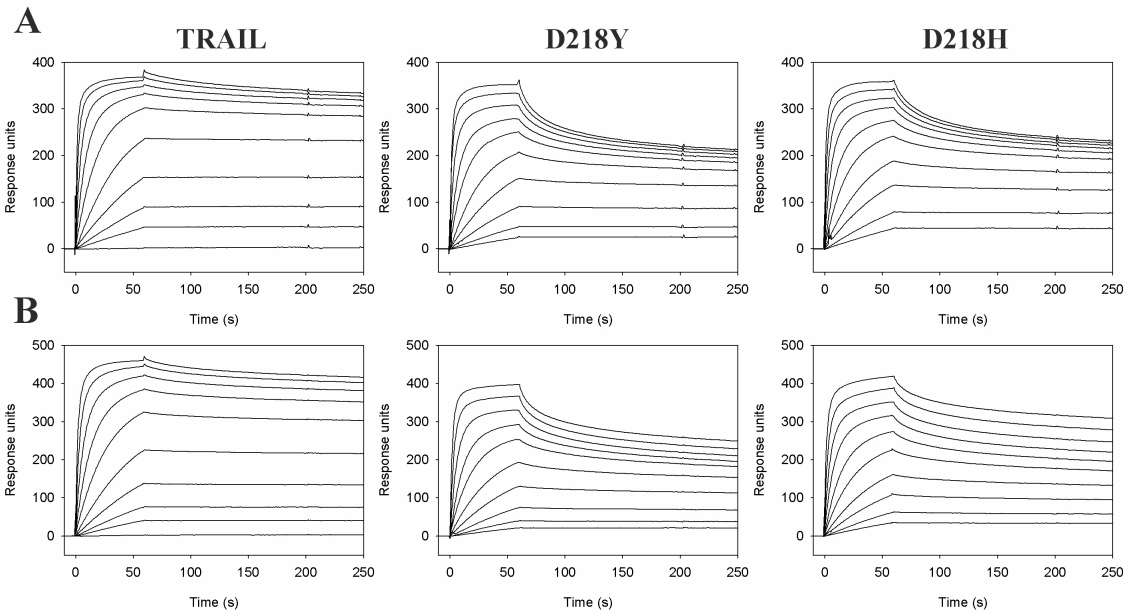

Figure 5. Time versus response SPR sensorgrams. (A) Receptor binding of rhTRAIL WT, D218H and D218Y towards DR5-Ig as determined by SPR at 25 ^{o}C. (B) or towards DR4-Ig at 25 ^{o}C. Depicted are the responses to concentrations of TRAIL or variants ranging from 250 nM to 0.5 nM.

Biological activity

To test the biological activity of D218Y and D218H variants, Colo205 and EM-2 cells were treated with this variant. Previously, it was established that Colo205 cells are sensitive towards TRAIL-induced apoptosis primarily mediated by DR5[108]. ML-1 cells, in contrast, are mainly sensitive towards TRAIL-induced apoptosis mediated by DR4[108]. The EM-2 cell line expresses only the DR4 receptor and hence is only sensitive towards TRAIL-induced apoptosis mediated by the DR4 receptor[108]. In Colo205 a large decrease in apoptosis inducing activity of D218Y and D218H was observed when compared to rhTRAIL WT and the DR5 selective D269HE195R variant (figure 6a). In contrast, in cell lines EM-2 and ML-1, D218Y and D218H variants were able to efficiently induce apoptosis at concentrations above 100 ng/ml (Figure 6B and C) whereas the DR5 selective variant D269H/E195R essentially lacks apoptosis inducing activity. The D218H showed enhanced apoptosis inducing activity when compared to D218Y but both variants are considerably less active than rhTRAIL WT. With regard to potential DR4 selective behavior it is important to correct for rhTRAIL WT sensitivity and to determine at what concentration the variants in comparison with rhTRAIL WT start to induce apoptosis (figure 7). In Colo205 cells

rhTRAIL WT induces a maximum level of apoptosis at a protein concentration of ~20 ng/ml. In ML-1 and EM-2 cells rhTRAIL WT induces a maximum level of apoptosis at a concentration of ~100 ng/ml.

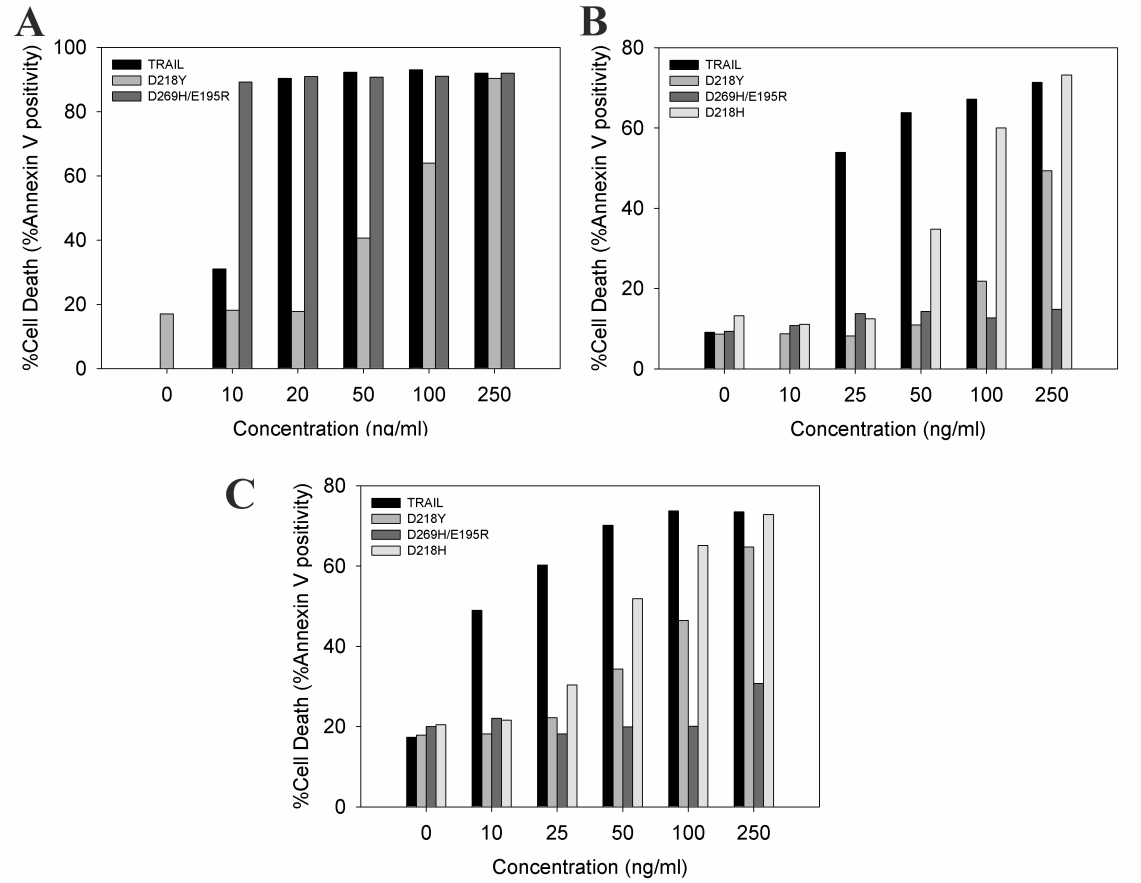

Figure 6. Biological activity of rhTRAIL WT, D218Y and D218H variants and the DR5 selective ligand D269HE195R in DR5 sensitive Colo205 cells and in DR4 sensitive ML-1 and EM-2 cells. Percentage apoptosis was measured as percentage Annexin V positivity after 3 hrs of incubation.

While in Colo205 cells no significant apoptosis is induced by the D218Y variant at a concentration of 20 ng/ml, the D218Y variant is able to induce a significant amount of apoptosis in EM-2 cells and in ML-1 cells at a concentration of 100 ng/ml. This is illustrated in figure 6 for rhTRAIL WT, D218Y and the DR5 selective variant D269H/E195R. Whereas the D218Y ligand is able to efficiently induce apoptosis in EM-2 cells, it shows a marked decrease in biological activity in Colo205 cells (figure 6). Taken together, these results indicate that the D218Y and D218H variants induce apoptosis preferentially via DR4.

Discussion

TRAIL interacts with five different receptors of the TNF-R family; however, only receptors DR4 and DR5 transmit the apoptosis inducing signal. Interestingly, it was shown that the expression levels of DR4 and/or DR5 were up-regulated in cancer cells in response to

certain chemotherapeutic drugs[19]. Previously we used computational protein design to construct a DR5 receptor selective TRAIL variant[108]. The existence of certain cancer cells exclusively responding to DR4-mediated apoptosis[108] and favorable results obtained with agonistic anti-DR4 antibodies[192], encouraged us to design a DR4 selective TRAIL variant using computational protein design.

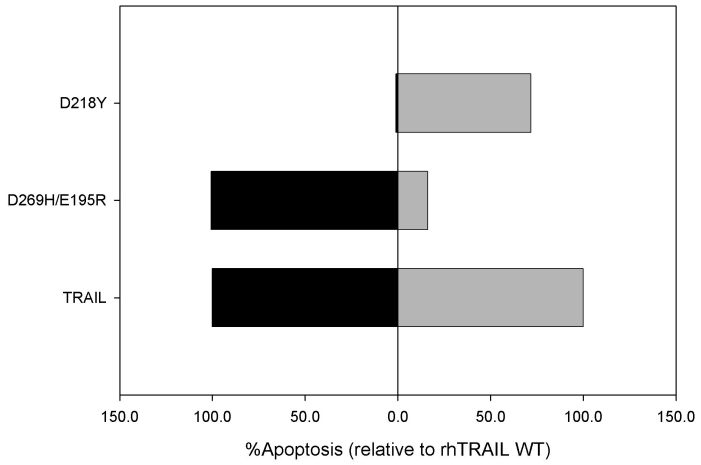

Figure 7. Biological activity of rhTRAIL WT, the D218Y variant and the DR5 selective ligand D269H/E195R in DR5 sensitive Colo205 cells and in DR4 sensitive EM-2 cells. Percentage apoptosis was measured as percentage Annexin V positivity after 3 hrs of incubation with 20 ng/ml (Colo205) or 100 ng/ml (EM-2) of rhTRAIL WT or variant. These concentrations were chosen as these are the concentrations were rhTRAIL WT starts to show its maximum apoptosis inducing activity. Apoptosis inducing activity is calculated relative to the apoptosis inducing activity of rhTRAIL WT at these concentrations.

It was demonstrated by us and others that computational protein design methods are a valuable addition to other established protein engineering methodologies, such as directed evolution methods using phage display, as a tool for the improvement and modification of protein-protein interactions[85-87,89,104,108]. Kelley *et al.,* recently described a DR4 selective TRAIL variant selected from a TRAIL saturation mutagenesis library using phage display[109]. However, subsequent analysis revealed that this DR4 selective TRAIL variant—comprising of 6 mutations relative to rhTRAIL WT—was biologically largely inactive[194]. Biological activity was restored partially after changing one of the mutations back to the wild-type amino acid[194]. In this study we focused on position Asp 218 predicted by the FOLD-X algorithm to be important for selectivity towards the DR4 receptor and not identified before with the phage-display approach of Kelley *et al*. Although the biological activity data indicate that the D218Y and D218H variants induce apoptosis preferentially via DR4 and thus seem DR4 selective, the SPR receptor binding data prevent any definitive conclusions with regard to receptor binding. Additional experiments have to be performed to resolve remaining questions; e.g. DR4 receptor coating density dependent effects on ligand binding have to be investigated. In addition, the biological activity of the D218H and D218Y variants should also be determined in a DR5 deficient cell line, e.g. A2780, as at higher protein concentrations Colo205 cells are sensitive towards DR4 mediated TRAIL-induced apoptosis. In any case, the goal to design a high affinity DR4 selective variant has not been fully reached yet. The lack of clear success in the design of a DR4 selective

TRAIL variant with high affinity for the DR4 receptor can, at least in part, be attributed to the quality of the TRAIL-DR4 homology model. Despite the validation of the currently used TRAIL-DR4 model, apparently not all important interactions are correctly captured in this model. As the computational protein design process critically depends on the quality of this DR4 homology model, improving the accuracy of the model is therefore of paramount importance. Allowing protein backbone flexibility in the construction of the binding interface between TRAIL and the DR4 receptor will probably already improve the quality of the model. Additional options are also available, short of determining the crystal structure of the TRAIL-DR4 complex. Although computationally demanding, recent advantages in homology modeling[195], in *de novo* protein structure prediction[149] and protein-protein docking will eventually allow the prediction of more accurate structural models of target complexes[196]. This in turn will allow more accurate designs with a reduced amount of false positive and false negative predictions. An alternative approach would be to use computational design to construct a library of (putative) receptor selective TRAIL variants enriched for structural stability and combing this with an *in vitro* screening or selection procedure to select the most receptor selective variants. Such an enriched library approach would allow the use of relatively coarse homology models to populate the library with amino acid substitutions having a putative receptor selective effect. High resolution crystal structural data of TRAIL can be used to assess the structural stability of the proposed amino acids substitutions and finally include only the structural favorable ones in the library. Structural stability of TRAIL can already be predicted as demonstrated by us in a previous work[65] and the concept of using computational design to devise "enriched libraries" has also been successfully demonstrated[100,146].

In summary, the first design predictions for DR4 selective rhTRAIL variants resulted in variants that do show DR4 specificity in cell line assays. Preliminary analytical SPR binding tests showed under standard conditions (immobilized receptor in presence of BSA) a lowered DR5 affinity and unchanged DR4 affinity in concert with the increased DR4 specificity. However, these binding studies were not conclusive in experiments without BSA.
In order to design a variant with higher affinity for the DR4 receptor the currently used homology model of the TRAIL-DR4 complex needs to be refined. The computational method used in our study is based on general applicable principles and it can be used on any other protein as template structure, spanning the whole sequence and structure space of protein families and protein folds. This was convincingly demonstrated in other protein design works using FOLD-X[65,85,108,183-185,197]. From a practical point of view, the FOLD-X computational design algorithm enables one to modify several key properties of proteins within a short time frame. Using directed evolution methods, the time from creating initial target diversity to obtain—by several rounds of selection—the final target can take several months to complete. In contrast, the time from initial design to the final target using a computational design method is substantially shorter. However, these methods are not necessarily mutually exclusive; combining computationally designed "quality enriched libraries" and *in vitro* screening or selection techniques combines the best of both methodologies, especially in cases when accurate structural information is lacking. Computational design methods in combination with *de novo* structure prediction methods

and/or in combination with traditional screening or selections methods will become tools of increasing importance in the development of successful protein therapeutics.

Methods

All reagents were of analytical grade unless specified otherwise. Isopropyl-β-D-1-thiogalactoside (IPTG), ampicillin and dithiotreitol (DTT) were from Duchefa. Chromatographic columns and media were from Amersham Biosciences. Restriction enzymes used were purchased from New England Biolabs. Recombinant TRAIL-receptor Ig fusion proteins formulated with and without BSA were ordered from R&D systems. All other chemicals were from Sigma.

Modeling of TRAIL-receptor complexes

At present only crystal structures of TRAIL in complex with the DR5 receptor are known. The template selected was 1D4V[18], the structure at 2.2 Å resolution and of monomeric human TRAIL in complex with the ectodomain of DR5 (TRAIL-R2) receptor. The homotrimer was generated using the protein quaternary structure server from the EBI (http://pqs.ebi.ac.uk), having the symmetry coordinates in the PDB file. From the sequence alignment of the different TRAIL receptors[187] it is observed that the receptor cysteine rich domains (CRDs) involved in the interaction with TRAIL (CRD2 and CRD3) are highly conserved, with the exception of the soluble receptor OPG[108]. Indeed, when compared to DR5, the sequence identity of any other membrane-attached TRAIL receptor is higher than 50% in each case, and there are neither insertions nor deletions in the sequence (with the exception of a glycine deletion in the middle of the CRD3 in DcR1). In addition, all the cysteines involved in the formation of internal disulfide bridges are conserved and share the same sequence position. Thus it is possible to build homology models of all TRAIL receptors except for OPG. The homology models were built using the WHAT IF[186] web interface (http://swift.cmbi.kun.nl/WIWWWI//), using the above mentioned template. The receptor models were superimposed on the structure of the TRAIL-DR5 complex, and after removal of the template receptor the initial complex models were obtained. Afterwards, these models were refined using the protein design options of FOLD-X, removing incorrect side chain torsion angles, eliminating Van der Waals clashes and accommodating TRAIL and receptor residues to their new interface (see Methods). Similar results are obtained if the whole modelling exercise is done directly with FOLD-X, however with the current FOLD-X version the modelling is faster if WHAT IF is used first to place the side chains, subsequently followed by the use of FOLD-X to refine the structure (data not shown).

Computational design of the mutants

A detailed description of the empirical force field FOLD-X is available elsewhere[160] (and at http://fold-x.embl-heidelberg.de). Briefly, this force field calculates the free energy of unfolding (ΔG) of a target protein or protein complex combining the physical description of the interactions with empirical data obtained from experiments on proteins. Force field components (polar and hydrophobic solvation energies, van der Waals' interactions, van der Waals clashes, H-bond energies, electrostatics in the complex and its effects on the k_{on} and backbone and side chain entropies) are calculated evaluating the properties of the structure, such as its atomic contact map, the accessibility of its atoms and residues, the

backbone dihedral angles, the H-bond network and the electrostatic network of the protein. Water molecules making two or more H-bonds with the protein are also taken into account[183].

In addition, the modified version of FOLD-X used in this work[150] is able to perform amino acid mutations accommodating this new residue and its surrounding amino acids the following way: It first mutates the selected position to alanine and annotates the side chain energies of the neighbour residues. Then it mutates this alanine to the selected amino acid and re-calculates the side chain energies of the same neighboring residues. Those that exhibit an energy difference are then mutated to themselves to see if another rotamer will be more favorable.

This procedure was also used to reconstruct the binding interface of TRAIL in complex with the modeled receptors DR4, DcR1 and DcR2 in order to repair residues with bad torsion angles or with Van der Waals' clashes between TRAIL and receptor residues, and to build up the putative interactions between TRAIL and the three non-crystallized receptors through rotamer substitution (see above). The crystal complex structure of TRAIL with DR5 receptor was also refined this way.

This new feature allows proceeding through the whole computational design process using just one single force field, avoiding the use of PERLA[158,159] for rotamer substitution used in similar methodology works[65,85].

Side directed mutagenesis, Expression and Purification of selectivity mutants

cDNA corresponding to human soluble TRAIL (aa 114-281) was cloned in pET15B (Novagen) using *Nco*I and *BamH*I restriction sites. Mutants were constructed by PCR as described before.[65] Homotrimeric TRAIL proteins were purified using a 3 step purification as described before[65].

Determination of Receptor binding

Binding experiments were performed using a surface plasmon resonance-based biosensor Biacore 3000 (Biacore AB, Uppsala, Sweden), at 25 ^{o}C or at 37 ^{o}C. Immobilization of the DR4-Ig and DR5-Ig receptors on the sensor surface of a Biacore CM5 sensor chip was performed following a standard amine coupling procedure according to the manufacturer's instructions at 25 ^{o}C. Receptors or receptors and BSA were coated at a level of ~600-800 RU. Purified TRAIL and TRAIL mutants were injected in three-fold at concentrations ranging from 250 nM to 0.1 nM at 70 µl/min flow rate. Binding of ligands to the receptors was monitored in real-time. Between injections the receptor/sensor surface was regenerated using 3 M sodium acetate pH 5.2 injections in case of DR4-Ig and DR5-Ig chimeras formulated with BSA or with a 1:1 mixture of 10 mM glycine, 1.5 M NaCl pH2 and ethylene glycol in case of regenerating immobilized DR4-Ig and DR5-Ig chimeras formulated without BSA.

Biological activity

Cell line and treatment: Colo205 colon cancer cells, ML-1 myeloid leukaemia cells and the EM-2 cell lines were maintained in RPMI1640 medium, 10% FCS, 1% penicillin, 1% streptomycin in humidified incubator, 37 °C, in 5 % CO_2 environment. *Annexin V staining*: The Colo205 cells, EM-2 cells and ML-1 cells were seeded the day before the experiment at 10^5 cells/ml in 24 well plates (1ml/well). Concentrations ranging from 10-250 ng/ml rhTRAIL WT, D269HE195R, D218H or D218Y was added to the cells and incubated for 2h and 30 minutes. After treatment, the cells were harvested by scraping them gently off the wells and spun down. Control or treated Colo205 cells, EM-2 cells and ML-1 cells were harvested and collected by centrifugation, washed once in Annexin V incubation buffer and resuspended in 400 µl fresh incubation buffer. 1 µl Annexin V was added to the samples, incubated at room temperature for 10 minutes and measured immediately on a FACSCalibur Flow cytometer (Beckton Dickinson), results were expressed as % of Annexin V positive cells.

6

Enhanced anti-cancer activity of a DR5 selective TRAIL variant in combination with a proteasome inhibitor or radiation therapy in a cervical cancer model

Almer M. van der Sloot, John H. Maduro, Robbert H. Cool,
Steven de Jong and Wim J. Quax

Abstract

Combination treatment with radiation therapy or chemotherapy can sensitize TRAIL resistant tumor cells and vice versa. In this study, we show that treatment of TRAIL resistant HeLa S3 cells with 10 μM of the proteasome inhibitor MG132 combined with a low concentration (10 ng/ml) of a DR5 selective TRAIL variant is able to induce apoptosis in this cell line in a synergistic fashion. Moreover, this combination is significantly more potent than similar concentrations of MG132 and rhTRAIL. Preliminary results suggest that also the sequential combination of 10 Gγ ionizing radiation and low concentrations (5-10 ng/ml) of the DR5 selective TRAIL variant is able to induce significantly more apoptosis in HeLa S3 cells than either treatment alone and that this combination is more potent than 10 Gγ ionizing radiation and 5-10 ng/ml rhTRAIL. Although the exact molecular mechanism of the enhanced potency of the DR5 selective TRAIL variant when used in combination with radiotherapy or a proteasome inhibitor remains to be elucidated, DR5 receptor selective TRAIL variants permit novel targeted and tumor selective anti-cancer therapies.

Introduction

Tumor necrosis factor (TNF) related apoptosis inducing-ligand (TRAIL) is currently attracting great interest as a potential cancer therapeutic. TRAIL in its soluble form selectively induces apoptosis in tumor cells *in vitro* and *in vivo* in several preclinical models[19]. TRAIL binds to five cognate receptors; to the death receptors DR4 (TRAIL-R1) and DR5 (TRAIL-R2) and to the decoy receptors DcR1 (TRAIL-R3), DcR2 (TRAIL-R4) and osteoprotegerin (OPG)[19]. Binding of TRAIL to the DR4 and DR5 receptors induces apoptosis by activating the cell-extrinsic or death receptor-mediated apoptosis pathway. Upon binding with TRAIL the death receptors trimerize and an intracellular death-inducing signaling complex (DISC) is assembled; the intracellular death domains of DR4 and DR5 recruit Fas associated death domain (FADD)[20-22], which bind and activate the apoptosis initiator caspases 8 and 10[23-26]. This leads to the activation of the apoptosis executioner caspase 3, followed by the activation of other proteases and nucleases resulting finally in apoptosis[27,28]. This process can be inhibited by the cellular FLICE like-inhibitory protein (cFLIP), an inhibitor of caspase activation, or by inhibitor of apoptosis proteins (IAPs) such as X-IAP[29]. DcR1 or DcR2 do not contain an intracellular death domain or contain a truncated death domain, respectively. Binding to these receptors does not induce apoptosis, in contrast, it could prevent apoptosis by sequestering available TRAIL or by interfering in the formation of a TRAIL DR4 or DR5 signaling complex[30]. The physiological relevance of the third decoy receptor OPG is unclear; this soluble receptor is able to bind TRAIL although the affinity at physiological temperature is rather low[188]**.** Recently, we designed DR5 selective TRAIL variants, which show reduced binding to the DR4 receptor as well as reduced binding to both decoy receptors and OPG[108].

It has been shown that TRAIL treatment enhances the efficacy of irradiation and chemotherapeutic treatment or, alternatively, these treatments can resensitize TRAIL resistant tumor cells[198]. Moreover, in experimental anti-cancer treatment, the receptors DR4 and/or DR5 were shown to be up-regulated after treatment with chemotherapeutic drugs or irradiation and the response to TRAIL-induced apoptosis was significantly increased[19,107,182]. Exposure to most anticancer chemotherapeutics and irradiation triggers the cell-intrinsic or mitochondrial apoptosis pathway, this in contrast to TRAIL treatment which induces the cell-extrinsic or death receptor-mediated apoptosis pathway[28]. Upon activation of the cell-intrinsic or mitochondrial pathway by DNA damaging chemotherapeutics or irradiation, apoptogenic factors such as cytochrome-c and smac/diablo are released from the mitochondria into the cytosol by pro-apoptotic members of the Bcl-2 family. Cytochrome-c binds in the cytosol the adaptor protein apoptosis–activating factor-1 (Apaf-1), forming an "apoptosome" resulting in the recruitment and activation of apoptosis initiator caspase—caspase 9—of the cell-intrinsic pathway. Similar to the activation of the initiator caspase of the death receptor-mediated apoptosis pathway, activation of caspase 9 also results in the activation of the downstream "executioner" or effector caspases (caspase 3, 6 and 7), ultimately resulting in apoptosis[105,199].

The death receptor-mediated pathway and the mitochondrial pathway are connected via the pro-apoptotic Bcl-2 family member Bid, a substrate of caspase 3 and 8. Depending on the particular cell type, activation of the effector caspases (e.g. caspase 3) is induced directly after stimulating the death-receptor pathway and subsequent activation of caspase 8 (type I

cells). However in type II cells, amplification via the mitochondrial pathway through activated truncated Bid (tBid) is required to activate the effector caspases. Translocation of tBid to the mitochondria triggers the release of cytochrome-c and smac/diablo, in cooperation with two other pro-apoptotic Bcl-2 family members Bak or Bax. A decrease in expression levels of these pro-apoptotic Bcl-2 family members or increases in the expression levels of anti-apoptotic Bcl-2 family members such as Bcl-2 or Bcl-x_L, disrupts apoptotic signaling of the cell-intrinsic pathway and causing resistance to anticancer therapy[19,29,198].

Whereas apoptosis induction by the intrinsic pathway often depends on the presence of functional p53, TRAIL has been shown to induce apoptosis independently of p53 function. Irradiation appears to specifically up-regulate DR5 receptor expression and the combination of irradiation and TRAIL treatment has been demonstrated to have an additive or synergistic effect[107,200]. Up-regulation of DR5 receptor expression in response to irradiation was demonstrated being both dependent as well as independent on the presence of functional p53[200-202]. Treatment with proteasome inhibitors have also been reported to up-regulate DR5 and/or DR4 receptor expression[203-205]. Proteasome inhibitors can sensitize tumor cells to TRAIL-mediated apoptosis by several mechanisms including, inactivation of the nuclear factor kappa Beta (NF-κB) pathway, modulating the balance between pro- and anti-apoptotic Bcl-2 members resulting in the accumulation of pro-apoptotic members, reducing levels of IAPs (e.g. X-IAP), reduction of cFLIP levels, or reduced degradation of p53. In the present study, we have investigated the co-treatment of TRAIL or a DR5 selective variant in combination with a proteasome inhibitor or irradiation in the human cervical cancer cell line HeLa S3. We reasoned that a DR5 receptor selective TRAIL variant in combination with irradiation or a proteasome inhibitor might show enhanced synergistic or additive activity when compared to rhTRAIL WT in apoptosis induction. The HeLa S3 cell line has a wild type functional p53[206] and harbors the HPV18 oncogene[207]. This oncogene encodes the HPV E6 protein which inactivates p53 by targeting it to the proteasome for degradation[208]. In addition, this cell line is only slightly sensitive to TRAIL induced apoptosis but can be sensitized when treated with a proteasome inhibitor[205]. Preliminary results indicate an enhanced synergistic behavior between the DR5 selective TRAIL variant in combination with a proteasome inhibitor or irradiation when compared to rhTRAIL WT. Combination of a DR5 selective TRAIL variant with a proteasome inhibitor or irradiation could therefore be a highly complementary treatment strategy.

Results

Treatment with radiation therapy and rhTRAIL WT or D269H/E195R.

The viability of HeLa cells upon treatment with rhTRAIL WT or DR5 selective TRAIL variant D269H/E195R in combination with 10 Gγ ionizing radiation was determined using a MTT assay. After exposing the cells to the required dose of ionizing radiation (0.9 Gy/min, 10 Gy total) the cells were further incubated with 5, 10 or 50 ng/ml rhTRAIL WT or D269H/E195R. Cells treated only with 5 or 50 ng/ml rhTRAIL WT or D269H/E195R were used as control. After treatment the viability of the cells was assessed using a MTT assay. Upon treatment with only rhTRAIL WT or D269H/E195R the viability of the HeLa

cells was hardly affected, at the highest concentration tested (50 ng/ml) rhTRAIL WT reduces the viability with less than 20% and D269H/E195R causes a reduction in viability of less than 5%. This low sensitivity of HeLa cells for rhTRAIL WT is in agreement with a previous study of Hougardy et al.,[205]. Conversely, after an accumulated dose of 10 Gy of ionizing irradiation the response to rhTRAIL WT treatment was markedly increased. The decrease in viability of the HeLa cells sequentially treated with 10 Gy of irradiation and 50 ng/ml rhTRAIL WT was more than doubled when compared to cells only treated with 50 ng/ml rhTRAIL WT (Figure 1a). The combination of D269H/E195R and radiotherapy gave even a more pronounced effect. Although the maximum effect on viability of D269H/E195R in combination with radiation therapy was equal to the effect of rhTRAIL WT at 50 ng/ml in combination with radiation therapy, this effect was already reached at 5 ng/ml while rhTRAIL WT reached the same level of effect only at 50 ng/ml (Figure 1a). In a second experiment the more potent effect of D269H/E195R in combination with radiotherapy was confirmed, at concentrations of both 1 ng/ml and 5 ng/ml the decrease in viability was more pronounced than that of similar concentrations of rhTRAIL WT (Figure 1b).

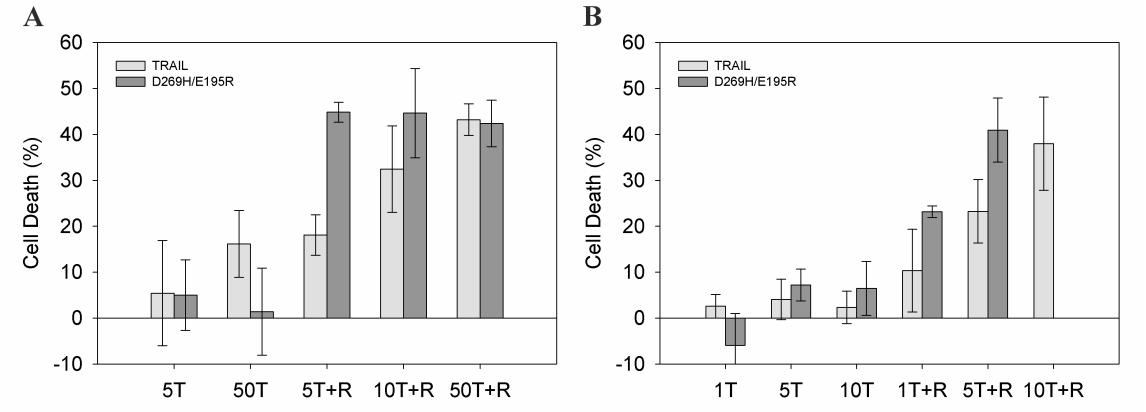

Figure 1. A and B. Cell death induced by radiation therapy in combination with rhTRAIL WT or a DR5 selective TRAIL variant in HeLa cells. Cells were sequentially treated with 10 Gy of irradiation and 1-50 ng/ml rhTRAIL WT or D269H/E195R. Figure 1A and 1B are two independent experiments; the error bars depict the variation (standard deviation) within a single experiment. Legend; WT: rhTRAIL WT; D/E: D269H/E195R; T: treated with 1-50 ng/ml rhTRAIL WT or D269H/E195R; R: 10 Gy of irradiation.

In order to confirm that the observed increase in cell death upon treatment with rhTRAIL WT or D269H/E195R in combination with radiotherapy was indeed caused by apoptosis, HeLa cells were treated with 10 ng/ml rhTRAIL WT or D269H/E195R with and without 10 Gy ionizing radiation and apoptosis was determined with acridine orange staining. The combination of 10 ng/ml rhTRAIL WT or D269H/E195R with 10 Gy ionizing radiation induces a high level of apoptosis (>50%) while when treating cells with only 10 ng/ml rhTRAIL WT or D269H/E195R only 5% of the cells appear to be apoptotic (Figure 2). Taken together, these results suggest that the DR5 selective TRAIL variant might be more potent than rhTRAIL WT when combined with radiotherapy. Both the DR5 selective variant and rhTRAIL WT when combined with radiotherapy appear to exert their effect by an increase in the level of apoptosis.

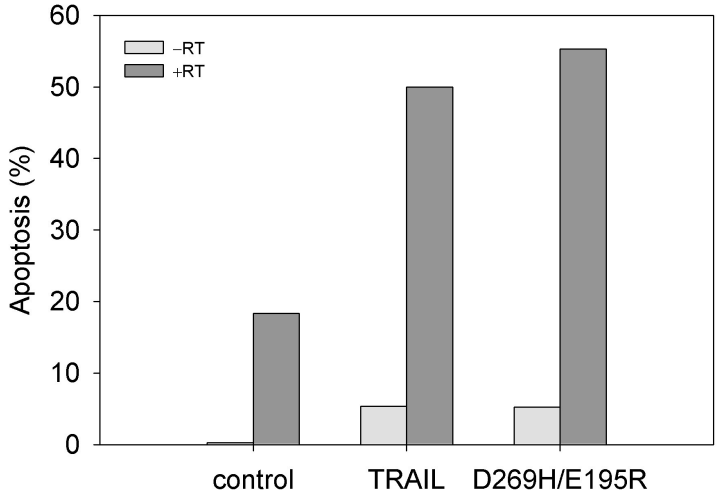

Figure 2. Apoptosis induced in HeLa cells by radiation therapy in combination with rhTRAIL WT or a DR5 selective TRAIL variant. Cells were sequentially treated with 10 Gy of irradiation and 10 ng/ml rhTRAIL WT or D269H/E195R. Legend; WT: rhTRAIL WT; D/E: D269H/E195R; -RT: no radiation therapy; +RT: 10 Gy of irradiation.

Treatment with proteasome inhibitor and rhTRAIL WT or D269H/E195R

Recently, it was demonstrated that co-treatment of HeLa cells with the proteasome inhibitor MG132 could sensitize these cells for TRAIL induced apoptosis[205]. Both the DR5 receptor and, to a lesser extend, the DR4 receptor were found to be upregulated in response to treatment with MG132. However, the apoptotic inducing capability of rhTRAIL WT upon co-treatment with MG132 could partially be inhibited by an antagonistic DR4 antibody[205]. To examine the efficacy of a DR5 selective TRAIL variant in this setting, HeLa cells were pretreated with 10 μM of the proteasome inhibitor MG132. After 2 hr, 10 ng/ml rhTRAIL WT or D269H/E195R were added to the cells and incubated for another 4 and 6 hours. Untreated HeLa cells and HeLa cells treated only with 10 ng/ml rhTRAIL WT, D269H/E195R or 10 μM MG132 were used as controls. Following incubation the number of apoptotic cells was determined using acridine orange staining. After incubation for 4 and 6 hours, cells treated with only rhTRAIL WT, D269H/E195R or MG132 showed only a small increase in the number of apoptotic cells when compared to the untreated cells, in all cases the percentage of apoptotic cells was well below 10% (Figure 3). Treatment with MG132 and rhTRAIL WT for 6 h, caused a ~2-fold increase in the number of apoptotic HeLa cells when compared to the controls. In cells treated with MG132 and D269H/E195R this effect was much more pronounced. Even after 4 h of incubation with D269H/E195R the number of apoptotic cells was more than 3-fold higher then after treatment with only MG132 or D269H/E195R. A 7-fold increase in the number of apoptotic cells was observed after 6 h of incubation with D269H/E195R and MG132 (Figure 3). Both at 4 h as well as at 6 h of treatment with D269H/E195R in combination with MG132, this combination was significantly more potent than the combination of rhTRAIL WT and MG132 ($p = 0.006$ and $p = 0.02$, for 4 and 6 h treatment, respectively). These results demonstrate that TRAIL variants can be used to trigger apoptosis through a DR5 receptor mediated pathway when combined with a proteasome inhibitor in HeLa cells in a synergistic fashion. Moreover, the

DR5 selective TRAIL variant shows higher potency than rhTRAIL WT when used in combination with a proteasome inhibitor.

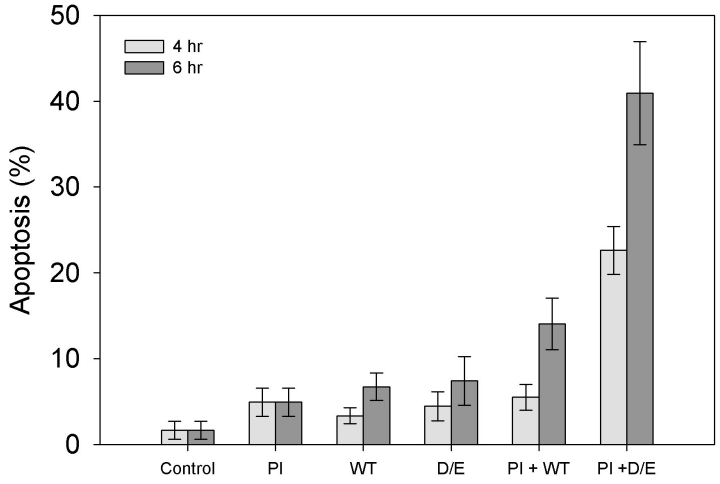

Figure 3. Combined treatment of proteasome inhibitor and rhTRAIL WT or DR5 selective TRAIL variant in HeLa cells. Legend; WT: 10 ng/ml rhTRAIL WT; D/E: 10 ng/ml D269H/E195R; PI: proteasome inhibitor MG132 (10 μM). Apoptosis was determined after 4 and 6 hr of treatment with rhTRAIL WT or D269H/E195R. Mean and standard error of three independent experiments.

Discussion

TRAIL interacts with five different receptors of the TNF-R family; however, only DR4 and DR5 transmit the apoptosis inducing signal. Furthermore, it was shown that the expression levels of DR5 were up-regulated in cancer cells in response to certain chemotherapeutic drugs (15) and in response to ionizing radiation (16). Therefore, we recently developed DR5 receptor selective variants of TRAIL in order to permit novel tumor selective anti-cancer therapies[108].

Treatment of HeLa cancer cells with either rhTRAIL WT, D269H/E195R or the proteasome inhibitor MG132 only gave a marginal effect. However, treatment of HeLa cells with MG132 followed by treatment with rhTRAIL WT or D269H/E195R was shown to have a synergistic effect, this treatment resulted in a manifest increase in cell death when compared to either treatment alone. Radiotherapy as well sensitized HeLa cells towards apoptosis induced by rhTRAIL WT or D269H/E195R. In this study we compared the efficacy of rhTRAIL WT and the DR5 selective TRAIL variant D269H/E195R, the combination of the proteasome inhibitor MG132 and D269H/E195R was shown to be significantly more potent in the induction of apoptosis than the combination MG132 and rhTRAIL WT. Furthermore, the available data indicates that the combination of radiotherapy and D269H/E195R might be more potent than the combination of radiotherapy and rhTRAIL WT.
Sensitization of TRAIL resistant cancer cells by chemotherapeutics or radiotherapy are mediated by both p53 dependent and p53 independent mechanisms[202]. Activation of p53 by DNA damaging stressors or inhibition of p53 degradation by using proteasome inhibitors,

causes an increase in the expression levels of several proteins implicated in apoptosis signaling[198,209]. DNA damage induced p53 activation results in transcriptional activation of FAS and DR5 death receptors through their p53 transactivation sites in the genes encoding these death receptors. Other examples are the activation in a p53 dependent manner of Bax, Bid, Noxa and other pro-apoptotic Bcl-2 members and the p53 dependent transcriptional activation of caspase 10[29,198,209]. Chemotherapeutic drugs induce the expression levels of DR4 and DR5 and enhance the efficacy of TRAIL induced apoptosis, both in p53 wild-type and p53 negative or mutant cells[198,210,211]. DR5 up-regulation in response to treatment with the proteasome inhibitor MG132 was found to be induced both at the transcriptional level and protein level through the CCAAT/Enhancer-binding protein homologues protein (CHOP) and this up-regulation was (probably) independent from p53 function[212]. Up-regulation of DR5 receptor expression in response to irradiation was demonstrated being both dependent as well as independent on the presence of functional p53[107,200-202,213]. However, the surface expression level of DR4 or DR5 receptors does not always correlate with the sensitivity for TRAIL induced apoptosis mediated by those receptors[108,214]. Similarly, no tight correlation was observed between irradiation induced DR5 up-regulation and tumor cell sensitization to TRAIL[200]. Apart from DR4 and DR5 receptor expression levels and the involvement of p53, the direct contribution of pro-apoptotic Bcl-2 members in the sensitization to TRAIL induced apoptosis in response to irraditiation or treatment with proteasome inhibitors is equally complex. In irradiation-induced sensitization to TRAIL induced apoptosis the levels of Bax and Bak were upregulated in a prostate cancer model[202], in another prostate cancer model and in a colon cancer model Bax was reported to be essential and Bak to be dispensable for the synergy between TRAIL induced apoptosis and irradiation[215], and in a mesothelioma cancer model Bid was found to be essential[216]. The sensitization to TRAIL induced apoptosis in response to treatment with the proteasome inhibitor MG132 was reported to be independent of Bax in a colon cancer model[204]. The pro-apoptotic Bcl-2 family member Bik was reported to be involved in the sensitization toward TRAIL induced apoptosis upon treatment with proteasome inhibitors in colon cancer models[217].

In a recent study, Hougardy et al., examined the effects of combination treatment of a proteasome inhibitor with rhTRAIL WT in HeLa cells[205]. Treatment with the proteasome inhibitor MG132 strongly sensitized cells to TRAIL induced apoptosis. In response to treatment with MG132 both the DR5 receptor and, to a lesser extend, the DR4 receptor were up-regulated. DR5 receptor up-regulation was found to be partially dependent on p53 up-regulation while DR4 up-regulation was independent of p53, as was the effect on TRAIL induced apoptosis. In addition, inactivation of XIAP was found to contribute to proteasome inhibitor-induced sensitization to TRAIL-induced apoptosis[205]. Radiotherapy also induced DR5 membrane expression levels in HeLa cells without affecting DR4 receptor expression levels (Maduro et al., manuscript in preparation). The increase in DR5 receptor membrane expression levels was found to be dependent on an increase in p53 expression levels and the increase in apoptosis after irradiation was not dependent on increased p53 expression levels. Irradiation did not change the expression levels of the pro- and anti- apoptotic mitochondrial proteins like Bax, Bak or Bcl2. Surprisingly, using siRNA to block DR4 and DR5 receptor expression, it was found that both the DR4 and DR5 receptors mediate the TRAIL induced apoptosis after irradiation rather than the DR5 receptor (Maduro et al., manuscript in preparation). In the present study we demonstrate

that triggering of the DR5 receptor mediated pathway by a DR5 selective TRAIL variant also efficiently induces apoptosis after sensitization by a proteasome inhibitor or ionizing radiation. How to explain the results in the present study with the observed DR4 dependency in the previous study? Blocking experiments with siRNA and antagonistic antibodies in the previous study revealed that at least a fraction of the cell death could still be mediated by the DR5 receptor. A partial explanation of the observed efficacy of the DR5 selective TRAIL variant could then be the higher affinity of D269H/E195R for the DR5 receptor and the lower affinity for decoy receptors[108], allowing D269H/E195R to make more efficiently use of the available (functional) DR5 receptors than similar concentrations of rhTRAIL WT. Additionally, the observed efficacy of the DR5 selective TRAIL variant could also be in part due to utilizing DR5 receptor-induced Caspase 10 mediated apoptosis. It was previously demonstrated that at low TRAIL concentrations or at early assessed time points TRAIL could induce caspase 10 mediated apoptosis via a DR5-mediated mechanism but not via a DR4-mediated mechanism[218]. The DR5 selective variant could possibly trigger this particular route with enhanced efficacy compared to rhTRAIL WT due to its higher affinity for DR5 and its inability to form DR4/DR5 heteromeric complexes as, in contrast, has been demonstrated for rhTRAIL WT[23]. Further research using receptor specific antagonistic antibodies and siRNA experiments should further elucidate the role of each death and decoy receptor and of intracellular components responsible for the observed potency of the DR5 selective TRAIL variant. Despite the uncertainty of the exact molecular mechanism responsible for the observed potency of the DR5 selective TRAIL variant in HeLa cells, the DR5 receptor is a viable target for receptor mediated apoptosis by DR5 selective ligands in combination with radiotherapy or a proteasome inhibitor. Several examples support this notion; Buchsbaum and co-workers successfully used the agonistic anti-DR5 mAb TRA-8 in combination with radiotherapy and/or chemotherapy in vitro and in vivo in breast cancer models and in cervical cancer models[219,220]. Treatment with a proteasome inhibitor or radiotherapy was able to enhance, in additive or synergistic manner, the apoptosis inducing activity of the agonistic anti-DR5 mAb HGS-ETR2 in various cell lines[214,221,222]. In an in vivo Colo205 xenograft model this latter antibody was found to have a higher activity than the agonistic anti-DR4 mAb HGS-ETR1[222].

Unlike other apoptosis inducing TNF family members, soluble TRAIL appears to be inactive against normal healthy tissue[13]. Reports in which TRAIL induces apoptosis in normal cells could be attributed to the specific preparations of TRAIL used[14,15]. The few available tests regarding DR5 selective TRAIL variants[108,109] and the extensive available information regarding several TRAIL death receptor specific antibodies (see for example Ichikawa et al.,[180]) indicate that death receptor specific ligands, just as normal promiscuous rhTRAIL WT, also have low toxicity in normal cells. In this respect, rhTRAIL WT is currently evaluated in a phase I clinical trial and a death receptor specific ligand (the agonistic anti-DR4 mAb HGS-ETR1) is currently already being evaluated in a phase II clinical trail in combination with the proteasome inhibitor bortezomib (PS-341). However, combination treatment with chemotherapeutics or radiotherapy might also sensitize normal healthy tissues to TRAIL induced apoptosis. This must be properly investigated for both rhTRAIL WT as well as any death receptor specific ligands, especially in cases when both treatments have to be systemically administered or applied. Encouragingly, sensitization to

TRAIL induced apoptosis in combination with 10 Gy irradiation could not be demonstrated using a panel of several normal non-cancer cell lines including hepatocytes[200].

In conclusion, our results show that a combination of the DR5 selective TRAIL variant D269H/E195R and the proteasome inhibitor MG132 is significantly more potent in the induction of apoptosis than the combination MG132 and rhTRAIL WT. Preliminary results also suggest that the combination of radiotherapy and D269H/E195R is more potent than the combination of radiation therapy and rhTRAIL WT. Although the exact molecular mechanism of the enhanced potency of the DR5 selective TRAIL variant when used in combination with radiation therapy or with a proteasome inhibitor remains to be elucidated and safety of these combination treatment regimens towards non cancer cells needs to be addressed, this DR5 receptor selective TRAIL variant permits novel targeted and tumor selective anti-cancer therapies.

Material and Methods

Reagents and chemicals
Dulbecco's MEM and Nutrient Mixture F-12 (HAM) were obtained from Invitrogen-Life Technologies (Merelbeke, Belgium) and fetal calf serum (FCS) from Bodinco (Alkmaar, the Netherlands). 3-(4, 5-dimethylthiazol-2-yl) 2, 5-diphenyltetrazolium bromide (MTT) was purchased from Sigma-Aldrich (Zwijndrecht, the Netherlands), dimethyl sulfoxide (DMSO) from Merck (Amsterdam, the Netherlands), trypsin stock (10×) solution and EDTA from Invitrogen-Life Technologies and the proteasome inhibitor MG132 from Calbiochem (Breda, the Netherlands). RhTRAIL WT and the DR5 selective TRAIL variant D269H/E195R[108] were produced following a protocol described previously[65].

Cell line and cell culture
The human cervical carcinoma cell line HeLa S3 (HeLa) was obtained from the American Type Culture Collection (ATCC, Manassas, VA, USA). This HeLa cell line is human papillomavirus type 18 (HPV-18) positive[207] and contains wild-type p53[206]. Cells were grown at 37^{o}C in a humidified atmosphere with 5% CO_2 in 1:1 DMEM/HAM medium supplemented with 10% FCS. Cells were detached with 0.05% trypsin/0.5 mM EDTA in phosphate-buffered saline (PBS, 0.14 M NaCl, 2.7 M KCl, 6.4 M Na_2HPO_4. $2H_2O$, 1.5 M KH_2PO_4, pH 7.4).

Irradiation
Cells were irradiated with a 137 Cesium γ-ray machine (IBL 637, CIS Bio International Gif/Yvette, France) at 0.9 Gy/ min. After receiving the required dose of ionizing radiation (10 Gy) the cells were treated with 5, 10 or 50 ng/ml rhTRAIL WT or D269H/E195R. Cells treated only with 5 or 50 ng/ml rhTRAIL WT or D269H/E195R were used as control. To correct for loss of viability due to irradiation and to compare the efficacy of the TRAIL and D269H/E195R treatment, data was normalized to 100% viability at 0 ng/ml rhTRAIL WT or D269H/E195R and for each treatment all other values were calculated relative to the value at 0 ng/ml.

Cytotoxicity assay

The 3-(4,5-Dimethylthiazol-2-yl)-2,5-diphenyl tetrazolium bromide (MTT) assay was used to determine the cytotoxic activity of rhTRAIL WT in combination with irradiation. In a 96-well culture plate, 3,000 cells per well (to obtain logarithmic cell growth at day 4) were incubated in a total volume of 200 µl. Treatment consisted of irradiation followed by continuous incubation with rhTRAIL WT in various concentrations. Cytotoxicity was determined after 4 days by adding 20 µl MTT-solution and incubated for 3.5 h at 37°C. After centrifugation, the culture supernatant was discarded and the blue formazan crystals, which are only formed in living cells by oxidation, were dissolved by adding DMSO. The plate was read immediately at 520 nm using a microtiter plate spectrometer (Benchmark Microplate Reader, Bio-Rad Laboratories Inc., Veenendaal, the Netherlands). Controls consisted of media without cells. Cell survival was defined as the growth of treated cells compared to untreated cells. The assay was performed in quadruplicate.

Proteasome inhibition

In a 96-wells culture plate 15,000 cells per well were seeded in 100 µl culture medium. Cells were pretreated for 2 hr with 10 µM MG132 (dissolved in DMSO) followed by treatment with 10 ng/ml rhTRAIL WT or D269H/E195R for 4 hr and 6 hr. At the end of the experimental period acridine orange was added and apoptotic cells were counted using a fluorescence microscope. Apoptosis was defined by the appearance of apoptotic bodies and/or chromatin condensation. Results are expressed as the percentage of apoptotic cells in a culture (by counting at least 300 cells per well). This assay was performed three times.

Statistical analysis

Statistical analysis was performed using the two sample t-test. Differences associated with p-values < 0.05 were considered significant.

7

Summary and general discussion

Introduction

Tumor necrosis factor (TNF) ligand family members and their corresponding receptors of the TNF receptor family activate several signaling pathways, eliciting activities ranging from cell-proliferation to the induction of apoptosis. TNF ligands and TNF receptors are involved in a variety of biological processes, such as host defense, development, (auto)immunity, inflammation and tumor surveillance. Many TNF ligand and TNF receptor family members are attractive drug targets for treating autoimmune diseases and cancer. Blocking TNF-α signaling is a clinically well established treatment strategy for rheumatoid arthritis and some other auto-immune diseases. The inhibition or, reversely, activation of other signaling pathways modulated by members of TNF ligand and TNF receptor families are currently under investigation as potential treatment strategies to combat cancer or to alleviate autoimmune diseases.

One member of the TNF ligand family, Tumor necrosis factor (TNF) related apoptosis inducing-ligand (TRAIL), is currently attracting great interest as a potential anti-cancer therapeutic. TRAIL in its soluble form selectively induces apoptosis in tumor cells *in vitro* and *in vivo* in several preclinical models. Unlike other apoptosis inducing TNF ligand family members, soluble TRAIL appears to be inactive against normal healthy tissue. TRAIL binds to five cognate receptors of the TNF receptor family; to the death receptors DR4 and DR5 and to the decoy receptors DcR1, DcR2 and osteoprotegerin (OPG). Binding of TRAIL to the DR4 and DR5 receptors induces apoptosis by activating the cell-extrinsic or death receptor-mediated apoptosis pathway. Binding to the decoy receptors and OPG does not induce apoptosis; in contrast, it could prevent apoptosis.

Currently, approximately twenty five percent of all new therapeutics entering the market are protein based therapeutics. Since endogenous proteins are not "designed" by Nature to function as therapeutic agents, additional optimization might be required. Modifying a protein's amino acid sequence can be a useful strategy to improve several properties relevant to a potential protein drug, such as stability, affinity, specificity, solubility, immunogenicity and pharmacokinetic (PK) properties, in order to obtain a variant with the desired characteristics. Both classical protein engineering approaches (expert design) and directed evolution methods have been successfully applied in the development of improved protein therapeutics. More recently, structure based computational protein design methods combine computer design steps with *in silico* screening/selection, permitting screening of a much larger fraction of sequence space (up to 10^{80}) than is experimentally possible. Structure based computational design algorithms employ usually an inverse protein folding approach, i.e. the algorithm determines which amino acid sequence is most compatible with a protein 3-dimensional backbone structure. A particular 3-dimensional backbone structure will have many sequences compatible with it while any given amino acid sequence has only one compatible 3-dimensional structure. Computational design methods have been successfully employed to improve various properties of several proteins but have yet hardly been applied to improve the efficacy of (prospective) protein therapeutics. In this thesis, structure based computational design methods are used to improve the structural stability of TRAIL and to modify the receptor binding characteristics of TRAIL in order to enhance its efficacy.

Stability is an important property for protein therapeutics. Protein stability is important throughout the production process and for the shelf-life of the final product. In addition, stability influences pharmacokinetic and pharmacodynamic properties of a protein therapeutic and increasing the structural stability can also be constructive in reducing potential immunogenicity by decreasing protein aggregation. The shelf-life of a protein therapeutic can be enhanced using proper formulation technology, increasing physical stability and chemical stability for prolonged periods of time and pharmacokinetic- and immunogenic properties can for example be improved using pegylation technology. However, it is also possible to increase the intrinsic stability of a protein by modifying its amino acid sequence. **Chapter 3** reports the design of rhTRAIL WT variants with higher thermostability. Using a crystal structure of TRAIL as a template, stabilizing amino acid substitutions were selected by employing a computational design algorithm. Information derived from a TNF-ligand family alignment was used to focus the design on non-conserved residues only. Conserved residues are often retained in a protein family for good reason, such as structural stability. Focusing on non-conserved residues only left the existing stability causing amino acid residue networks intact and, as additional benefit, this approach also reduced the use of computational resources. The automated design algorithms PERLA/FOLD-X were subsequently employed to identify favorable substitutions at those non-conserved residue positions. Various biophysical and biological assays were performed to assess the thermostability of the TRAIL variants as a read out for structural stability. A rhTRAIL variant (M1) containing only 2 mutations showed an 8 ^{o}C increase in thermal stability when compared to rhTRAIL WT. In an accelerated thermal stability study this rhTRAIL variant retained full biological activity upon incubation for 1 hour at 73 ^{o}C while rhTRAIL WT was all but inactivated within 30 minutes of incubation at 73 ^{o}C. Importantly, we could demonstrate that computational design techniques can involve both residues involved in inter-chain contacts as well as residues involved in intra-chain contacts to successfully stabilize the quaternary structure of a protein. In particular, it was shown that stabilization of the CD loop in a single TRAIL monomer resulted in stabilization of the entire trimeric molecule.

In **chapter 4** the design of DR5 selective TRAIL variants is described. Use of TRAIL receptor selective variants could permit novel tumor-specific therapies. The computational design of DR5 selective TRAIL variants was facilitated by the available crystal structures of TRAIL in complex with the DR5 receptor. However, no crystal structures were available of TRAIL in complex with the other receptors. Structures of these complexes were derived by homology modeling. Using the FOLD-X protein design algorithm, amino acid substitutions were selected (and combined) which contributed favorably to the binding energy between TRAIL and DR5 and disfavored binding to the other receptors, resulting in DR5 selective TRAIL variants. A fast surface plasmon resonance (SPR) based *in vitro* receptor binding screen was used to further refine the *in silico* selection to select for variants having favorable DR5 over DR4 binding ratios. Subsequent receptor binding experiments using surface plasmon resonance (SPR) and competition ELISA experiments confirmed the modeling predictions. Several variants were between 70 to 150 fold more selective for the DR5 receptor than for the DR4 when compared with rhTRAIL WT, one double mutant variant did not bind to DR4 at all. Many DR5 specific TRAIL variants had a higher affinity for the DR5 receptor when compared to rhTRAIL WT. This study revealed

that residues 269 and 214 of TRAIL are important in determining specificity for the DR5 receptor. Biological activity assays showed that these variants did not induce apoptosis in DR4-responsive cell lines but, in contrast, the DR5 selective variants show high activity towards DR5 responsive cancer cells without the need for additional cross-linking. Consequently, these variants are of interest for the development as a potential anti-cancer therapeutic.

Chapter 5 discusses the design of DR4 selective TRAIL variants. In contrast to the design of DR5 selective TRAIL variants no crystal structure is available of the TRAIL-DR4 complex and a homology model of the TRAIL-DR4 complex needs to be used. This makes the design of a DR4 selective variant with improved affinity for the DR4 receptor, in addition to decreased affinity for the other receptors, much harder. The FOLD-X design process proposed several TRAIL receptor interface positions and (single) amino-acid substitutions important for obtaining DR4 selectivity. Amino acid substitutions at position 218 of TRAIL (D218Y and D218H) were predicted to cause the highest change in DR4 selectivity by improving the interaction with DR4 and decreasing the interaction with DR5. Although the receptor binding assays needs further work, biological activity assays indicated that both variants induce apoptosis preferentially via DR4. However, to make these variants more potent in inducing apoptosis, the affinity of both variants for DR4 needs to increase. The lack of success in the design of a high affinity DR4 selective TRAIL variant can, at least in part, be attributed to the quality of the TRAIL-DR4 homology model; not all important interactions are apparently modeled correctly. Improving the accuracy of the TRAIL-DR4 model by crystallization is therefore of paramount importance in obtaining high affinity DR4 selective TRAIL variants.

Combination treatment with radiation therapy or chemotherapy can sensitize TRAIL resistant tumor cells and vice versa. Furthermore, it was shown that the expression levels of DR5 were up-regulated in cancer cells in response to certain chemotherapeutic drugs and in response to ionizing radiation (radiation therapy). **Chapter 6** reports on the treatment efficacy of a DR5 selective TRAIL variant in combination with a proteasome inhibitor or radiation therapy in a cervical cancer model. In this study it was shown that treatment of TRAIL resistant HeLa S3 cells with the proteasome inhibitor MG132 combined with a low concentration of the DR5 selective TRAIL variant D269H/E195R was able to induce apoptosis in this cell line in a synergistic fashion. Moreover, this combination was significantly more potent than similar concentrations of rhTRAIL WT and MG132. Preliminary results suggest that also the sequential combination of ionizing radiation and low concentrations of the DR5 selective TRAIL variant were able to induce apoptosis in HeLa S3 cells in a synergistic manner and that this combination was more potent than ionizing radiation and rhTRAIL WT. This study strongly suggests that DR5 receptor selective TRAIL variants permit novel targeted and tumor selective anti-cancer therapies.

In conclusion, the results described in this thesis demonstrate that the use of computational protein design methods is a successful approach to enhance protein thermostability and modifying protein-protein interactions. The use and development of computational design algorithms provides new insights into the fundamentals of protein structure, folding and function. From a practical point of view, computational protein design methods are a

valuable addition to other protein engineering methodologies, such as directed evolution, as a tool for the improvement and modification of protein properties. However, the importance of using accurate high quality structural information as a template, which is especially critical in the design of energetically favorable interactions, is being demonstrated in the design of DR4 receptor selective TRAIL variants that still needs improvement. Structural genomics initiatives and regular structural biology studies are determining an increasing amount of structures of proteins and protein complexes, making more and more proteins directly amenable to design or providing templates with high sequence identity for structurally similar targets allowing the modeling of more accurate homology models. Moreover, recent advantages in homology modeling, *de novo* protein structure prediction and protein-protein docking will eventually allow the prediction of more accurate structural models of target complexes. These developments will allow successful designs with a reduced amount of false positive and false negative predictions.

The demonstrated apoptosis inducing efficacy of DR5 receptor selective TRAIL variants in DR5 responsive cancer cells or in combination with a proteasome inhibitor or radiation therapy, indicate that these DR5 receptor selective TRAIL variants might be a potential anti-cancer therapeutic. Additional preclinical efficacy and safety studies are currently being established to determine and validate its use as a potential anti-cancer therapeutic. These DR5 receptor selective TRAIL variants are promising potential anti-cancer agents, permitting novel targeted and tumor selective anti-cancer therapies, both as single treatment or in combination with chemotherapeutics or radiation therapy.

References

1. Locksley, R. M., Killeen, N., & Lenardo, M. J. (2001). The TNF and TNF receptor superfamilies: integrating mammalian biology. *Cell* **104**, 487-501.

2. Bodmer, J. L., Schneider, P., & Tschopp, J. (2002). The molecular architecture of the TNF superfamily. *Trends Biochem. Sci.* **27**, 19-26.

3. Aggarwal, B. B. (2003). Signalling pathways of the TNF superfamily: a double-edged sword. *Nat. Rev. Immunol.* **3**, 745-756.

4. Collette, Y., Gilles, A., Pontarotti, P., & Olive, D. (2003). A co-evolution perspective of the TNFSF and TNFRSF families in the immune system. *Trends Immunol.* **24**, 387-394.

5. Bossen, C., Ingold, K., Tardivel, A., Bodmer, J. L., Gaide, O., Hertig, S., Ambrose, C., Tschopp, J., & Schneider, P. (2006). Interactions of tumor necrosis factor (TNF) and TNF receptor family members in the mouse and human. *J. Biol. Chem.* **281**, 13964-13971.

6. Zhang, G. (2004). Tumor necrosis factor family ligand-receptor binding. *Curr. Opin. Struct. Biol.* **14**, 154-160.

7. Chan, F. K., Chun, H. J., Zheng, L., Siegel, R. M., Bui, K. L., & Lenardo, M. J. (2000). A domain in TNF receptors that mediates ligand-independent receptor assembly and signaling. *Science* **288**, 2351-2354.

8. Siegel, R. M., Frederiksen, J. K., Zacharias, D. A., Chan, F. K., Johnson, M., Lynch, D., Tsien, R. Y., & Lenardo, M. J. (2000). Fas preassociation required for apoptosis signaling and dominant inhibition by pathogenic mutations. *Science* **288**, 2354-2357.

9. Bradley, J. R. & Pober, J. S. (2001). Tumor necrosis factor receptor-associated factors (TRAFs). *Oncogene* **20**, 6482-6491.

10. Fesik, S. W. (2000). Insights into programmed cell death through structural biology. *Cell* **103**, 273-282.

11. Fesik, S. W. (2005). Promoting apoptosis as a strategy for cancer drug discovery. *Nat. Rev. Cancer* **5**, 876-885.

12. Cha, S. S., Sung, B. J., Kim, Y. A., Song, Y. L., Kim, H. J., Kim, S., Lee, M. S., & Oh, B. H. (2000). Crystal structure of TRAIL-DR5 complex identifies a critical role of the unique frame insertion in conferring recognition specificity. *J. Biol. Chem.* **275**, 31171-31177.

13. Ashkenazi, A., Pai, R. C., Fong, S., Leung, S., Lawrence, D. A., Marsters, S. A., Blackie, C., Chang, L., McMurtrey, A. E., Hebert, A., Deforge, L., Koumenis, I.

L., Lewis, D., Harris, L., Bussiere, J., Koeppen, H., Shahrokh, Z., & Schwall, R. H. (1999). Safety and antitumor activity of recombinant soluble Apo2 ligand. *J. Clin. Invest* **104**, 155-162.

14. Lawrence, D., Shahrokh, Z., Marsters, S., Achilles, K., Shih, D., Mounho, B., Hillan, K., Totpal, K., Deforge, L., Schow, P., Hooley, J., Sherwood, S., Pai, R., Leung, S., Khan, L., Gliniak, B., Bussiere, J., Smith, C. A., Strom, S. S., Kelley, S., Fox, J. A., Thomas, D., & Ashkenazi, A. (2001). Differential hepatocyte toxicity of recombinant Apo2L/TRAIL versions. *Nat. Med.* **7**, 383-385.

15. Qin, J., Chaturvedi, V., Bonish, B., & Nickoloff, B. J. (2001). Avoiding premature apoptosis of normal epidermal cells. *Nat. Med.* **7**, 385-386.

16. Hymowitz, S. G., Christinger, H. W., Fuh, G., Ultsch, M., O'Connell, M., Kelley, R. F., Ashkenazi, A., & de Vos, A. M. (1999). Triggering cell death: the crystal structure of Apo2L/TRAIL in a complex with death receptor 5. *Mol. Cell* **4**, 563-571.

17. Hymowitz, S. G., O'Connell, M. P., Ultsch, M. H., Hurst, A., Totpal, K., Ashkenazi, A., de Vos, A. M., & Kelley, R. F. (2000). A unique zinc-binding site revealed by a high-resolution X-ray structure of homotrimeric Apo2L/TRAIL. *Biochemistry* **39**, 633-640.

18. Mongkolsapaya, J., Grimes, J. M., Chen, N., Xu, X. N., Stuart, D. I., Jones, E. Y., & Screaton, G. R. (1999). Structure of the TRAIL-DR5 complex reveals mechanisms conferring specificity in apoptotic initiation. *Nat. Struct. Biol.* **6**, 1048-1053.

19. LeBlanc, H. N. & Ashkenazi, A. (2003). Apo2L/TRAIL and its death and decoy receptors. *Cell Death. Differ.* **10**, 66-75.

20. Chaudhary, P. M., Eby, M., Jasmin, A., Bookwalter, A., Murray, J., & Hood, L. (1997). Death receptor 5, a new member of the TNFR family, and DR4 induce FADD-dependent apoptosis and activate the NF-kappaB pathway. *Immunity.* **7**, 821-830.

21. Schneider, P., Thome, M., Burns, K., Bodmer, J. L., Hofmann, K., Kataoka, T., Holler, N., & Tschopp, J. (1997). TRAIL receptors 1 (DR4) and 2 (DR5) signal FADD-dependent apoptosis and activate NF-kappaB. *Immunity.* **7**, 831-836.

22. Kuang, A. A., Diehl, G. E., Zhang, J., & Winoto, A. (2000). FADD is required for DR4- and DR5-mediated apoptosis: lack of trail-induced apoptosis in FADD-deficient mouse embryonic fibroblasts. *J. Biol. Chem.* **275**, 25065-25068.

23. Kischkel, F. C., Lawrence, D. A., Chuntharapai, A., Schow, P., Kim, K. J., & Ashkenazi, A. (2000). Apo2L/TRAIL-dependent recruitment of endogenous FADD and caspase-8 to death receptors 4 and 5. *Immunity.* **12**, 611-620.

24. Sprick, M. R., Weigand, M. A., Rieser, E., Rauch, C. T., Juo, P., Blenis, J., Krammer, P. H., & Walczak, H. (2000). FADD/MORT1 and caspase-8 are recruited to TRAIL receptors 1 and 2 and are essential for apoptosis mediated by TRAIL receptor 2. *Immunity.* **12**, 599-609.

25. Bodmer, J. L., Holler, N., Reynard, S., Vinciguerra, P., Schneider, P., Juo, P., Blenis, J., & Tschopp, J. (2000). TRAIL receptor-2 signals apoptosis through FADD and caspase-8. *Nat. Cell Biol.* **2**, 241-243.

26. Kischkel, F. C., Lawrence, D. A., Tinel, A., LeBlanc, H., Virmani, A., Schow, P., Gazdar, A., Blenis, J., Arnott, D., & Ashkenazi, A. (2001). Death receptor recruitment of endogenous caspase-10 and apoptosis initiation in the absence of caspase-8. *J. Biol. Chem.* **276**, 46639-46646.

27. Jin, Z. & El Deiry, W. S. (2005). Overview of cell death signaling pathways. *Cancer Biol. Ther.* **4**, 139-163.

28. Debatin, K. M. & Krammer, P. H. (2004). Death receptors in chemotherapy and cancer. *Oncogene* **23**, 2950-2966.

29. Van Geelen, C. M., de Vries, E. G., & de Jong, S. (2004). Lessons from TRAIL-resistance mechanisms in colorectal cancer cells: paving the road to patient-tailored therapy. *Drug Resist. Updat.* **7**, 345-358.

30. Kimberley, F. C. & Screaton, G. R. (2004). Following a TRAIL: update on a ligand and its five receptors. *Cell Res.* **14**, 359-372.

31. Clancy, L., Mruk, K., Archer, K., Woelfel, M., Mongkolsapaya, J., Screaton, G., Lenardo, M. J., & Chan, F. K. (2005). Preligand assembly domain-mediated ligand-independent association between TRAIL receptor 4 (TR4) and TR2 regulates TRAIL-induced apoptosis. *Proc. Natl. Acad. Sci. U. S. A* **102**, 18099-18104.

32. Kelley, S. K., Harris, L. A., Xie, D., Deforge, L., Totpal, K., Bussiere, J., & Fox, J. A. (2001). Preclinical studies to predict the disposition of Apo2L/tumor necrosis factor-related apoptosis-inducing ligand in humans: characterization of in vivo efficacy, pharmacokinetics, and safety. *J. Pharmacol. Exp. Ther.* **299**, 31-38.

33. Pavlou, A. K. & Reichert, J. M. (2004). Recombinant protein therapeutics--success rates, market trends and values to 2010. *Nat. Biotechnol.* **22**, 1513-1519.

34. Brannigan, J. A. & Wilkinson, A. J. (2002). Protein engineering 20 years on. *Nat. Rev. Mol. Cell Biol.* **3**, 964-970.

35. Otten, L. G. & Quax, W. J. (2005). Directed evolution: selecting today's biocatalysts. *Biomol. Eng* **22**, 1-9.

36. Patrick, W. M. & Firth, A. E. (2005). Strategies and computational tools for improving randomized protein libraries. *Biomol. Eng* **22**, 105-112.

37. Yuan, L., Kurek, I., English, J., & Keenan, R. (2005). Laboratory-directed protein evolution. *Microbiol. Mol. Biol. Rev.* **69**, 373-392.

38. Amstutz, P., Forrer, P., Zahnd, C., & Pluckthun, A. (2001). In vitro display technologies: novel developments and applications. *Curr. Opin. Biotechnol.* **12**, 400-405.

39. Dahiyat, B. I. (1999). In silico design for protein stabilization. *Curr. Opin. Biotechnol.* **10**, 387-390.

40. Dahiyat, B. I. & Mayo, S. L. (1997). De novo protein design: fully automated sequence selection. *Science* **278**, 82-87.

41. Kuhlman, B., Dantas, G., Ireton, G. C., Varani, G., Stoddard, B. L., & Baker, D. (2003). Design of a novel globular protein fold with atomic-level accuracy. *Science* **302**, 1364-1368.

42. Looger, L. L. & Hellinga, H. W. (2001). Generalized dead-end elimination algorithms make large-scale protein side-chain structure prediction tractable: implications for protein design and structural genomics. *J. Mol. Biol.* **307**, 429-445.

43. Gordon, D. B., Marshall, S. A., & Mayo, S. L. (1999). Energy functions for protein design. *Curr. Opin. Struct. Biol.* **9**, 509-513.

44. Mendes, J., Guerois, R., & Serrano, L. (2002). Energy estimation in protein design. *Curr. Opin. Struct. Biol.* **12**, 441-446.

45. Voigt, C. A., Gordon, D. B., & Mayo, S. L. (2000). Trading accuracy for speed: A quantitative comparison of search algorithms in protein sequence design. *J. Mol. Biol.* **299**, 789-803.

46. Desjarlais, J. R. & Handel, T. M. (1995). De novo design of the hydrophobic cores of proteins. *Protein Sci.* **4**, 2006-2018.

47. Koehl, P. & Levitt, M. (1999). De novo protein design. I. In search of stability and specificity. *J. Mol. Biol.* **293**, 1161-1181.

48. Koehl, P. & Delarue, M. (1994). Application of a self-consistent mean field theory to predict protein side-chains conformation and estimate their conformational entropy. *J. Mol. Biol.* **239**, 249-275.

49. Desmet, J., Maeyer, M. D., Hazes, B., & Lasters, I. (1992). The dead-end elimination theorem and its use in protein side-chain positioning. *Nature* **356**, 539-542.

50. Fersht, A. & Winter, G. (1992). Protein engineering. *Trends Biochem. Sci.* **17**, 292-295.

51. Van den Burg, B. & Eijsink, V. G. (2002). Selection of mutations for increased protein stability. *Curr. Opin. Biotechnol.* **13**, 333-337.

52. Pantoliano, M. W., Ladner, R. C., Bryan, P. N., Rollence, M. L., Wood, J. F., & Poulos, T. L. (1987). Protein engineering of subtilisin BPN': enhanced stabilization through the introduction of two cysteines to form a disulfide bond. *Biochemistry* **26**, 2077-2082.

53. Matsumura, M., Signor, G., & Matthews, B. W. (1989). Substantial increase of protein stability by multiple disulphide bonds. *Nature* **342**, 291-293.

54. Van den Burg, B., Vriend, G., Veltman, O. R., Venema, G., & Eijsink, V. G. (1998). Engineering an enzyme to resist boiling. *Proc. Natl. Acad. Sci. U. S. A* **95**, 2056-2060.

55. Villegas, V., Viguera, A. R., Aviles, F. X., & Serrano, L. (1996). Stabilization of proteins by rational design of alpha-helix stability using helix/coil transition theory. *Fold. Des* **1**, 29-34.

56. Giver, L., Gershenson, A., Freskgard, P. O., & Arnold, F. H. (1998). Directed evolution of a thermostable esterase. *Proc. Natl. Acad. Sci. U. S. A* **95**, 12809-12813.

57. Jung, S., Honegger, A., & Pluckthun, A. (1999). Selection for improved protein stability by phage display. *J. Mol. Biol.* **294**, 163-180.

58. Finucane, M. D., Tuna, M., Lees, J. H., & Woolfson, D. N. (1999). Core-directed protein design. I. An experimental method for selecting stable proteins from combinatorial libraries. *Biochemistry* **38**, 11604-11612.

59. Malakauskas, S. M. & Mayo, S. L. (1998). Design, structure and stability of a hyperthermophilic protein variant. *Nat. Struct. Biol.* **5**, 470-475.

60. Ventura, S., Vega, M. C., Lacroix, E., Angrand, I., Spagnolo, L., & Serrano, L. (2002). Conformational strain in the hydrophobic core and its implications for protein folding and design. *Nat. Struct. Biol.* **9**, 485-493.

61. Dantas, G., Kuhlman, B., Callender, D., Wong, M., & Baker, D. (2003). A large scale test of computational protein design: folding and stability of nine completely redesigned globular proteins. *J. Mol. Biol.* **332**, 449-460.

62. Korkegian, A., Black, M. E., Baker, D., & Stoddard, B. L. (2005). Computational thermostabilization of an enzyme. *Science* **308**, 857-860.

63. Luo, P., Hayes, R. J., Chan, C., Stark, D. M., Hwang, M. Y., Jacinto, J. M., Juvvadi, P., Chung, H. S., Kundu, A., Ary, M. L., & Dahiyat, B. I. (2002). Development of a cytokine analog with enhanced stability using computational ultrahigh throughput screening. *Protein Sci.* **11**, 1218-1226.

64. Filikov, A. V., Hayes, R. J., Luo, P., Stark, D. M., Chan, C., Kundu, A., & Dahiyat, B. I. (2002). Computational stabilization of human growth hormone. *Protein Sci.* **11**, 1452-1461.

65. van der Sloot, A. M., Mullally, M. M., Fernandez-Ballester, G., Serrano, L., & Quax, W. J. (2004). Stabilization of TRAIL, an all-beta-sheet multimeric protein, using computational redesign. *Protein Eng Des Sel* **17**, 673-680.

66. Domingues, H., Peters, J., Schneider, K. H., Apeler, H., Sebald, W., Oschkinat, H., & Serrano, L. (2000). Improving the refolding yield of interleukin-4 through the optimization of local interactions. *J. Biotechnol.* **84**, 217-230.

67. Lehmann, M., Kostrewa, D., Wyss, M., Brugger, R., D'Arcy, A., Pasamontes, L., & van Loon, A. P. (2000). From DNA sequence to improved functionality: using protein sequence comparisons to rapidly design a thermostable consensus phytase. *Protein Eng* **13**, 49-57.

68. Imanaka, T., Shibazaki, M., & Takagi, M. (1986). A new way of enhancing the thermostability of proteases. *Nature* **324**, 695-697.

69. Serrano, L., Day, A. G., & Fersht, A. R. (1993). Step-wise mutation of barnase to binase. A procedure for engineering increased stability of proteins and an experimental analysis of the evolution of protein stability. *J. Mol. Biol.* **233**, 305-312.

70. Steipe, B., Schiller, B., Pluckthun, A., & Steinbacher, S. (1994). Sequence statistics reliably predict stabilizing mutations in a protein domain. *J. Mol. Biol.* **240**, 188-192.

71. Lehmann, M. & Wyss, M. (2001). Engineering proteins for thermostability: the use of sequence alignments versus rational design and directed evolution. *Curr. Opin. Biotechnol.* **12**, 371-375.

72. Lehmann, M., Loch, C., Middendorf, A., Studer, D., Lassen, S. F., Pasamontes, L., van Loon, A. P., & Wyss, M. (2002). The consensus concept for thermostability engineering of proteins: further proof of concept. *Protein Eng* **15**, 403-411.

73. Zakrzewska, M., Krowarsch, D., Wiedlocha, A., & Otlewski, J. (2004). Design of fully active FGF-1 variants with increased stability. *Protein Eng Des Sel* **17**, 603-611.

74. Zakrzewska, M., Krowarsch, D., Wiedlocha, A., Olsnes, S., & Otlewski, J. (2005). Highly stable mutants of human fibroblast growth factor-1 exhibit prolonged biological action. *J. Mol. Biol.* **352**, 860-875.

75. Frenz, C. M. (2005). Neural network-based prediction of mutation-induced protein stability changes in Staphylococcal nuclease at 20 residue positions. *Proteins* **59**, 147-151.

76. Capriotti, E., Fariselli, P., & Casadio, R. (2005). I-Mutant2.0: predicting stability changes upon mutation from the protein sequence or structure. *Nucleic Acids Res.* **33**, W306-W310.

77. Cheng, J., Randall, A., & Baldi, P. (2006). Prediction of protein stability changes for single-site mutations using support vector machines. *Proteins* **62**, 1125-1132.

78. Wang, W. (2005). Protein aggregation and its inhibition in biopharmaceutics. *Int. J. Pharm.* **289**, 1-30.

79. Schellekens, H. (2002). Bioequivalence and the immunogenicity of biopharmaceuticals. *Nat. Rev. Drug Discov.* **1**, 457-462.

80. Chiti, F., Stefani, M., Taddei, N., Ramponi, G., & Dobson, C. M. (2003). Rationalization of the effects of mutations on peptide and protein aggregation rates. *Nature* **424**, 805-808.

81. Dubay, K. F., Pawar, A. P., Chiti, F., Zurdo, J., Dobson, C. M., & Vendruscolo, M. (2004). Prediction of the absolute aggregation rates of amyloidogenic polypeptide chains. *J. Mol. Biol.* **341**, 1317-1326.

82. Fernandez-Escamilla, A. M., Rousseau, F., Schymkowitz, J., & Serrano, L. (2004). Prediction of sequence-dependent and mutational effects on the aggregation of peptides and proteins. *Nat. Biotechnol.* **22**, 1302-1306.

83. Fowler, S. B., Poon, S., Muff, R., Chiti, F., Dobson, C. M., & Zurdo, J. (2005). Rational design of aggregation-resistant bioactive peptides: reengineering human calcitonin. *Proc. Natl. Acad. Sci. U. S. A* **102**, 10105-10110.

84. Grauer, A., Ziegler, R., & Raue, F. (1995). Clinical significance of antibodies against calcitonin. *Exp. Clin. Endocrinol. Diabetes* **103**, 345-351.

85. Reina, J., Lacroix, E., Hobson, S. D., Fernandez-Ballester, G., Rybin, V., Schwab, M. S., Serrano, L., & Gonzalez, C. (2002). Computer-aided design of a PDZ domain to recognize new target sequences. *Nat. Struct. Biol.* **9**, 621-627.

86. Havranek, J. J. & Harbury, P. B. (2003). Automated design of specificity in molecular recognition. *Nat. Struct. Biol.* **10**, 45-52.

87. Shifman, J. M. & Mayo, S. L. (2002). Modulating calmodulin binding specificity through computational protein design. *J. Mol. Biol.* **323**, 417-423.

88. Shifman, J. M. & Mayo, S. L. (2003). Exploring the origins of binding specificity through the computational redesign of calmodulin. *Proc. Natl. Acad. Sci. U. S. A* **100**, 13274-13279.

89. Kortemme, T., Joachimiak, L. A., Bullock, A. N., Schuler, A. D., Stoddard, B. L., & Baker, D. (2004). Computational redesign of protein-protein interaction specificity. *Nat. Struct. Mol. Biol.* **11**, 371-379.

90. Clackson, T. & Wells, J. A. (1995). A hot spot of binding energy in a hormone-receptor interface. *Science* **267**, 383-386.

91. Massova, I. & Kollman, P. A. (1999). Computational alanine scanning to probe protein-protein interactions: A novel approach to evaluate binding free energies. *Journal of the American Chemical Society* **121**, 8133-8143.

92. Kortemme, T., Kim, D. E., & Baker, D. (2004). Computational alanine scanning of protein-protein interfaces. *Sci. STKE.* **2004**, l2.

93. Schymkowitz, J., Borg, J., Stricher, F., Nys, R., Rousseau, F., & Serrano, L. (2005). The FoldX web server: an online force field. *Nucleic Acids Res.* **33**, W382-W388.

94. Bolon, D. N., Grant, R. A., Baker, T. A., & Sauer, R. T. (2005). Specificity versus stability in computational protein design. *Proc. Natl. Acad. Sci. U. S. A* **102**, 12724-12729.

95. Selzer, T., Albeck, S., & Schreiber, G. (2000). Rational design of faster associating and tighter binding protein complexes. *Nat. Struct. Biol.* **7**, 537-541.

96. Kiel, C., Selzer, T., Shaul, Y., Schreiber, G., & Herrmann, C. (2004). Electrostatically optimized Ras-binding Ral guanine dissociation stimulator mutants increase the rate of association by stabilizing the encounter complex. *Proc. Natl. Acad. Sci. U. S. A* **101**, 9223-9228.

97. Clark, L. A., Boriack-Sjodin, P. A., Eldredge, J., Fitch, C., Friedman, B., Hanf, K. J., Jarpe, M., Liparoto, S. F., Li, Y., Lugovskoy, A., Miller, S., Rushe, M., Sherman, W., Simon, K., & Van Vlijmen, H. (2006). Affinity enhancement of an in vivo matured therapeutic antibody using structure-based computational design. *Protein Sci.* **15**, 949-960.

98. Marvin, J. S. & Lowman, H. B. (2003). Redesigning an antibody fragment for faster association with its antigen. *Biochemistry* **42**, 7077-7083.

99. Clynes, R. A., Towers, T. L., Presta, L. G., & Ravetch, J. V. (2000). Inhibitory Fc receptors modulate in vivo cytoxicity against tumor targets. *Nat. Med.* **6**, 443-446.

100. Lazar, G. A., Dang, W., Karki, S., Vafa, O., Peng, J. S., Hyun, L., Chan, C., Chung, H. S., Eivazi, A., Yoder, S. C., Vielmetter, J., Carmichael, D. F., Hayes, R. J., & Dahiyat, B. I. (2006). Engineered antibody Fc variants with enhanced effector function. *Proc. Natl. Acad. Sci. U. S. A* **103**, 4005-4010.

101. Anderson, M. E. & Siahaan, T. J. (2003). Targeting ICAM-1/LFA-1 interaction for controlling autoimmune diseases: designing peptide and small molecule inhibitors. *Peptides* **24**, 487-501.

102. Shimaoka, M. & Springer, T. A. (2003). Therapeutic antagonists and conformational regulation of integrin function. *Nat. Rev. Drug Discov.* **2**, 703-716.

103. Song, G., Lazar, G. A., Kortemme, T., Shimaoka, M., Desjarlais, J. R., Baker, D., & Springer, T. A. (2006). Rational design of intercellular adhesion molecule-1 (ICAM-1) variants for antagonizing integrin lymphocyte function-associated antigen-1-dependent adhesion. *J. Biol. Chem.* **281**, 5042-5049.

104. Steed, P. M., Tansey, M. G., Zalevsky, J., Zhukovsky, E. A., Desjarlais, J. R., Szymkowski, D. E., Abbott, C., Carmichael, D., Chan, C., Cherry, L., Cheung, P., Chirino, A. J., Chung, H. H., Doberstein, S. K., Eivazi, A., Filikov, A. V., Gao, S. X., Hubert, R. S., Hwang, M., Hyun, L., Kashi, S., Kim, A., Kim, E., Kung, J., Martinez, S. P., Muchhal, U. S., Nguyen, D. H., O'Brien, C., O'Keefe, D., Singer, K., Vafa, O., Vielmetter, J., Yoder, S. C., & Dahiyat, B. I. (2003). Inactivation of TNF signaling by rationally designed dominant-negative TNF variants. *Science* **301**, 1895-1898.

105. Ashkenazi, A. (2002). Targeting death and decoy receptors of the tumour-necrosis factor superfamily. *Nat. Rev. Cancer* **2**, 420-430.

106. de Vries, E. G., Gietema, J. A., & de Jong, S. (2006). Tumor necrosis factor-related apoptosis-inducing ligand pathway and its therapeutic implications. *Clin. Cancer Res.* **12**, 2390-2393.

107. Chinnaiyan, A. M., Prasad, U., Shankar, S., Hamstra, D. A., Shanaiah, M., Chenevert, T. L., Ross, B. D., & Rehemtulla, A. (2000). Combined effect of tumor necrosis factor-related apoptosis-inducing ligand and ionizing radiation in breast cancer therapy. *Proc. Natl. Acad. Sci. U. S. A* **97**, 1754-1759.

108. van der Sloot, A. M., Tur, V., Szegezdi, E., Mullally, M. M., Cool, R. H., Samali, A., Serrano, L., & Quax, W. J. (2006). Designed tumor necrosis factor-related apoptosis-inducing ligand variants initiating apoptosis exclusively via the DR5 receptor. *Proc. Natl. Acad. Sci. U. S. A* **103**, 8634-8639.

109. Kelley, R. F., Totpal, K., Lindstrom, S. H., Mathieu, M., Billeci, K., Deforge, L., Pai, R., Hymowitz, S. G., & Ashkenazi, A. (2005). Receptor-selective mutants of apoptosis-inducing ligand 2/tumor necrosis factor-related apoptosis-inducing ligand reveal a greater contribution of death receptor (DR) 5 than DR4 to apoptosis signaling. *J. Biol. Chem.* **280**, 2205-2212.

110. Bolon, D. N., Voigt, C. A., & Mayo, S. L. (2002). De novo design of biocatalysts. *Curr. Opin. Chem. Biol.* **6**, 125-129.

111. Uil, T. G., Haisma, H. J., & Rots, M. G. (2003). Therapeutic modulation of endogenous gene function by agents with designed DNA-sequence specificities. *Nucleic Acids Res.* **31**, 6064-6078.

112. Bibikova, M., Carroll, D., Segal, D. J., Trautman, J. K., Smith, J., Kim, Y. G., & Chandrasegaran, S. (2001). Stimulation of homologous recombination through targeted cleavage by chimeric nucleases. *Mol. Cell Biol.* **21**, 289-297.

113. Bibikova, M., Beumer, K., Trautman, J. K., & Carroll, D. (2003). Enhancing gene targeting with designed zinc finger nucleases. *Science* **300**, 764.

114. Porteus, M. H. & Baltimore, D. (2003). Chimeric nucleases stimulate gene targeting in human cells. *Science* **300**, 763.

115. Urnov, F. D., Miller, J. C., Lee, Y. L., Beausejour, C. M., Rock, J. M., Augustus, S., Jamieson, A. C., Porteus, M. H., Gregory, P. D., & Holmes, M. C. (2005). Highly efficient endogenous human gene correction using designed zinc-finger nucleases. *Nature* **435**, 646-651.

116. Chevalier, B. S., Kortemme, T., Chadsey, M. S., Baker, D., Monnat, R. J., & Stoddard, B. L. (2002). Design, activity, and structure of a highly specific artificial endonuclease. *Mol. Cell* **10**, 895-905.

117. Ashworth, J., Havranek, J. J., Duarte, C. M., Sussman, D., Monnat, R. J., Jr., Stoddard, B. L., & Baker, D. (2006). Computational redesign of endonuclease DNA binding and cleavage specificity. *Nature* **441**, 656-659.

118. Marvin, J. S. & Hellinga, H. W. (2001). Conversion of a maltose receptor into a zinc biosensor by computational design. *Proc. Natl. Acad. Sci. U. S. A* **98**, 4955-4960.

119. Dwyer, M. A., Looger, L. L., & Hellinga, H. W. (2003). Computational design of a Zn2+ receptor that controls bacterial gene expression. *Proc. Natl. Acad. Sci. U. S. A* **100**, 11255-11260.

120. Yang, W., Jones, L. M., Isley, L., Ye, Y., Lee, H. W., Wilkins, A., Liu, Z. R., Hellinga, H. W., Malchow, R., Ghazi, M., & Yang, J. J. (2003). Rational design of a calcium-binding protein. *J. Am. Chem. Soc.* **125**, 6165-6171.

121. Cochran, F. V., Wu, S. P., Wang, W., Nanda, V., Saven, J. G., Therien, M. J., & DeGrado, W. F. (2005). Computational de novo design and characterization of a four-helix bundle protein that selectively binds a nonbiological cofactor. *J. Am. Chem. Soc* **127**, 1346-1347.

122. Looger, L. L., Dwyer, M. A., Smith, J. J., & Hellinga, H. W. (2003). Computational design of receptor and sensor proteins with novel functions. *Nature* **423**, 185-190.

123. Allert, M., Rizk, S. S., Looger, L. L., & Hellinga, H. W. (2004). Computational design of receptors for an organophosphate surrogate of the nerve agent soman. *Proc. Natl. Acad. Sci. U. S. A* **101**, 7907-7912.

124. Benkovic, S. J. & Hammes-Schiffer, S. (2003). A perspective on enzyme catalysis. *Science* **301**, 1196-1202.

125. Garcia-Viloca, M., Gao, J., Karplus, M., & Truhlar, D. G. (2004). How enzymes work: analysis by modern rate theory and computer simulations. *Science* **303**, 186-195.

126. Bolon, D. N. & Mayo, S. L. (2001). Enzyme-like proteins by computational design. *Proc. Natl. Acad. Sci. U. S. A* **98**, 14274-14279.

127. Kaplan, J. & DeGrado, W. F. (2004). De novo design of catalytic proteins. *Proc. Natl. Acad. Sci. U. S. A* **101**, 11566-11570.

128. Dwyer, M. A., Looger, L. L., & Hellinga, H. W. (2004). Computational design of a biologically active enzyme. *Science* **304**, 1967-1971.

129. Tang, L., Persky, A. M., Hochhaus, G., & Meibohm, B. (2004). Pharmacokinetic aspects of biotechnology products. *J. Pharm. Sci.* **93**, 2184-2204.

130. Rao, B. M., Lauffenburger, D. A., & Wittrup, K. D. (2005). Integrating cell-level kinetic modeling into the design of engineered protein therapeutics. *Nat. Biotechnol.* **23**, 191-194.

131. Sarkar, C. A., Lowenhaupt, K., Horan, T., Boone, T. C., Tidor, B., & Lauffenburger, D. A. (2002). Rational cytokine design for increased lifetime and enhanced potency using pH-activated "histidine switching". *Nat. Biotechnol.* **20**, 908-913.

132. Chirino, A. J., Ary, M. L., & Marshall, S. A. (2004). Minimizing the immunogenicity of protein therapeutics. *Drug Discov. Today* **9**, 82-90.

133. Hermeling, S., Crommelin, D. J., Schellekens, H., & Jiskoot, W. (2004). Structure-immunogenicity relationships of therapeutic proteins. *Pharm. Res.* **21**, 897-903.

134. Oberg, K. & Alm, G. V. (1989). Development of neutralizing interferon antibodies after treatment with recombinant interferon-alpha 2b in patients with malignant carcinoid tumors. *J. Interferon Res.* **9 Suppl 1**, S45-S49.

135. Casadevall, N. (2002). Antibodies against rHuEPO: native and recombinant. *Nephrol. Dial. Transplant.* **17 Suppl 5**, 42-47.

136. Casadevall, N., Nataf, J., Viron, B., Kolta, A., Kiladjian, J. J., Martin-Dupont, P., Michaud, P., Papo, T., Ugo, V., Teyssandier, I., Varet, B., & Mayeux, P. (2002). Pure red-cell aplasia and antierythropoietin antibodies in patients treated with recombinant erythropoietin. *N. Engl. J. Med.* **346**, 469-475.

137. Brusic, V., Bajic, V. B., & Petrovsky, N. (2004). Computational methods for prediction of T-cell epitopes--a framework for modelling, testing, and applications. *Methods* **34**, 436-443.

138. De Groot, A. S. & Berzofsky, J. A. (2004). From genome to vaccine--new immunoinformatics tools for vaccine design. *Methods* **34**, 425-428.

139. De Groot, A. S. (2006). Immunomics: discovering new targets for vaccines and therapeutics. *Drug Discov. Today* **11**, 203-209.

140. Voigt, C. A., Mayo, S. L., Arnold, F. H., & Wang, Z. G. (2001). Computationally focusing the directed evolution of proteins. *J. Cell Biochem. Suppl* **Suppl 37**, 58-63.

141. Saven, J. G. (2002). Combinatorial protein design. *Curr. Opin. Struct. Biol.* **12**, 453-458.

142. Moore, G. L. & Maranas, C. D. (2004). Computational challenges in combinatorial library design for protein engineering. *Aiche Journal* **50**, 262-272.

143. Voigt, C. A., Martinez, C., Wang, Z. G., Mayo, S. L., & Arnold, F. H. (2002). Protein building blocks preserved by recombination. *Nat. Struct. Biol.* **9**, 553-558.

144. Otey, C. R., Landwehr, M., Endelman, J. B., Hiraga, K., Bloom, J. D., & Arnold, F. H. (2006). Structure-guided recombination creates an artificial family of cytochromes P450. *PLoS. Biol.* **4**, e112.

145. Saraf, M. C., Moore, G. L., Goodey, N. M., Cao, V. Y., Benkovic, S. J., & Maranas, C. D. (2006). IPRO: an iterative computational protein library redesign and optimization procedure. *Biophys. J.* **90**, 4167-4180.

146. Hayes, R. J., Bentzien, J., Ary, M. L., Hwang, M. Y., Jacinto, J. M., Vielmetter, J., Kundu, A., & Dahiyat, B. I. (2002). Combining computational and experimental screening for rapid optimization of protein properties. *Proc. Natl. Acad. Sci. U. S. A* **99**, 15926-15931.

147. Dahiyat, B. I. (2006). In silico protein design: fitting sequence onto structure. *Methods Mol. Biol.* **316**, 359-374.

148. Chandonia, J. M. & Brenner, S. E. (2006). The impact of structural genomics: expectations and outcomes. *Science* **311**, 347-351.

149. Bradley, P., Misura, K. M., & Baker, D. (2005). Toward high-resolution de novo structure prediction for small proteins. *Science* **309**, 1868-1871.

150. Schymkowitz, J. W., Rousseau, F., Martins, I. C., Ferkinghoff-Borg, J., Stricher, F., & Serrano, L. (2005). Prediction of water and metal binding sites and their affinities by using the Fold-X force field. *Proc. Natl. Acad. Sci. U. S. A* **102**, 10147-10152.

151. Jiang, L., Kuhlman, B., Kortemme, T., & Baker, D. (2005). A "solvated rotamer" approach to modeling water-mediated hydrogen bonds at protein-protein interfaces. *Proteins* **58**, 893-904.

152. Vizcarra, C. L. & Mayo, S. L. (2005). Electrostatics in computational protein design. *Curr. Opin. Chem. Biol.* **9**, 622-626.

153. Wang, L., Xie, J., & Schultz, P. G. (2006). Expanding the genetic code. *Annu. Rev. Biophys. Biomol. Struct.* **35**, 225-249.

154. Allen, B. D. & Mayo, S. L. (2006). Dramatic performance enhancements for the FASTER optimization algorithm. *J. Comput. Chem.* **27**, 1071-1075.

155. Socolich, M., Lockless, S. W., Russ, W. P., Lee, H., Gardner, K. H., & Ranganathan, R. (2005). Evolutionary information for specifying a protein fold. *Nature* **437**, 512-518.

156. Marshall, S. A., Lazar, G. A., Chirino, A. J., & Desjarlais, J. R. (2003). Rational design and engineering of therapeutic proteins. *Drug Discov. Today* **8**, 212-221.

157. DeGrado, W. F., Summa, C. M., Pavone, V., Nastri, F., & Lombardi, A. (1999). De novo design and structural characterization of proteins and metalloproteins. *Annu. Rev. Biochem.* **68**, 779-819.

158. Fisinger, S., Serrano, L., & Lacroix, E. (2001). Computational estimation of specific side chain interaction energies in alpha helices. *Protein Sci.* **10**, 809-818.

159. Lacroix, E. (1999). *Protein design: a computer based approach, Ph.D.thesis* U. Libre de Bruxelles.

160. Guerois, R., Nielsen, J. E., & Serrano, L. (2002). Predicting changes in the stability of proteins and protein complexes: a study of more than 1000 mutations. *J. Mol. Biol.* **320**, 369-387.

161. Wiley, S. R., Schooley, K., Smolak, P. J., Din, W. S., Huang, C. P., Nicholl, J. K., Sutherland, G. R., Smith, T. D., Rauch, C., Smith, C. A., & . (1995). Identification and characterization of a new member of the TNF family that induces apoptosis. *Immunity.* **3**, 673-682.

162. Pitti, R. M., Marsters, S. A., Ruppert, S., Donahue, C. J., Moore, A., & Ashkenazi, A. (1996). Induction of apoptosis by Apo-2 ligand, a new member of the tumor necrosis factor cytokine family. *J. Biol. Chem.* **271**, 12687-12690.

163. Cha, S. S., Kim, M. S., Choi, Y. H., Sung, B. J., Shin, N. K., Shin, H. C., Sung, Y. C., & Oh, B. H. (1999). 2.8 A resolution crystal structure of human TRAIL, a cytokine with selective antitumor activity. *Immunity.* **11**, 253-261.

164. Bodmer, J. L., Meier, P., Tschopp, J., & Schneider, P. (2000). Cysteine 230 is essential for the structure and activity of the cytotoxic ligand TRAIL. *J. Biol. Chem.* **275**, 20632-20637.

165. Lopez, D. L. P., Lacroix, E., Ramirez-Alvarado, M., & Serrano, L. (2001). Computer-aided design of beta-sheet peptides. *J. Mol. Biol.* **312**, 229-246.

166. Angrand, I., Serrano, L., & Lacroix, E. (2001). Computer-assisted re-design of spectrin SH3 residue clusters. *Biomol. Eng* **18**, 125-134.

167. Koradi, R., Billeter, M., & Wuthrich, K. (1996). MOLMOL: a program for display and analysis of macromolecular structures. *J. Mol. Graph.* **14**, 51-32.

168. Eck, M. J., Ultsch, M., Rinderknecht, E., de Vos, A. M., & Sprang, S. R. (1992). The structure of human lymphotoxin (tumor necrosis factor-beta) at 1.9-A resolution. *J. Biol. Chem.* **267**, 2119-2122.

169. Vriend, G. & Eijsink, V. (1993). Prediction and analysis of structure, stability and unfolding of thermolysin-like proteases. *J. Comput. Aided Mol. Des* **7**, 367-396.

170. Chiti, F., Taddei, N., White, P. M., Bucciantini, M., Magherini, F., Stefani, M., & Dobson, C. M. (1999). Mutational analysis of acylphosphatase suggests the importance of topology and contact order in protein folding. *Nat. Struct. Biol.* **6**, 1005-1009.

171. Narhi, L. O., Philo, J. S., Li, T., Zhang, M., Samal, B., & Arakawa, T. (1996). Induction of alpha-helix in the beta-sheet protein tumor necrosis factor-alpha: thermal- and trifluoroethanol-induced denaturation at neutral pH. *Biochemistry* **35**, 11447-11453.

172. Morris, A. E., Remmele, R. L., Jr., Klinke, R., Macduff, B. M., Fanslow, W. C., & Armitage, R. J. (1999). Incorporation of an isoleucine zipper motif enhances the biological activity of soluble CD40L (CD154). *J. Biol. Chem.* **274**, 418-423.

173. Willard, D., Chen, W. J., Barrett, G., Blackburn, K., Bynum, J., Consler, T., Hoffman, C., Horne, E., Iannone, M. A., Kadwell, S., Parham, J., & Ellis, B. (2000). Expression, purification, and characterization of the human receptor activator of NF-kappaB ligand (RANKL) extracellular domain. *Protein Expr. Purif.* **20**, 48-57.

174. Filikov, A. V., Hayes, R. J., Luo, P., Stark, D. M., Chan, C., Kundu, A., & Dahiyat, B. I. (2002). Computational stabilization of human growth hormone. *Protein Sci.* **11**, 1452-1461.

175. Luo, P., Hayes, R. J., Chan, C., Stark, D. M., Hwang, M. Y., Jacinto, J. M., Juvvadi, P., Chung, H. S., Kundu, A., Ary, M. L., & Dahiyat, B. I. (2002). Development of a cytokine analog with enhanced stability using computational ultrahigh throughput screening. *Protein Sci.* **11**, 1218-1226.

176. Steipe, B., Schiller, B., Pluckthun, A., & Steinbacher, S. (1994). Sequence statistics reliably predict stabilizing mutations in a protein domain. *J. Mol. Biol.* **240**, 188-192.

177. Guex, N. & Peitsch, M. C. (1997). SWISS-MODEL and the Swiss-PdbViewer: an environment for comparative protein modeling. *Electrophoresis* **18**, 2714-2723.

178. Picard, V., Ersdal-Badju, E., Lu, A., & Bock, S. C. (1994). A rapid and efficient one-tube PCR-based mutagenesis technique using Pfu DNA polymerase. *Nucleic Acids Res.* **22**, 2587-2591.

179. Griffith, T. S., Rauch, C. T., Smolak, P. J., Waugh, J. Y., Boiani, N., Lynch, D. H., Smith, C. A., Goodwin, R. G., & Kubin, M. Z. (1999). Functional analysis of TRAIL receptors using monoclonal antibodies. *J. Immunol.* **162**, 2597-2605.

180. Ichikawa, K., Liu, W., Zhao, L., Wang, Z., Liu, D., Ohtsuka, T., Zhang, H., Mountz, J. D., Koopman, W. J., Kimberly, R. P., & Zhou, T. (2001). Tumoricidal activity of a novel anti-human DR5 monoclonal antibody without hepatocyte cytotoxicity. *Nat. Med.* **7**, 954-960.

181. Chuntharapai, A., Dodge, K., Grimmer, K., Schroeder, K., Marsters, S. A., Koeppen, H., Ashkenazi, A., & Kim, K. J. (2001). Isotype-dependent inhibition of tumor growth in vivo by monoclonal antibodies to death receptor 4. *J. Immunol.* **166**, 4891-4898.

182. Wen, J., Ramadevi, N., Nguyen, D., Perkins, C., Worthington, E., & Bhalla, K. (2000). Antileukemic drugs increase death receptor 5 levels and enhance Apo-2L-induced apoptosis of human acute leukemia cells. *Blood* **96**, 3900-3906.

183. Kiel, C., Serrano, L., & Herrmann, C. (2004). A detailed thermodynamic analysis of ras/effector complex interfaces. *J. Mol. Biol.* **340**, 1039-1058.

184. Kiel, C., Wohlgemuth, S., Rousseau, F., Schymkowitz, J., Ferkinghoff-Borg, J., Wittinghofer, F., & Serrano, L. (2005). Recognizing and defining true Ras binding domains II: in silico prediction based on homology modelling and energy calculations. *J. Mol. Biol.* **348**, 759-775.

185. Kempkens, O., Medina, E., Fernandez-Ballester, G., Ozuyaman, S., Le Bivic, A., Serrano, L., & Knust, E. (2006). Computer modelling in combination with in vitro studies reveals similar binding affinities of Drosophila Crumbs for the PDZ domains of Stardust and DmPar-6. *Eur. J. Cell Biol.* **85**, 753-767.

186. Vriend, G. (1990). WHAT IF: a molecular modeling and drug design program. *J. Mol. Graph.* **8**, 52-6, 29.

187. Strausberg, R. L., Feingold, E. A., Grouse, L. H., Derge, J. G., Klausner, R. D., Collins, F. S., Wagner, L., Shenmen, C. M., Schuler, G. D., Altschul, S. F., Zeeberg, B., Buetow, K. H., Schaefer, C. F., Bhat, N. K., Hopkins, R. F., Jordan, H., Moore, T., Max, S. I., Wang, J., Hsieh, F., Diatchenko, L., Marusina, K., Farmer, A. A., Rubin, G. M., Hong, L., Stapleton, M., Soares, M. B., Bonaldo, M. F., Casavant, T. L., Scheetz, T. E., Brownstein, M. J., Usdin, T. B., Toshiyuki, S., Carninci, P., Prange, C., Raha, S. S., Loquellano, N. A., Peters, G. J., Abramson, R. D., Mullahy, S. J., Bosak, S. A., McEwan, P. J., McKernan, K. J., Malek, J. A., Gunaratne, P. H., Richards, S., Worley, K. C., Hale, S., Garcia, A. M., Gay, L. J., Hulyk, S. W., Villalon, D. K., Muzny, D. M., Sodergren, E. J., Lu, X., Gibbs, R. A., Fahey, J., Helton, E., Ketteman, M., Madan, A., Rodrigues, S., Sanchez, A., Whiting, M., Madan, A., Young, A. C., Shevchenko, Y., Bouffard, G. G.,

Blakesley, R. W., Touchman, J. W., Green, E. D., Dickson, M. C., Rodriguez, A. C., Grimwood, J., Schmutz, J., Myers, R. M., Butterfield, Y. S., Krzywinski, M. I., Skalska, U., Smailus, D. E., Schnerch, A., Schein, J. E., Jones, S. J., & Marra, M. A. (2002). Generation and initial analysis of more than 15,000 full-length human and mouse cDNA sequences. *Proc. Natl. Acad. Sci. U. S. A* **99**, 16899-16903.

188. Truneh, A., Sharma, S., Silverman, C., Khandekar, S., Reddy, M. P., Deen, K. C., McLaughlin, M. M., Srinivasula, S. M., Livi, G. P., Marshall, L. A., Alnemri, E. S., Williams, W. V., & Doyle, M. L. (2000). Temperature-sensitive differential affinity of TRAIL for its receptors. DR5 is the highest affinity receptor. *J. Biol. Chem.* **275**, 23319-23325.

189. Thomas, L. R., Johnson, R. L., Reed, J. C., & Thorburn, A. (2004). The C-terminal tails of tumor necrosis factor-related apoptosis-inducing ligand (TRAIL) and Fas receptors have opposing functions in Fas-associated death domain (FADD) recruitment and can regulate agonist-specific mechanisms of receptor activation. *J. Biol. Chem.* **279**, 52479-52486.

190. Muhlenbeck, F., Schneider, P., Bodmer, J. L., Schwenzer, R., Hauser, A., Schubert, G., Scheurich, P., Moosmayer, D., Tschopp, J., & Wajant, H. (2000). The tumor necrosis factor-related apoptosis-inducing ligand receptors TRAIL-R1 and TRAIL-R2 have distinct cross-linking requirements for initiation of apoptosis and are non-redundant in JNK activation. *J. Biol. Chem.* **275**, 32208-32213.

191. Wajant, H., Moosmayer, D., Wuest, T., Bartke, T., Gerlach, E., Schonherr, U., Peters, N., Scheurich, P., & Pfizenmaier, K. (2001). Differential activation of TRAIL-R1 and -2 by soluble and membrane TRAIL allows selective surface antigen-directed activation of TRAIL-R2 by a soluble TRAIL derivative. *Oncogene* **20**, 4101-4106.

192. Yagita, H., Takeda, K., Hayakawa, Y., Smyth, M. J., & Okumura, K. (2004). TRAIL and its receptors as targets for cancer therapy. *Cancer Sci.* **95**, 777-783.

193. MacFarlane, M., Inoue, S., Kohlhaas, S. L., Majid, A., Harper, N., Kennedy, D. B., Dyer, M. J., & Cohen, G. M. (2005). Chronic lymphocytic leukemic cells exhibit apoptotic signaling via TRAIL-R1. *Cell Death. Differ.* **12**, 773-782.

194. MacFarlane, M., Kohlhaas, S. L., Sutcliffe, M. J., Dyer, M. J., & Cohen, G. M. (2005). TRAIL receptor-selective mutants signal to apoptosis via TRAIL-R1 in primary lymphoid malignancies. *Cancer Res.* **65**, 11265-11270.

195. Misura, K. M., Chivian, D., Rohl, C. A., Kim, D. E., & Baker, D. (2006). Physically realistic homology models built with ROSETTA can be more accurate than their templates. *Proc. Natl. Acad. Sci. U. S. A* **103**, 5361-5366.

196. Schueler-Furman, O., Wang, C., Bradley, P., Misura, K., & Baker, D. (2005). Progress in modeling of protein structures and interactions. *Science* **310**, 638-642.

197. Wohlgemuth, S., Kiel, C., Kramer, A., Serrano, L., Wittinghofer, F., & Herrmann, C. (2005). Recognizing and defining true Ras binding domains I: biochemical analysis. *J. Mol. Biol.* **348**, 741-758.

198. Shankar, S. & Srivastava, R. K. (2004). Enhancement of therapeutic potential of TRAIL by cancer chemotherapy and irradiation: mechanisms and clinical implications. *Drug Resist. Updat.* **7**, 139-156.

199. French, L. E. & Tschopp, J. (2003). Protein-based therapeutic approaches targeting death receptors. *Cell Death. Differ.* **10**, 117-123.

200. Marini, P., Schmid, A., Jendrossek, V., Faltin, H., Daniel, P. T., Budach, W., & Belka, C. (2005). Irradiation specifically sensitises solid tumour cell lines to TRAIL mediated apoptosis. *BMC. Cancer* **5**, 5.

201. Sheikh, M. S., Burns, T. F., Huang, Y., Wu, G. S., Amundson, S., Brooks, K. S., Fornace, A. J., Jr., & El Deiry, W. S. (1998). p53-dependent and -independent regulation of the death receptor KILLER/DR5 gene expression in response to genotoxic stress and tumor necrosis factor alpha. *Cancer Res.* **58**, 1593-1598.

202. Shankar, S., Singh, T. R., & Srivastava, R. K. (2004). Ionizing radiation enhances the therapeutic potential of TRAIL in prostate cancer in vitro and in vivo: Intracellular mechanisms. *Prostate* **61**, 35-49.

203. Johnson, T. R., Stone, K., Nikrad, M., Yeh, T., Zong, W. X., Thompson, C. B., Nesterov, A., & Kraft, A. S. (2003). The proteasome inhibitor PS-341 overcomes TRAIL resistance in Bax and caspase 9-negative or Bcl-xL overexpressing cells. *Oncogene* **22**, 4953-4963.

204. He, Q., Huang, Y., & Sheikh, M. S. (2004). Proteasome inhibitor MG132 upregulates death receptor 5 and cooperates with Apo2L/TRAIL to induce apoptosis in Bax-proficient and -deficient cells. *Oncogene* **23**, 2554-2558.

205. Hougardy, B. M., Maduro, J. H., van der Zee, A. G., de Groot, D. J., van den Heuvel, F. A., de Vries, E. G., & de Jong, S. (2006). Proteasome inhibitor MG132 sensitizes HPV-positive human cervical cancer cells to rhTRAIL-induced apoptosis. *Int. J. Cancer* **118**, 1892-1900.

206. Yaginuma, Y. & Westphal, H. (1991). Analysis of the p53 gene in human uterine carcinoma cell lines. *Cancer Res.* **51**, 6506-6509.

207. Yee, C., Krishnan-Hewlett, I., Baker, C. C., Schlegel, R., & Howley, P. M. (1985). Presence and expression of human papillomavirus sequences in human cervical carcinoma cell lines. *Am. J. Pathol.* **119**, 361-366.

208. Scheffner, M. & Whitaker, N. J. (2003). Human papillomavirus-induced carcinogenesis and the ubiquitin-proteasome system. *Semin. Cancer Biol.* **13**, 59-67.

209. Hougardy, B. M., Maduro, J. H., van der Zee, A. G., Willemse, P. H., de Jong, S., & de Vries, E. G. (2005). Clinical potential of inhibitors of survival pathways and activators of apoptotic pathways in treatment of cervical cancer: changing the apoptotic balance. *Lancet Oncol.* **6**, 589-598.

210. Singh, T. R., Shankar, S., Chen, X., Asim, M., & Srivastava, R. K. (2003). Synergistic interactions of chemotherapeutic drugs and tumor necrosis factor-related apoptosis-inducing ligand/Apo-2 ligand on apoptosis and on regression of breast carcinoma in vivo. *Cancer Res.* **63**, 5390-5400.

211. Shankar, S., Singh, T. R., Chen, X., Thakkar, H., Firnin, J., & Srivastava, R. K. (2004). The sequential treatment with ionizing radiation followed by TRAIL/Apo-2L reduces tumor growth and induces apoptosis of breast tumor xenografts in nude mice. *Int. J. Oncol.* **24**, 1133-1140.

212. Yoshida, T., Shiraishi, T., Nakata, S., Horinaka, M., Wakada, M., Mizutani, Y., Miki, T., & Sakai, T. (2005). Proteasome inhibitor MG132 induces death receptor 5 through CCAAT/enhancer-binding protein homologous protein. *Cancer Res.* **65**, 5662-5667.

213. Gong, B. & Almasan, A. (2000). Apo2 ligand/TNF-related apoptosis-inducing ligand and death receptor 5 mediate the apoptotic signaling induced by ionizing radiation in leukemic cells. *Cancer Res.* **60**, 5754-5760.

214. Georgakis, G. V., Li, Y., Humphreys, R., Andreeff, M., O'Brien, S., Younes, M., Carbone, A., Albert, V., & Younes, A. (2005). Activity of selective fully human agonistic antibodies to the TRAIL death receptors TRAIL-R1 and TRAIL-R2 in primary and cultured lymphoma cells: induction of apoptosis and enhancement of doxorubicin- and bortezomib-induced cell death. *Br. J. Haematol.* **130**, 501-510.

215. Wendt, J., von Haefen, C., Hemmati, P., Belka, C., Dorken, B., & Daniel, P. T. (2005). TRAIL sensitizes for ionizing irradiation-induced apoptosis through an entirely Bax-dependent mitochondrial cell death pathway. *Oncogene* **24**, 4052-4064.

216. Broaddus, V. C., Dansen, T. B., Abayasiriwardana, K. S., Wilson, S. M., Finch, A. J., Swigart, L. B., Hunt, A. E., & Evan, G. I. (2005). Bid mediates apoptotic

synergy between tumor necrosis factor-related apoptosis-inducing ligand (TRAIL) and DNA damage. *J. Biol. Chem.* **280**, 12486-12493.

217. Zhu, H., Guo, W., Zhang, L., Wu, S., Teraishi, F., Davis, J. J., Dong, F., & Fang, B. (2005). Proteasome inhibitors-mediated TRAIL resensitization and Bik accumulation. *Cancer Biol. Ther.* **4**, 781-786.

218. Engels, I. H., Totzke, G., Fischer, U., Schulze-Osthoff, K., & Janicke, R. U. (2005). Caspase-10 sensitizes breast carcinoma cells to TRAIL-induced but not tumor necrosis factor-induced apoptosis in a caspase-3-dependent manner. *Mol. Cell Biol.* **25**, 2808-2818.

219. Buchsbaum, D. J., Zhou, T., Grizzle, W. E., Oliver, P. G., Hammond, C. J., Zhang, S., Carpenter, M., & LoBuglio, A. F. (2003). Antitumor efficacy of TRA-8 anti-DR5 monoclonal antibody alone or in combination with chemotherapy and/or radiation therapy in a human breast cancer model. *Clin. Cancer Res.* **9**, 3731-3741.

220. Straughn, J. M., Jr., Oliver, P. G., Zhou, T., Wang, W., Alvarez, R. D., Grizzle, W. E., & Buchsbaum, D. J. (2006). Anti-tumor activity of TRA-8 anti-death receptor 5 (DR5) monoclonal antibody in combination with chemotherapy and radiation therapy in a cervical cancer model. *Gynecol. Oncol.* **101**, 46-54.

221. Zheng, B., Georgakis, G. V., Li, Y., Bharti, A., McConkey, D., Aggarwal, B. B., & Younes, A. (2004). Induction of cell cycle arrest and apoptosis by the proteasome inhibitor PS-341 in Hodgkin disease cell lines is independent of inhibitor of nuclear factor-kappaB mutations or activation of the CD30, CD40, and RANK receptors. *Clin. Cancer Res.* **10**, 3207-3215.

222. Marini, P., Denzinger, S., Schiller, D., Kauder, S., Welz, S., Humphreys, R., Daniel, P. T., Jendrossek, V., Budach, W., & Belka, C. (2006). Combined treatment of colorectal tumours with agonistic TRAIL receptor antibodies HGS-ETR1 and HGS-ETR2 and radiotherapy: enhanced effects in vitro and dose-dependent growth delay in vivo. *Oncogene* **25**, 5145-5154.

Nederlandse Samenvatting

Het humane eiwit TRAIL ("*Tumor necrosis factor-related apoptosis-inducing ligand*") wordt beschouwd als veelbelovend toekomstig antikankermiddel. In tegenstelling tot veel van de huidige generatie antikankermiddelen induceert TRAIL alleen celdood (apoptose) in bepaalde typen kankercellen zonder gezonde cellen aan te tasten. In dit proefschrift wordt onderzocht of het TRAIL-eiwit ook geoptimaliseerd kan worden voor gebruik als geneesmiddel, als een zogenaamd therapeutisch eiwit, door gebruik te maken van een nieuwe technologie, te weten computergestuurde eiwit-ontwerp-technologie).

Therapeutische eiwitten vormen een steeds belangrijker onderdeel van het beschikbare geneesmiddelenarsenaal. Bekende voorbeelden van therapeutische eiwitten zijn: insuline, groeihormoon, erytropoëtine (EPO; Eprex) en infliximab (Remicade). Deze middelen zijn onmisbaar in de behandeling van respectievelijk, diabetes, dwerggroei, diverse vormen van anemie en reuma. Tot de jaren 80 van de vorige eeuw werden de toen beschikbare therapeutische eiwitten gezuiverd uit materiaal afkomstig van humane, dierlijke of microbiële oorsprong. Dit had verschillende nadelen, zoals bijvoorbeeld het optreden van immuunreacties tegen de lichaamsvreemde dierlijke of microbiële eiwitten, gebrek aan donormateriaal en het risco op besmetting met virale infectieziektes zoals AIDS en hepatitus C. De ontwikkeling van recombinant DNA (rDNA) technieken sinds het begin jaren 70 maakte het mogelijk om humane eiwitten in bijvoorbeeld bacteriële of zoogdiercelcultures te produceren. Door rDNA-technieken kan het gen dat codeert voor een bepaald eiwit in een ander organisme worden ingebracht. Door introductie van deze rDNA-technieken kan het geneesmiddel onder gecontroleerde omstandigheden worden geproduceerd, worden virale infecties voorkomen en kan het risico van een immuunreactie worden verkleind. In 1982 werd het eerste humane recombinante therapeutische eiwit geïntroduceerd. Dit was humaan insuline, voorheen werd dit uit de alvleesklier van varkens geïsoleerd. Inmiddels zijn in de tussenliggende 25 jaar meer dan 70 recombinante therapeutische eiwitten op de markt verschenen en zijn er op dit moment ongeveer 80 andere in verschillende stadia van klinische ontwikkeling. Tegenwoordig is ongeveer een kwart van alle nieuwe geneesmiddelen die op de markt worden toegelaten een therapeutisch eiwit.

Is het gebruik van recombinante (humane) therapeutische eiwitten al een grote verbetering, het betekent niet dat recombinante eiwitten per definitie geschikt zijn als geneesmiddel. Aan een therapeutisch eiwit kunnen / moeten geheel andere eisen aan eigenschappen zoals stabiliteit, selectiviteit en kinetiek worden gesteld dan het eiwit onder fysiologische omstandigheden bezit. Bovendien moet het eiwit makkelijk te produceren zijn en gedurende langere tijd houdbaar en stabiel zijn. Een eiwit is opgebouwd uit een keten van 20 verschillende bouwstenen (aminozuren) en deze aminozuurketen is opgevouwen tot een unieke driedimensionale structuur die de uiteindelijke werking van het eiwit bepaald. Tot voor kort waren er grofweg twee methodes om eiwitten te veranderen. De eerste methode van rationeel ontwerp berust op het gericht introduceren van een aminozuursubstitutie in de aminozuurketen door het introduceren van een specifieke mutatie in het voor het eiwit coderende gen. Aan de hand van een alignment van de aminozuurketen met de aminozuurketens van verwante eiwitten of op basis van de driedimensionale structuur wordt bepaald op welke positie van het eiwit een aminozuur veranderd dient te worden in een ander aminozuur. Nadeel van deze methode is dat slechts een klein aantal

veranderingen geprobeerd kan worden. De tweede methode, gerichte evolutie, berust op het aanbrengen van willekeurige mutaties in het voor het eiwit coderende gen. Bij deze methode wordt een mutantenbank gemaakt van een heleboel verschillende varianten van het gen (vaak meer dan een miljard). Veel van deze genvarianten zullen echter een eiwit coderen dat in eigenschappen niet verschilt of juist slechter is dan het oorspronkelijke eiwit en slechts een klein aantal varianten zal over verbeterde eigenschappen beschikken. Om dit kleine aantal verbeterde varianten te isoleren uit het vele malen grotere aantal niet verbeterde varianten wordt een selectiemethode toegepast waarbij het gen van de verbeterde variant een grotere overlevingskans heeft dan de niet verbeterde varianten. Door dit selectieproces een aantal malen te herhalen worden de varianten met de verbeterde eigenschappen verrijkt ten opzichte van de niet verbeterde varianten en kunnen de verbeterde varianten geïsoleerd worden. Nadeel van deze techniek is dat men over een goede selectietechniek dient te beschikken en deze zijn niet altijd voor alle gewenste eigenschappen beschikbaar. Tegenwoordig is een derde methode in opkomst, te weten computational protein design (of computergestuurde eiwit-ontwerp-technologie). Deze methode maakt gebruik van computeralgoritmes voor het ontwerpen van eiwitten en combineert een rationeel aspect met de mogelijkheid om heel veel verschillende varianten te beoordelen. In deze algoritmes is veel kennis samengebracht over wat de wetenschap de afgelopen decennia over eiwitten en eiwitstructuren heeft geleerd. Aan de hand van een gegeven driedimensionale structuur kan algoritme vaststellen wat het beste aminozuur is op een bepaalde positie in de aminozuurketen van het eiwit. Ook bezitten deze algoritmes efficiente zoekfuncties waardoor heel veel verschillende varianten van een eiwit doorgerekend kunnen worden; veel meer dan ooit mogelijk is om met experimentele technieken te maken en te selecteren. Uit de vele doorgerekende varianten selecteert het algoritme de varianten met de beste score en deze kunnen vervolgens daadwerkelijk gemaakt en getest worden. In hoofdstuk 2 worden recente toepassingen van computergestuurde eiwit-ontwerp-algoritmes beschreven.

TRAIL behoort tot de *tumor necrosis factor* (TNF) ligand familie. Deze TNF-ligand familie bestaat bij de mens uit ongeveer negentien verschillende eiwitten. Deze eiwitten zijn verwant aan elkaar. De aminozuurketens van deze eiwitten hebben onderling veel overeenkomsten en net als de driedimensionale structuur van deze eiwitten. Biologisch actieve TNF-liganden zijn trimeren; ze zijn opgebouwd uit drie identieke eiwitketens (monomeren) en de driedimensionale vorm van een TNF-ligand lijkt een beetje op een scheepsklok. Dit geldt dus ook voor TRAIL. Aangezien deze driedimensionale vorm essentieel is voor de celdood inducerende activiteit van TRAIL, is het voor een therapeutische toepassing van belang om deze structuur zo stabiel mogelijk te maken.

TNF-liganden vertonen een breed spectrum aan activiteiten. Sommige TNF-ligand eiwitten kunnen celgroei en –deling bevorderen, terwijl andere TNF-ligand eiwitten juist celdood induceren. TNF-liganden fungeren als boodschappermoleculen tussen verschillende celtypes, nadat een TNF-ligand bindt aan een voor de ligand specifiek receptoreiwit op de celmembraan van een doelwitcel wordt het signaal doorgegeven. Deze receptoreiwitten voor TNF-ligand eiwitten behoren tot de TNF receptorfamilie. TRAIL behoort tot de subgroep van TNF-ligand eiwitten die doelwitcellen aanzet tot geprogrammeerde celdood (“apoptose”). TRAIL induceert apoptose door te binden aan de “death receptors” DR4 en

DR5. Deze "death receptors" behoren tot de TNF receptorfamilie. Naast het binden aan deze receptoren kan TRAIL ook binden aan de "decoy receptors" DcR1, DcR2 en OPG,. Binding aan deze receptoren voorkomt echter de inductie van apoptosis. Ook is het bekend dat bepaalde chemotherapieën de hoeveelheid DR4- en/of DR5-receptoren op de kankercel kunnen verhogen en radiotherapie ("bestraling") verhoogt selectief de hoeveelheid DR5-receptoren op de kankercel. Voor een therapeutische toepassing zou het dus gewenst kunnen zijn om een variant te ontwikkelen die selectief aan of de DR5-receptor of de DR4-receptor, bindt en niet aan de overige decoy-receptoren.

Hoofdstuk 3 beschrijft het ontwerpen en testen van recombinante humane (rh)TRAIL varianten met een hogere (thermische) stabiliteit. De computergestuurde eiwit-ontwerp-algoritmes PERLA en FOLD-X werden gebruikt om aminozuursubstituties te selecteren die voor een grotere stabiliteit zorgen. Hiervoor werd de driedimensionale kristalstructuur van TRAIL als sjabloon gebruikt. Na doorrekenen van een groot aantal verschillende mogelijkheden, werden de vijf TRAIL-varianten met de hoogst scorende aminozuursubstituties voor stabiliteit gemaakt. Omdat eiwitten door verwarming kunnen ontvouwen (denatureren), werd de temperatuur waarbij de TRAIL eiwitten ontvouwen als maat voor de stabiliteit genomen. Uit de experimenten bleek dat vier van de vijf gemaakte varianten inderdaad de gewenste hogere stabiliteit bezaten. Deze varianten behielden bij hogere temperatuur zowel de driedimensionale structuur als de apoptosis inducerende activiteit. Terwijl voor rhTRAIL WT bij deze hogere temperatuur zowel de driedimensionale structuur als de biologische activiteit verloren ging. rhTRAIL WT denatureerde bij 73 ^{o}C, terwijl de twee beste varianten (M1 en C1) pas bij 81 ^{o}C begonnen te ontvouwen. Wanneer deze twee stabielere varianten gedurende een uur werden verwarmd bij 73 ^{o}C, behielden deze hun structuur en biologische activiteit. rhTRAIL WT verloor binnen dertig minuten zowel structuur als biologische activiteit. Nu zal een geneesmiddel nooit bij 73 ^{o}C worden bewaard of toegediend, echter bij hogere temperaturen verlopen diverse degradatiereacties sneller. Door verwarmen bij 73 ^{o}C kon in korte tijd worden getest of de TRAIL varianten inderdaad stabieler waren dan rhTRAIL WT, terwijl dit bij kamertemperatuur veel langer zou hebben geduurd. Deze hogere stabiliteit van de TRAIL M1 en C1 varianten kan betekenen dat ze veel langer houdbaar zijn dan rhTRAIL WT en als geneesmiddel in het lichaam veel langer actief blijven.

Hoofdstuk 4 en 5 beschrijven ontwerp en ontwikkeling van receptorselectieve TRAIL-varianten die alleen binden aan één van de twee celdood inducerende receptoren DR4 of DR5. Om deze TRAIL-varianten te ontwerpen is gebruik gemaakt van het FOLD-X algoritme. In hoofdstuk 4 werd het ontwerp van DR5-selectieve TRAIL-varianten beschreven. Voor het ontwerp van deze varianten kon gebruik worden gemaakt van de kristalstructuur van TRAIL in complex met de DR5-receptor. Met het FOLD-X algoritme zijn vervolgens enkele duizenden TRAIL-varianten *in silico* (in de computer) doorgerekend op verbeterde bindingsaffiniteit voor de DR5-receptor en een verminderde bindingsaffiniteit voor de DR4- en decoy-receptoren. Enkele van de hoogstscorende varianten werden gemaakt en vervolgens getest. Deze varianten bleken inderdaad de voorspelde eigenschappen te bezitten: een verbeterde affiniteit voor de DR5-receptor en een verminderde affiniteit voor de overige receptoren. Voor het verkrijgen van selectiviteit voor de DR5-receptor waren slechts 2 aminozuursubstituties nodig ten opzichte van de natuurlijk

voorkomende variant. Door het kleine aantal substituties wordt de kans op een eventuele immunogene respons verminderd. Deze DR5-selectieve TRAIL-varianten, en in het bijzonder de D269H/E195R-variant, bleken een sterkere antikankeractiviteit tegen kankercellen met een actieve DR5-receptor te bezitten dan rhTRAIL WT, terwijl ze veel minder werkzaam zijn tegen kankercellen met alleen een actieve DR4-receptor. Net als rhTRAIL WT zijn deze nieuwe varianten niet toxisch voor normale cellen. De verhoogde activiteit en selectiviteit op kankercellen met een actieve DR5-receptor maken dat deze varianten interessant zijn voor verdere ontwikkeling als potentieel anti-kankergeneesmiddel.

Om ook kankercellen te kunnen bestrijden die alleen een actieve DR4-receptor bezitten, werd besloten om ook DR4-selectieve TRAIL-varianten te ontwikkelen (hoofdstuk 5). Hiervoor werd wederom het FOLD-X algoritme gebruikt. Bij het ontwerp van DR5-selectieve TRAIL-varianten kon gebruik worden gemaakt van de kristalstructuur van TRAIL in complex met de DR5-receptor, helaas bestaat er echter nog geen kristalstructuur van TRAIL in complex met de DR4-receptor. Er moest volstaan worden met een model van TRAIL in complex met de DR4-receptor Dit model kon gebasseerd worden op de structuur van TRAIL in complex met DR5, omdat DR4 en DR5 een aantal overeenkomsten bezitten. Helaas is het maken van een driedimensionale structuur op basis van een model doorgaans veel minder nauwkeurig dan een kristalstructuur. FOLD-X voorspelde dat twee varianten (D218H en D218Y) een gunstig effect op de selectiviteit van TRAIL voor de DR4 receptor zouden hebben. Hoewel receptorbindingsexperimenten geen eenduidig resultaat lieten zien met betrekking tot een grotere selectiviteit voor de DR4 receptor, gaven experimenten met kankercellen aan dat er waarschijnlijk wel grotere selectiviteit voor de DR4 receptor is. Deze DR4 selectieve varianten zijn zowel tegen kankercellen met alleen een actieve DR5-receptor als tegen kankercellen met alleen een actieve DR4-receptor minder actief dan rhTRAIL WT. Echter tegen kankercellen met alleen een actieve DR5-receptor zijn ze veel minder actief dan tegen kankercellen met alleen een actieve DR4 receptor. Om als uitgangspunt voor een potentieel geneesmiddel te kunnen dienen moet echter de activiteit van deze varianten nog wel vergroot worden. Door het aanpassen van het TRAIL-DR4-model zullen meer accurate voorspellingen door FOLD-X gedaan kunnen worden, wat tot sterker werkende DR4 selectieve rhTRAIL varianten zal leiden.

In hoofdstuk 6 worden de voordelen van de DR5 selectieve rhTRAIL variant D269H/E195R ten opzichte van rhTRAIL WT in combinatie met radio- en een bepaalde vorm van chemotherapie beschreven. Sommmige typen kankercellen zijn resistent voor behandeling met rhTRAIL WT. Door combinatie met chemotherapie of radiotherapie kunnen kankercellen weer gevoelig worden gemaakt voor behandeling met rhTRAIL en bovendien kan het effect van de combinatie groter zijn dan van beide behandelingen afzonderlijk. Dit laatste wordt ook wel een synergystisch effect genoemd. De baarmoederhalskanker cellijn HeLa is slechts matig gevoelig voor TRAIL geïnduceerde celdood. Eerder onderzoek toonde aan dat deze cellijn weer gevoelig gemaakt kon worden voor TRAIL door de HeLa-cellen voor te behandelen met de proteasoomremmer MG132. Wanneer HeLa-cellen alleen werden behandeld met rhTRAIL D269H/E195R of MG132 trad er nauwelijks celdood op. De combinatie tussen rhTRAIL D269H/E195R en MG132 zorgde voor een sterke stijging in celdood. Het effect van deze DR5 selectieve variant in

combinatie met MG132 was veel sterker dan het effect van rhTRAIL WT in combinatie met MG132. Ook radiotherapie kan HeLa-cellen weer gevoelig maken voor TRAIL geïnduceerde celdood. Gecombineerd met radiotherapie liet een lage concentratie rhTRAIL D269H/E195R al een sterker effect zien dan dezelfde concentratie rhTRAIL WT.

De in dit proefschrift beschreven ontwikkeling van DR5 selectieve rhTRAIL varianten is een veelbelovend startpunt voor de ontwikkeling van een nieuw anti-kankergeneesmiddel. Deze receptor selectieve TRAIL varianten maken een tumorselectieve behandeling mogelijk, zowel als monotherapie of in combinatie met radiotherapie of chemotherapie. Voordat een DR5 selectieve rhTRAIL variant kan worden toegepast als geneesmiddel dient er echter nog veel aanvullend onderzoek plaats te vinden. Zo moet er nog *in vivo* proefdieronderzoek plaatsvinden om de toxiciteit en effectiviteit te beoordelen. Hierna kan pas met klinische onderzoeken worden begonnen, waarin de effectiviteit en mogelijke bijwerkingen in patientstudies worden beoordeeld. Pas nadat al deze onderzoeken / stadia met goed gevolg zijn doorlopen kan de DR5 selective rhTRAIL variant als geneesmiddel worden toegelaten.

Dit proefschrift toont aan dat het gebruik van computeralgoritmes een waardevolle aanvulling is op de reeds beschikbare methodes voor optimalisatie van therapeutische eiwitten. De effectiviteit en efficiëntie van deze technologie, zoals beschreven in dit proefschrift, maakt de methode bij uitstek geschikt om ook andere eiwitten voor gebruik als geneesmiddel te ontwikkelen.

Dankwoord

Na een aantal weken stevig doorploeteren met het schrijven en lay-outen van de voorgaande hoofdstukken, kan ik dan eindelijk het meest gelezen onderdeel van een proefschrift schrijven: het dankwoord.

De afgelopen jaren zijn voorbij gevlogen. Ik heb met veel plezier aan het onderzoek gewerkt dat in dit proefschrift staat beschreven. Graag wil ik iedereen bedanken die mij, op welke manier dan ook, hebben geholpen om mijn promotie-onderzoek te volbrengen.

Beste Wim, ik wil je bedanken voor de mogelijkheid om binnen de groep farmaceutische biologie te promoveren en de vrijheid die je me hebt gegeven om me tot een zelfstandig onderzoeker te ontwikkelen.

I would like to thank the reading committee (Afshin Samali, Klaas Poelstra and Luis Serrano) for evaluating my thesis manuscript.

Dear Mags, I owe you a lot. As my former supervisor you introduced me to the world of science. You initiated the TRISKEL EU project and this enabled me to "harvest" most of the results described in this thesis. Thanks. Above all, you were also a good colleague and friend. We always had good discussions, both science related and unrelated. Unfortunately, I did not fulfill your wish of me having kids, my wedding and defending my thesis in the same year. I hope this does not disappoint you too much. Because we were always mixing Dutch and English also a few words in Dutch: Veel succes met het afronden van je MBA. Nu ik het proefschrift "uit de weg" heb hoop ik jou, Luigi en Orla snel een keer te kunnen bezoeken in Utrecht.

Beste Robbert, Naast kamergenoot was je ook mijn klankbord en heb je veel bijgedragen aan de totstandkoming van dit proefschrift. Bedankt. Veel succes met TRISKEL ltd./b.v. en de DR5 selectieve TRAIL varianten. Mijn excuses voor de papierlawine die altijd je kant op dreigde te komen.

Meelezers Barry, Mattijs, Robbert en Ykelien; Bedankt voor het corrigeren van het manuscript. Mattijs, bedankt voor het aanleveren van de template, dat heeft heel wat stress gescheeld. Carlos and Borgir, thank you for the nice cover design. Ykelien, bedankt voor het kleuradvies.

Beste Janita, Wim, Niesko, Oliver, Rein, Freeke, Albert, Elfahmi, Ronald van M., Mattijs, Monique, Aaron, Henco, Anna Margareta, Mark, Nikolay, Klazien, Bea, Johanna, Charles, Linda, Michiel (aka DJ Miguel), Dolf, Mags, Melloney, Ykelien, Robbert, Carlos, Lidia, Ronald D., Geeske, Peter, Mariana, Ilse, Jean-Yves, Helga, Patty, Asia, Agata, Jan Maarten en Sieb. Ik heb met heel veel plezier bij farmaceutische biologie gewerkt, bedankt voor de gezelligheid, zowel binnen als buiten het lab, en alle hulp in de afgelopen jaren! Ik hoop dat de "nieuwe ploeg" (Gerrit and the new batch of PhD students; Mariette, Marieke, Remco, Evelina, Pol and Luis) evenzeer met veel plezier bij "FaBio" zal werken. Ykelien, Manzanita en achterbuurvrouw, ik heb onze goede klets en ander gespreken altijd zeer gewaardeerd. Bedankt voor alle hulp en natuurlijk het PA zijn (en tegenwoordig zelfs PC!); ook al vergat ik altijd de bloemen en de secretaressedag. Over "Evilien" zal ik me maar niet

al te schuldig voelen aangezien je deze naam nu voert als je Nom de guerre. Veel succes met de laatste loodjes! Mattijs, bedankt voor alle hulp, samenwerking en goede gesprekken en natuurlijk dat je het zolang met me hebt uitgehouden ondanks mijn altijd aanwezige en niet te stuiten opruimwoede. Veel succes in (waarschijnlijk) Dortmund! Truus, ook al was je ver weg, je sprong bij toen ik je nodig had. Carlos, Thanks for being my paranimf and of course the TRAIL work. Michiel, bedankt voor je werkzaamheden in de laatste fase van mijn onderzoek. Charles, bedankt dat jij het ook met me hebt uitgehouden ondanks mijn hamstergedrag in de -20^{o}C. Het goede nieuws: ik heb al twee laden opgeruimd. (Ja, ik word nog wel eens volwassen). En natuurlijk: mi sofá es tu sofa.

I would like to thank all the people involved in the European Union funded TRISKEL project; Afshin Samali, Eva Szegezdi, Gregorio Fernandez-Ballester, Johanna Vrielink, Luis Serrano, Rob van Weeghel, Ron Suk and Vicente Tur your contributions were invaluable in writing this thesis. I enjoyed our collaboration very much, both on a scientific level and at a personal level. I will miss meeting you in real life at the various TRISKEL meetings in exotic places like Tenerife and Schiermonnikenoog, but I am sure we will meet each other soon again, either in Spain or at the next TRIDENT meeting. Rob en Ron, ook wij zullen elkaar nog wel vaker zien. Veel succes met Zebra Biosciences.

Ook wil ik Steven de Jong en John Maduro bedanken voor hun goede samenwerking. Ik heb veel van jullie geleerd met betrekking tot de celbiologische aspecten van TRAIL signalling en de medische invalshoek. Helaas ben ik er nog steeds niet ingeslaagd een fatsoenlijke naam voor D269H/E195R te vinden. Onder het motto “more to do with TRAIL”; JP, bedankt voor de goede samenwerking en het mij bijbrengen van farmaceutische en technologische aspecten van eiwit formuleringen. Marc T., thank you for your collaboration on drug targeting of TRAIL. I am sure we will meet again in Barcelona. I also would like to thank Ivan Plaza-Menacho for the collaboration on RET kinase, it had nothing to do with TRAIL but I liked it a lot.

Mijn bijvakstudenten Sjouke, Mariette, Catia en Wu Bian wil ik bedanken voor de goede en plezierige samenwerking. Bedankt, thanks and obrigado! Mariette and Wu good luck with your PhD projects!

Barry en Anneriek, ook jullie bedankt voor de etentjes en goede gesprekken. Barry, bedankt dat je mijn paranimf wilde zijn en heel veel succes met je project en onderzoek.

Als laatste wil ik mijn familie bedanken. Heit, Mem, Saco, Olga en Frank bedankt voor alle steun, goede zorgen en vertrouwen!

Bedankt,

Almer

Groningen, oktober 2006

List of Publications

van der Sloot A.M., Tur, V., Szegezdi E, Mullally M.M., Cool R.H., Samali A., Serrano L., Quax W.J. (2006). Designed TRAIL variants initiating apoptosis exclusively via the DR5 receptor. Proc Natl Acad Sci U S A. 103, 8634-8639.

Plaza-Menacho,I.P., Koster,R., **van der Sloot,A.M.**, Quax,W.J., Osinga,J., van der Sluis,S.T., Hollema,H., Burzynski,G.M., Gimm,O., Buys,C.H., Eggen,B.J., and Hofstra,R.M. (2005). RET-familial medullary thyroid carcinoma mutants Y791F and S891A activate a Src/JAK/STAT3 pathway, independent of glial cell line-derived neurotrophic factor. Cancer Res. *65*, 1729-1737.

Tur, V., **van der Sloot A.M.**, Mullally M.M., Cool R.H., Szegezdi E, Samali A., Fernandez-Ballester G., Serrano L, Quax W.J. (2003) Improved cytokine design, PCT patent application WO 2005/056596.

van der Sloot,A.M., Mullally,M.M., Fernandez-Ballester,G., Serrano,L., and Quax,W.J. (2004). Stabilization of TRAIL, an all-beta-sheet multimeric protein, using computational redesign. Protein Eng Des Sel *17*, 673-680.

Otten,L.G., Sio,C.F., **van der Sloot,A.M.**, Cool,R.H., and Quax,W.J. (2004). Mutational analysis of a key residue in the substrate specificity of a cephalosporin acylase. Chembiochem. *5*, 820-825.

Droge,M.J., Ruggeberg,C.J., **van der Sloot,A.M.**, Schimmel,J., Dijkstra,D.S., Verhaert,R.M., Reetz,M.T., and Quax,W.J. (2003). Binding of phage displayed Bacillus subtilis lipase A to a phosphonate suicide inhibitor. J. Biotechnol. *101*, 19-28.

Color figures

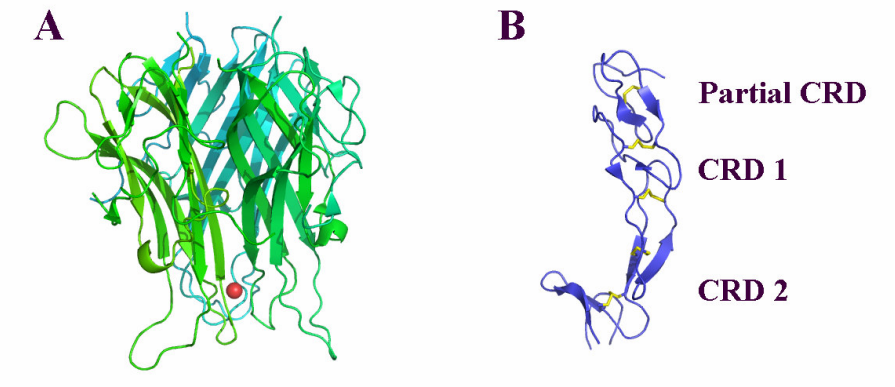

Figure 2. Chapter 1. Structure of the TRAIL trimer and DR5. A) Sideview of the TRAIL trimer, the individual TRAIL monomers are depicted in different shades of green. The zinc atom in the center of the TRAIL trimer is depicted as a red sphere. B) DR5 receptor monomer, disulphide bridges are depicted in yellow. In this orientation, the cell membrane of the DR5 containing cell is at the bottom of the figure. Picture is based on the structure of Cha *et al.*,[12].

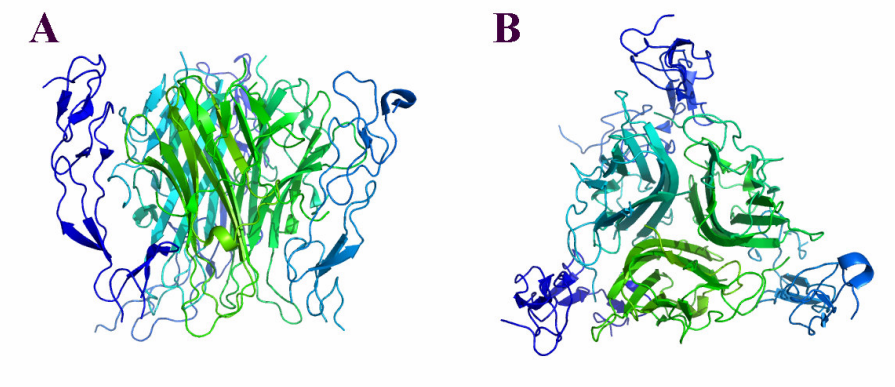

Figure 3. Chapter 1. Structure of the 3:3 TRAIL-DR5 complex. A) side view (same orientation as in figure 1). B) top view along the N-terminal to C-terminal axis of the DR5 receptor (i.e. looking towards the cell surface of DR5). Picture is based on the structure of the TRAIL-DR5 complex of Cha *et al.*,[12].

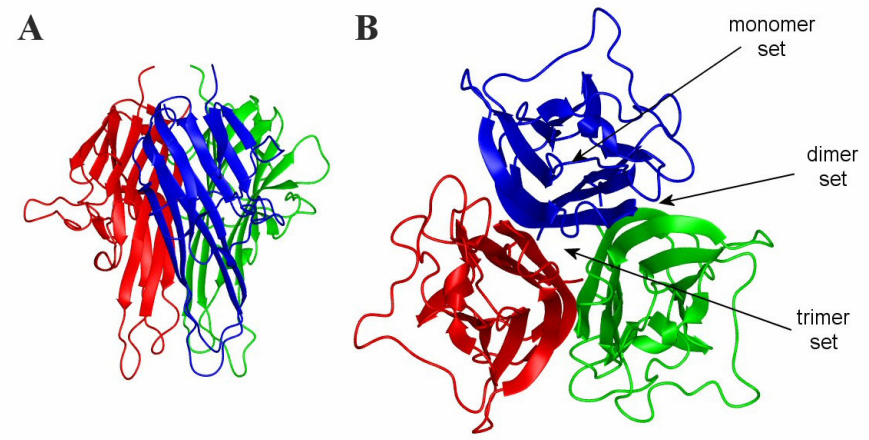

Figure 1. Chapter 3 A) Side view of the TRAIL trimeric complex, showing the three monomers in red, blue and green. B) Top view of the same complex but viewed along the longitudinal axis, depicting the different sets used for design. Structure figures were generated using MOLMOL[167].

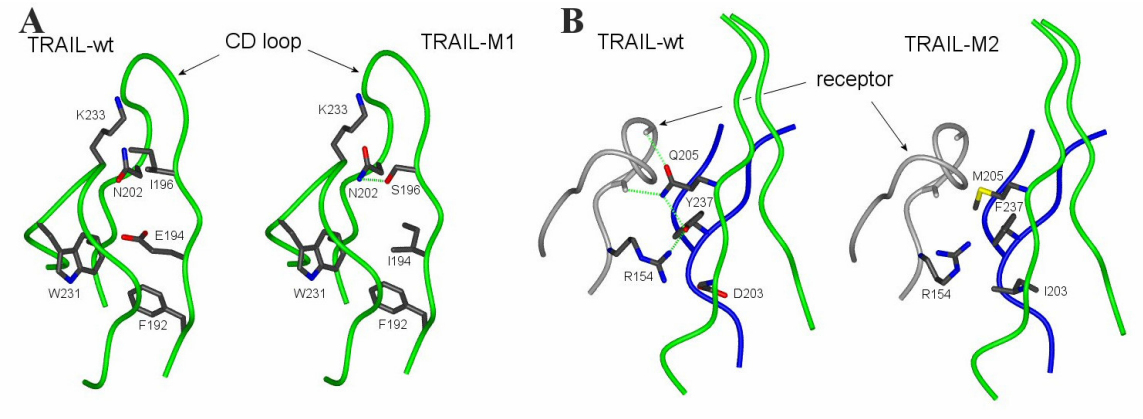

Figure 2. Chapter 3. A) Comparison, between rhTRAIL WT and M1, of the local environment around residues 194 and 196. B) Comparison between rhTRAIL WT and M2. Backbones of the two adjacent monomers are in green and blue, respectively, and the backbone of the DR5 receptor is in grey. Hydrogen bond interactions are depicted in dashed green lines.

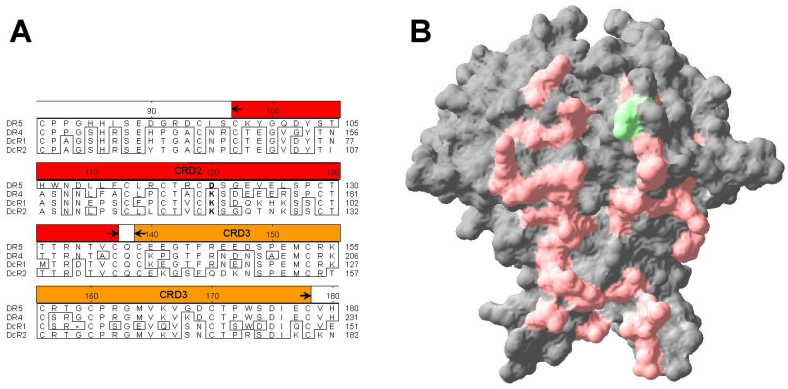

Figure 1. Chapter 4. (A) Sequence alignment of the four different TRAIL membrane receptors. Position Asp 120 of DR5 and corresponding residues of the other receptors are depicted in bold, residues of CRD2 in red and residues of CRD3 in orange. Identical amino acids to DR5 are boxed. (B) Side view of TRAIL receptor binding interface formed by two TRAIL monomers, highlighted in light red are all amino acids selected for the *in silico* screening. Tyr216 (depicted in green) was used as a reference and control.

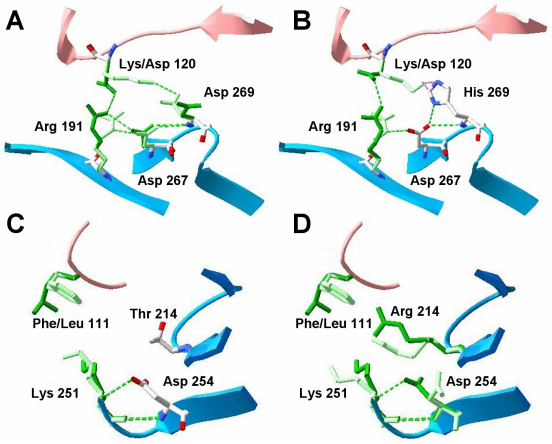

Figure 9. Chapter 4. Area of interaction of TRAIL and DR4/DR5 receptor around position 269: A) TRAIL; B) D269H variant and around position 214: C) TRAIL; D) T214R variant. Ribbons color is red for receptor and blue for TRAIL. Residues in DR5-complexes are in dark green and residues in DR4-complexes in light green. Arg 191 and Asp 267 are key TRAIL amino acids for DR5 receptor binding in the corresponding binding pocket of the receptor, as observed in the crystal structure of TRAIL in complex with DR5.